
2

Thermodynamics of Dilute Polymer Solutions

2.1 POLYMER SOLUTIONS AND THERMODYNAMICS

For a given polymer, there are solvents that dissolve the polymer well and solvents that do not dissolve the polymer. The former solvents are called “good solvents” and the latter “nonsolvents”. Table 2.1 lists a typical good solvent and a nonsolvent for polystyrene, poly(methyl methacrylate), and poly(ethylene glycol). *Polymer Handbook*¹¹ has a long list of solvents and nonsolvents for many polymers. The concentration of the polymer in the good solvent can be as high as 100%, yet the solution remains clear and uniform. Adding a nonsolvent to the solution causes the polymer to precipitate, if the nonsolvent mixes with the good solvent. A solvent with an intermediate quality dissolves the polymer to some extent.

Like low-molecular-weight solutes, a polymer dissolves in a solvent when solvation lowers the free energy. A good solvent lowers the free energy substantially. A nonsolvent increases the free energy.

Amorphous polymers (transparent in the solid state; to be precise, it is not a solid but rather a supercooled liquid) are usually easy to dissolve in the good solvent. In contrast, crystalline and semicrystalline polymers (opaque in the solid state) are sometimes not easy to dissolve. Within a crystallite, polymer chains are folded into a regular, thermodynamically stable arrangement. It is not easy to unfold the chain from the self-locked state into a disordered state in solution even if the latter state is thermodynamically more stable. Heating may help the dissolution because it facilitates the unfolding. Once dissolved, polymer chains take a random-coil conformation unless the chain is rigid.

TABLE 2.1 Good Solvents and Nonsolvents for Some Polymers

Polymer	Crystallinity	Good Solvent	Nonsolvent
Polystyrene	Amorphous	Toluene	Methanol
Poly(methyl methacrylate)	Amorphous	Tetrahydrofuran	Methanol
Poly(ethylene glycol)	Crystalline	Water (cold)	Ether

Thermodynamic properties of the polymer solution depend on how “good” the solvent is for the polymer as well as on the polymer itself. The interaction between the solvent and the polymer and the degree of polymerization dictate the properties, as we will see in the following sections of this chapter. We will examine the mean-field theory to understand the features of polymer solutions that are distinctly different from those of the other solutions. We will then examine static light scattering and size exclusion chromatography. These techniques belong to the most often used experimental methods to study dilute polymer solutions and to characterize the polymer in a state isolated from other polymer molecules. Our attention will be directed to understanding the measurement principles.

As we have learned in Section 1.8, there are a few concentration regimes in the polymer solution. Chapter 2 will primarily focus on the thermodynamics of dilute solutions, that is, below the overlap concentration, although we will also look at how the thermodynamics of the solution deviates from that of the ideal solution with an increasing concentration. Properties characteristic of nondilute solutions will be examined in detail in Chapter 4.

2.2 FLORY–HUGGINS MEAN-FIELD THEORY

2.2.1 Model

2.2.1.1 Lattice Chain Model Dissolution of a polymer into a solvent lowers the free energy of the polymer–solvent system when the enthalpy decreases by dissolution or, if it does not, when the product of the temperature and the entropy of mixing is greater than the enthalpy of mixing. Miscibility is much lower in polymer–solvent systems because adding solvent molecules to the polymer does not increase the entropy as much as it does to the low-molecular-weight solutes. Solvents that dissolve a given polymer are often limited to those that preferentially surround the polymer chain. We will learn in this section how small the entropy gain is in the polymer–solvent mixture. We will also learn what phenomena characteristic of polymer solutions are expected.

Miscibility of the polymer with a given solvent is well explained in the **mean-field theory**.³ The theory is an extension of the lattice fluid theory originally developed to explain the miscibility of two low-molecular-weight liquids. Flory pioneered the application of the mean-field lattice fluid theory to polymer solutions. The simplest version of this **lattice chain theory** is generally referred to as

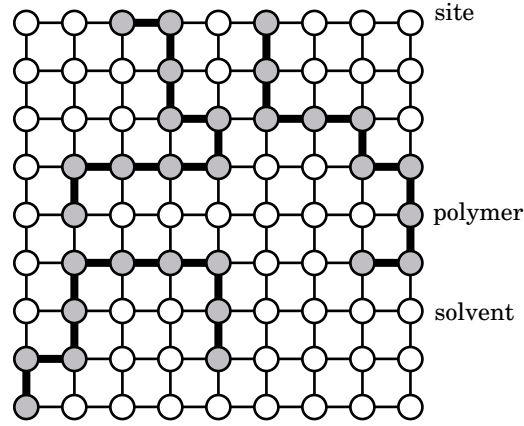


Figure 2.1. Lattice model for polymer solution. Gray sites are occupied by polymer chains, and white sites are occupied by solvent molecules.

Flory–Huggins mean-field theory. A similar mean-field theory successfully describes thermodynamics of polymer blends and, with some modifications, diblock copolymers and their blends with homopolymers.

The mean-field theory for the polymer solution compares the free energy of the polymer–solvent system before mixing and the free energy after mixing. We consider a simple situation: the polymer is a monodisperse homopolymer and is in an amorphous state or in a liquid state (melt) before mixing.

The Flory–Huggins theory uses the lattice model to arrange the polymer chains and solvents. We have looked at the lattice chain model in Section 1.4 for an excluded-volume chain. Figure 2.1 shows a two-dimensional version of the lattice model. The system consists of n_{site} sites. Each site can be occupied by either a monomer of the polymer or a solvent molecule (the monomer and the solvent molecule occupies the same volume). Double occupancy and vacancy are not allowed. A linear polymer chain occupies N sites on a string of $N-1$ bonds. There is no preference in the direction the next bond takes when a polymer chain is laid onto the lattice sites (flexible). Polymer chains consisting of N monomers are laid onto empty sites one by one until there are a total n_p chains. Then, the unoccupied sites are filled with solvent molecules. The volume fraction ϕ of the polymer is related to n_p by

$$n_p = n_{\text{site}}\phi/N \quad (2.1)$$

and the number of the solvent molecules n_s is given by

$$n_s = n_{\text{site}}(1 - \phi) \quad (2.2)$$

See Table 2.2 for summary.

TABLE 2.2 Lattice Chain Model

	Volume Fraction	Number of Molecules
Polymer	ϕ	$n_P = n_{\text{site}}\phi/N$
Solvent	$1 - \phi$	$n_S = n_{\text{site}}(1 - \phi)$

Before mixing, the polymer occupies the volume of $n_P N v_{\text{site}}$ and the solvent occupies the volume of $n_S v_{\text{site}}$, where v_{site} is the volume per site. The total volume $n_{\text{site}} v_{\text{site}}$ does not change upon mixing (incompressible). Thus, the enthalpy of mixing ΔH_{mix} in the constant-pressure process is equal to the change in the internal energy, ΔU_{mix} , and the Gibbs free energy change ΔG_{mix} is equal to the Helmholtz free energy change ΔA_{mix} .

2.2.1.2 Entropy of Mixing Flory counted the number of possible arrangements of n_P chains on n_{site} sites and compared it with the number of arrangements on $n_P N$ sites before mixing, that is, in the melt. Thus, he obtained the entropy of mixing ΔS_{mix} per site as

$$-\Delta S_{\text{mix}}/(k_B n_{\text{site}}) = \frac{\phi}{N} \ln \phi + (1 - \phi) \ln(1 - \phi) \quad \text{Flory-Huggins} \quad (2.3)$$

This expression is similar to the entropy of mixing for two gaseous substances. The difference is that the volume fraction appears in the argument of logarithm, in place of the mole fraction. Note that the first term is divided by the chain length. The division by a large N makes ΔS_{mix} small, especially at low concentrations ($\phi \ll 1$; the second term is near zero) compared with ΔS_{mix} for $N = 1$ (mixture of two solvents). The division also makes ΔS_{mix} asymmetric with respect to $\phi = 1/2$. As shown in Figure 2.2, longer chains decrease ΔS_{mix} at low ϕ and shift the maximum to the right. At $N = 100$, the plot is already close to the one for $N = \infty$ in which the entropy of mixing is determined by solvent molecules only.

We can show that ΔS_{mix} given by Eq. 2.3 is greater than the entropy of mixing for an ideal solution of n_P solute molecules and n_S solvent molecules (Problem 2.1). The difference is due to a greater number of conformations a polymer chain can take when the requirement that all the sites be occupied by the monomers is lifted.

2.2.1.3 χ Parameter The entropy of mixing is small for polymer-solvent systems, especially at low concentrations. Therefore, the change in the interactions upon mixing (= enthalpy of mixing) governs the miscibility. The interactions we are considering here are short-ranged ones only, typically van der Waals interactions (also known as dispersions), hydrogen-bonding, and dipole-dipole interactions.

The lattice fluid model considers interactions between nearest neighbors only. The interactions reside in the contacts. We denote by ϵ_{SS} , ϵ_{PP} , and ϵ_{PS} the interactions for a solvent-solvent (S-S) contact, a polymer-polymer (P-P) contact, and a polymer-solvent (P-S) contact, respectively. Mixing the solvent and polymer changes the overall interaction energy through rearrangement of contacts. Figure 2.3 illustrates the change in the two-dimensional rendering of the lattice.

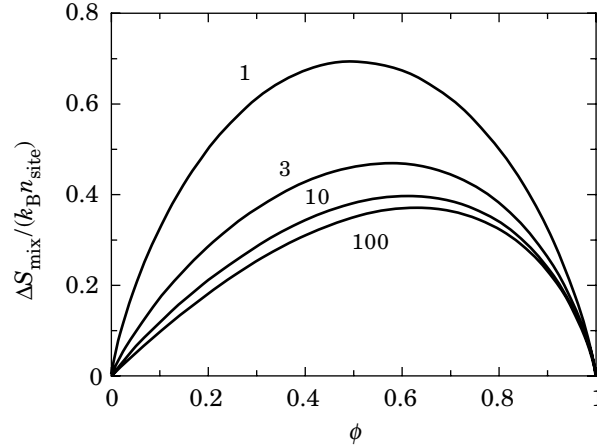


Figure 2.2. Entropy of mixing per site, $\Delta S_{\text{mix}}/(k_B n_{\text{site}})$, plotted as a function of polymer volume fraction ϕ . The number adjacent to each curve denotes N .

Before mixing, there are four P–P contacts and four S–S contacts between a total of eight sites. Mixing replaces two P–P contacts and two S–S contacts with four P–S contacts. The interaction energy on these eight bonds changes from $4\epsilon_{\text{SS}} + 4\epsilon_{\text{PP}}$ to $4\epsilon_{\text{PS}} + 2\epsilon_{\text{SS}} + 2\epsilon_{\text{PP}}$. The difference is $4\epsilon_{\text{PS}} - 2(\epsilon_{\text{SS}} + \epsilon_{\text{PP}})$. Per newly created P–S contact, the change is $\epsilon_{\text{PS}} - (\epsilon_{\text{SS}} + \epsilon_{\text{PP}})/2$. The χ (**chi**) **parameter**, also called **Flory’s χ parameter** or **Flory–Huggins χ parameter**, is defined as the product of the lattice coordinate Z and the energy change reduced by $k_B T$:

$$\chi = Z[\epsilon_{\text{PS}} - (\epsilon_{\text{PP}} + \epsilon_{\text{SS}})/2]/k_B T \quad (2.4)$$

A positive χ denotes that the polymer–solvent contacts are less favored compared with the polymer–polymer and solvent–solvent contacts (see Fig. 2.4). A negative χ means that polymer–solvent contacts are preferred, promoting solvation of the polymer. In general, χ decreases its magnitude with an increasing temperature because of $k_B T$ in the denominator, but the pair interactions also depend on the temperature in a manner characteristic of each polymer–solvent system. In a hydrogen bonding pair, for instance, χ usually changes from negative to positive with increasing temperature.

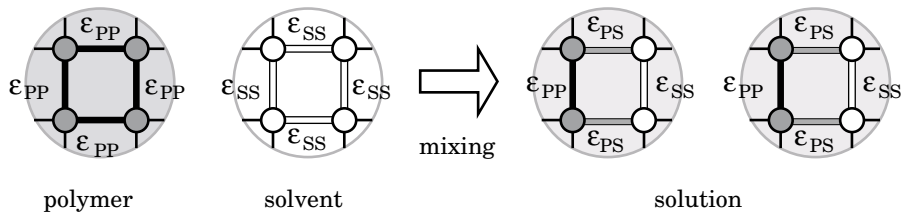


Figure 2.3. Change in the contacts between nearest neighbors when a polymer chain mixes with solvent molecules.

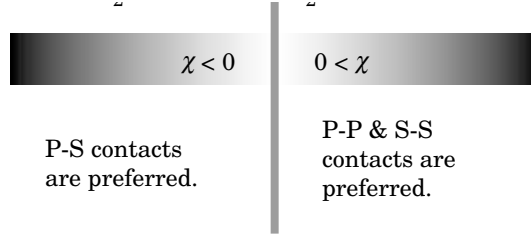


Figure 2.4. Negative χ promotes mixing of polymer with the solvent, whereas positive χ prefers polymer–polymer and solvent–solvent contacts to polymer–solvent contacts.

There are n_{site} sites, each with Z bonds. The product Zn_{site} is twice as large as the total number of bonds in the mixture because Zn_{site} counts each bond twice. Thus, $Z/2$ is the number of bonds per site. In the two-dimensional square lattice, the number is 2. In the three-dimensional cubic lattice, it is 3.

2.2.1.4 Interaction Change Upon Mixing For a site occupied by a monomer, two of its Z neighbors are always adjacent monomers on the same chain, except for the chain ends. Other monomers on the same chain are also likely to occupy some of the other neighbors. The mean-field theory neglects this fact and calculates the change in the interaction, ΔU_{mix} , by mixing $Nn_{\text{P}} = n_{\text{site}}\phi$ unconnected monomers and $n_{\text{S}} = n_{\text{site}}(1 - \phi)$ solvent molecules at random. The probability for a given bond to be a P–P contact is ϕ^2 , the probability for the S–S contact is $(1 - \phi)^2$, and the probability for the P–S contact is $2\phi(1 - \phi)$. Thus, the change ΔU_{mix} in the internal energy is

$$\Delta U_{\text{mix}} = \frac{Zn_{\text{site}}}{2} [\varepsilon_{\text{PS}} - (\varepsilon_{\text{PP}} + \varepsilon_{\text{SS}})/2] \cdot 2\phi(1 - \phi) \quad (2.5)$$

The change per site is

$$\boxed{\Delta U_{\text{mix}}/(n_{\text{site}}k_{\text{B}}T) = \chi\phi(1 - \phi) \quad \text{Flory–Huggins}} \quad (2.6)$$

As shown in Figure 2.5, ΔU_{mix} maximizes at $\phi = 1/2$. The sign of ΔU_{mix} is the same as that of χ .

ΔU_{mix} depends on the interaction through χ . A system with the same χ has the same ΔU_{mix} . For instance, a mixture with $\varepsilon_{\text{PP}} = \varepsilon_1$ and $\varepsilon_{\text{PS}} = \varepsilon_{\text{SS}} = 0$ is thermodynamically equivalent to a mixture with $\varepsilon_{\text{PP}} = \varepsilon_{\text{SS}} = 0$ and $\varepsilon_{\text{PS}} = -\varepsilon_1/2$.

Another way to arrive at Eq. 2.5 in the mean-field approximation is to tally all the contacts before and after the mixing. Table 2.3 lists the probability for a bond in the polymer–solvent system to be a P–P, P–S, or S–S contact before and after the mixing. The average contact energy is $\phi\varepsilon_{\text{PP}} + (1 - \phi)\varepsilon_{\text{SS}}$ before the mixing. After the mixing, it changes to $\phi^2\varepsilon_{\text{PP}} + 2\phi(1 - \phi)\varepsilon_{\text{PS}} + (1 - \phi)^2\varepsilon_{\text{SS}}$. The difference is $\phi(1 - \phi)(2\varepsilon_{\text{PS}} - \varepsilon_{\text{PP}} - \varepsilon_{\text{SS}})$. For a total $Zn_{\text{site}}/2$ bonds, we obtain Eq. 2.5.

TABLE 2.3 Probability of Nearest-Neighbor Contacts

Contact	Energy	Probability Before Mixing	Probability After Mixing
P-P	ε_{PP}	ϕ	ϕ^2
P-S	ε_{PS}	0	$2\phi(1 - \phi)$
S-S	ε_{SS}	$1 - \phi$	$(1 - \phi)^2$

A solution with $\chi = 0$ is called an **athermal solution**. There is no difference between the P-S contact energy and the average energy for the P-P and S-S contacts. In the athermal solution, $\Delta U_{\text{mix}} = \Delta H_{\text{mix}} = 0$ regardless of ϕ . We can regard that the polymer chain is dissolved in a sea of monomer molecules. Note however that, in an actual polymer-solvent system, the monomer before polymerization is chemically different from the repeating unit in the polymer. For instance, an oxyethylene repeating unit ($-\text{CH}_2-\text{CH}_2-\text{O}-$) in poly(ethylene glycol) is different from ethylene oxide or ethylene glycol.

2.2.2 Free Energy, Chemical Potentials, and Osmotic Pressure

2.2.2.1 General Formulas From Eqs. 2.3 and 2.6, the Helmholtz free energy of mixing, $\Delta A_{\text{mix}} = \Delta U_{\text{mix}} - T\Delta S_{\text{mix}}$, per site is given as

$$\frac{\Delta A_{\text{mix}}}{n_{\text{site}}k_{\text{B}}T} = \frac{\phi}{N} \ln \phi + (1 - \phi) \ln(1 - \phi) + \chi \phi(1 - \phi) \quad \text{Flory-Huggins} \quad (2.7)$$

For a total n_{site} sites,

$$\Delta A_{\text{mix}}/(k_{\text{B}}T) = n_{\text{p}} \ln \phi + n_{\text{s}} \ln(1 - \phi) + \chi N n_{\text{p}}(1 - \phi) \quad (2.8)$$

or

$$\Delta A_{\text{mix}}/(k_{\text{B}}T) = n_{\text{p}} \ln \phi + n_{\text{s}} \ln(1 - \phi) + \chi n_{\text{s}} \phi \quad (2.9)$$

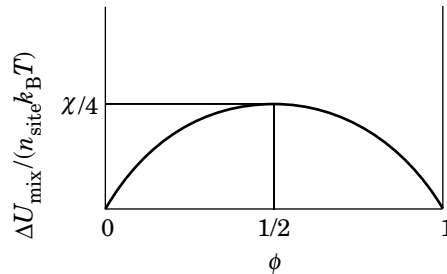


Figure 2.5. Change in the interaction by mixing, $\Delta U_{\text{mix}}/(k_{\text{B}}T n_{\text{site}})$, plotted as a function of polymer volume fraction ϕ . The plot is shown for a positive χ .

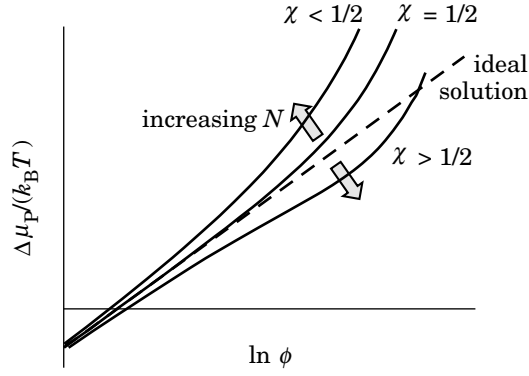


Figure 2.6. Chemical potential $\Delta\mu_P$ of the polymer chain plotted as a function of $\ln\phi$ for the ideal solution (dashed line) and for nonideal solutions of $\chi > 1/2$, $\chi = 1/2$, and $\chi < 1/2$. An increase in N inflates the deviation of the solid lines from the dashed line.

The following identities are useful:

$$\begin{aligned} \left(\frac{\partial \phi}{\partial n_P} \right)_{n_S} &= -\frac{\partial}{\partial n_P} (1 - \phi) = -\frac{\partial}{\partial n_P} \frac{n_S}{Nn_P + n_S} = \frac{Nn_S}{(Nn_P + n_S)^2} \\ &= \frac{1}{n_P} \phi(1 - \phi) = \frac{N}{n_S} (1 - \phi)^2 \end{aligned} \quad (2.10)$$

$$\begin{aligned} \left(\frac{\partial \phi}{\partial n_S} \right)_{n_P} &= \frac{\partial}{\partial n_S} \frac{Nn_P}{Nn_P + n_S} = -\frac{Nn_P}{(Nn_P + n_S)^2} = -\frac{\phi}{n_{\text{site}}} \\ &= -\frac{1}{n_S} \phi(1 - \phi) = -\frac{1}{Nn_P} \phi^2 \end{aligned} \quad (2.11)$$

The chemical potential difference $\Delta\mu_P$ of the polymer chain between the solution and the polymer melt is calculated from Eqs. 2.9 and 2.10 as

$$\frac{\Delta\mu_P}{k_B T} = \left(\frac{\partial}{\partial n_P} \frac{\Delta G_{\text{mix}}}{k_B T} \right)_{T,p,n_S} = \ln\phi - (N-1)(1-\phi) + \chi N(1-\phi)^2 \quad (2.12)$$

where $\Delta G_{\text{mix}} = \Delta A_{\text{mix}}$ was used. Likewise, the chemical potential difference $\Delta\mu_S$ of the solvent molecule between the solution and the pure solvent is calculated from Eqs. 2.8 and 2.11 as

$$\frac{\Delta\mu_S}{k_B T} = \left(\frac{\partial}{\partial n_S} \frac{\Delta G_{\text{mix}}}{k_B T} \right)_{T,p,n_P} = \ln(1-\phi) + \left(1 - \frac{1}{N}\right)\phi + \chi\phi^2 \quad (2.13)$$

Then, with Eq. 2.A.4 ($v^* = v_{\text{site}}$ in the lattice chain model), the osmotic pressure Π is given as

$$\boxed{\frac{\Pi v_{\text{site}}}{k_B T} = \frac{\Pi V}{n_{\text{site}} k_B T} = \frac{\phi}{N} - \ln(1-\phi) - \phi - \chi\phi^2 \quad \text{Flory-Huggins}} \quad (2.14)$$

where $V = v_{\text{site}} n_{\text{site}}$ is the volume of the solution. **Membrane osmometry** and **vapor pressure osmometry** measure the osmotic pressure (Appendix 2.A).

2.2.2.2 Chemical Potential of a Polymer Chain in Solution When $N \gg 1$, Eq. 2.12 is rearranged to

$$\Delta\mu_p/(k_B T) = \ln \phi + N[\chi - 1 + (1 - 2\chi)\phi + \chi\phi^2] \quad \text{Flory–Huggins} \quad (2.15)$$

The first term is the chemical potential of the ideal solution. $N(\chi - 1)$ is just a constant and therefore irrelevant to the further discussion. $N[(1 - 2\chi)\phi + \chi\phi^2]$ represents the nonideal part. Figure 2.6 illustrates how $\Delta\mu_p$ changes with ϕ . At low concentrations, $\Delta\mu_p/k_B T \cong \ln \phi$, and the solution is nearly ideal. As ϕ increases, the nonideal term increases its magnitude. The shape of the plot depends primarily on whether $\chi < 1/2$. When $\chi < 1/2$ on the one hand, the nonideal terms are positive and the plot deviates upward compared with the ideal solution. When $\chi > 1/2$ on the other hand, the leading term in the nonideal part is negative and therefore the plot deviates downward. At higher concentrations, the positive second-order term lets the plot eventually cross the line for the ideal solution. The nonideality minimizes at $\chi = 1/2$.

The deviation from the ideal solution is magnified by N . A small difference of χ from $1/2$ shows up as a large nonideality when N is large. Thus the polymer solutions, especially those of high-molecular-weight polymers, can be easily nonideal. When $\chi > 1/2$, in particular, $N(1 - 2\chi)$ can be easily as large as to cause a dip in the plot of $\Delta\mu_p$.

Equations 2.7, 2.14, and 2.15 serve as a starting point for further discussion of thermodynamics of the polymer solution in the lattice fluid model. Another approach to the thermodynamics based on these equations is given in Appendix 2.B.

The Flory–Huggins theory neglects the chain connectivity, the chain rigidity, and the shape of the monomer. Modifications to the Flory–Huggins theory are possible by taking into account these effects.^{12,13} The chain rigidity can be incorporated by giving preference to straight bonds over angled ones, for instance.

2.2.3 Dilute Solutions

2.2.3.1 Mean-Field Theory In this subsection, we consider dilute solutions. When $\phi \ll 1$, $\ln(1 - \phi) = -\phi - (1/2)\phi^2 - (1/3)\phi^3 - \dots$. Then, Eq. 2.14 is rewritten to

$$\frac{\Pi V}{n_{\text{site}} k_B T} = \frac{\phi}{N} + \left(\frac{1}{2} - \chi\right)\phi^2 + \frac{1}{3}\phi^3 + \dots \quad \text{Flory–Huggins, dilute solution} \quad (2.16)$$

In the low concentration limit, Eq. 2.16 gives the osmotic pressure Π_{ideal} of the ideal solution:

$$\Pi_{\text{ideal}} = \frac{n_{\text{site}}\phi}{NV} k_B T \quad (2.17)$$

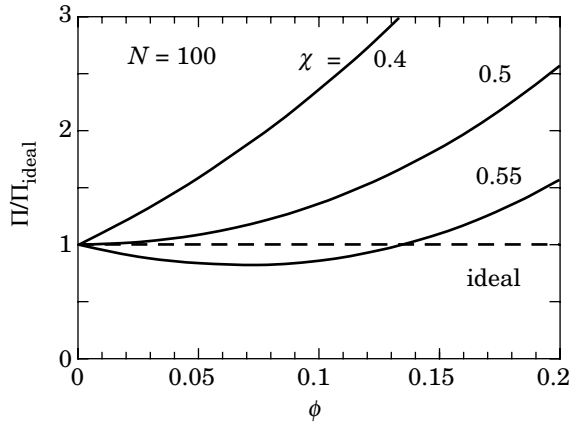


Figure 2.7. Osmotic compressibility (Π/Π_{ideal}) plotted as a function of ϕ for the ideal solution (dashed line) and nonideal solutions with $N = 100$ and $\chi = 0.4, 0.5,$ and 0.55 (solid lines).

Thus the ratio of Π to Π_{ideal} compared at the same concentration is

$$\frac{\Pi}{\Pi_{\text{ideal}}} = 1 + N \left[\left(\frac{1}{2} - \chi \right) \phi + \frac{1}{3} \phi^2 + \dots \right] \quad (2.18)$$

The ratio is often called the **(osmotic) compressibility**.

Figure 2.7 shows Π/Π_{ideal} as a function of ϕ . Three curves with $\chi = 0.4, 0.5,$ and 0.55 are plotted for chains of $N = 100$. The upward or downward deviation of Π from Π_{ideal} depends on whether $\chi < 1/2$. When $\chi = 1/2$, the solution is close to ideal. A small enthalpic penalty ($\chi = 1/2 > 0$; P-S contacts are disfavored) of mixing is compensated by the entropy of mixing, which gives rise to the coefficient $1/2$ in the linear term of Eq. 2.18. When $\chi > 1/2$, the entropy of mixing is not sufficient to offset the increase in the interaction due to unfavorable polymer-solvent contacts. Then, the polymer-polymer contacts are promoted, effectively lowering the osmotic pressure. At higher concentrations, the positive $(N/3)\phi^2$ drives Π above Π_{ideal} . When $\chi < 1/2$, in contrast, the entropy dominates, and $\Pi > \Pi_{\text{ideal}}$ in the entire range of ϕ (Problem 2.6). As χ decreases and turns negative, the polymer-solvent contacts are favored also in terms of the interaction. Then, Π is even greater. It is apparent in Eq. 2.18 that the deviation from Π_{ideal} is magnified by N . The nonideality is large in polymer solutions.

2.2.3.2 Virial Expansion To compare the theory with experiments, Π needs to be expressed in terms of mass concentration c , typically in g/L or mg/L. Using the identity

$$c = \frac{M}{N_A N} \frac{\phi}{v_{\text{site}}} \quad (2.19)$$

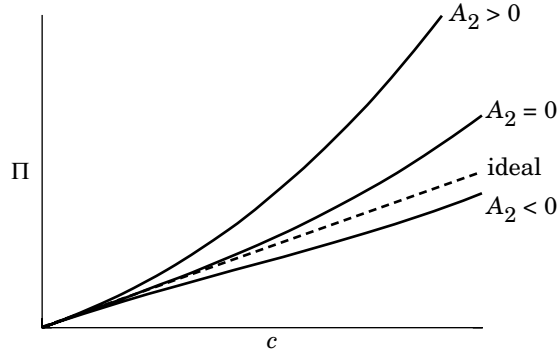


Figure 2.8. Osmotic pressure Π plotted as a function of polymer concentration c for the ideal solution (dashed line) and nonideal solutions with $A_2 > 0$, $= 0$, and < 0 (solid lines).

where $M/(N_A N)$ is the mass of the monomer (not molar mass), $\Pi/(N_A k_B T)$ is, in general, expanded in a power series of c :

$$\boxed{\frac{\Pi}{N_A k_B T} = \frac{c}{M} + A_2 c^2 + A_3 c^3 + \cdots \quad \text{virial expansion}} \quad (2.20)$$

In this **virial expansion**, A_2 is the (osmotic) **second virial coefficient**, and A_3 is the **third virial coefficient**. A positive A_2 deviates Π upward compared with that of the ideal solution ($\Pi_{\text{ideal}}/(N_A k_B T) = c/M$). When $A_2 = 0$, the solution is close to the ideal solution in a wide range of concentrations. Figure 2.8 illustrates how Π deviates from that of the ideal solution, depending on the sign of A_2 . The meanings of A_2 and A_3 will become clearer when we express them in the lattice model by comparing Eqs. 2.18 and 2.20:

$$\boxed{A_2 = \left(\frac{1}{2} - \chi\right) N_A v_{\text{site}} (N/M)^2} \quad (2.21)$$

$$A_3 = \frac{1}{3} (N_A v_{\text{site}})^2 (N/M)^3 \quad (2.22)$$

Table 2.4 summarizes the relationship between A_2 and χ . A_2 is a measure of the nonideality of the solution. $A_2 = 0$ when the entropy of mixing compensates repulsive polymer–solvent interactions or attractive polymer–polymer interactions.

As seen in the expansion of $\Pi/(N_A k_B T) = (c/M)[1 + A_2 M c + A_3 M c^2 + \cdots]$, the magnitude of $A_2 M c$ tells how much thermodynamics of the solution deviates from that of the ideal solution. A solution with a greater $A_2 M$ will develop a

TABLE 2.4 Relationship Between A_2 and χ

A_2	Π	χ
+	$> \Pi_{\text{ideal}}$	$< 1/2$
0	$\cong \Pi_{\text{ideal}}$	$= 1/2$
–	$< \Pi_{\text{ideal}}$	$> 1/2$

nonideality at a lower mass concentration. Separately in Section 1.8, we defined the overlap concentration c^* . We expect that c/c^* gives another measure of the nonideality. It is then natural to expect

$$A_2M \cong \frac{1}{c^*} \quad (2.23)$$

This equality applies to a sufficiently good solvent only in which A_2M dominates over the third term. Because $c^* \cong (M/N_A)/R_g^3$ (Eq. 1.108) and $R_g \cong b(M/M_b)^{\nu}$ with M_b being the molecular weight of the segment, $c^* \cong M_b^{3\nu}/(N_A b^3 M^{3\nu-1})$. With Eq. 2.23, we obtain

$$A_2 \cong \frac{N_A b^3 M^{3\nu-2}}{M_b^{3\nu}} \propto M^{3\nu-2} \quad (2.24)$$

The exponent on M is $-1/5$ or -0.23 . We thus find that A_2 decreases with M , but its dependence is weak. This dependence was verified in experiments.¹⁴

Likewise the virial expansion of Π/Π_{ideal} in terms of ϕ allows us to find the overlap volume fraction ϕ^* as $\phi^* \cong [N(1/2 - \chi)]^{-1}$. This result is, however, wrong. We know that ϕ^* should rather be $\sim N^{-4/5}$ or $\sim N^{-0.77}$ for real chains in a good solvent. Here, we see a shortcoming of the mean-field theory.

2.2.4 Coexistence Curve and Stability

2.2.4.1 Replacement Chemical Potential As χ exceeds $1/2$ and increases further, A_2 becomes negative and its absolute value increases. The unfavorable polymer-solvent interaction can be sufficiently strong to cause the solution to separate into two phases. We will examine the phase diagram of the solution in the mean-field theory for a system of a fixed volume.

In the lattice model, we cannot change n_p and n_s independently. A polymer chain, when added to the system, replaces N solvent molecules, thereby holding the total volume unchanged. It is convenient to introduce a replacement chemical potential $\Delta\mu_{\text{rep}} \equiv \Delta\mu_p - N\Delta\mu_s$. It is the change in the free energy of the solution when the polymer increases its concentration by removing N solvent molecules and placing a polymer chain. From Eqs. 2.12 and 2.13, $\Delta\mu_{\text{rep}}$ is expressed as

$$\frac{\Delta\mu_{\text{rep}}}{k_B T} = \ln\phi + 1 - N - N\ln(1 - \phi) + \chi N(1 - 2\phi) \quad (2.25)$$

This $\Delta\mu_{\text{rep}}$ is also calculated directly from ΔA_{mix} (Eq. 2.7) using

$$\frac{\Delta\mu_{\text{rep}}}{k_B T} = \left(\frac{\partial}{\partial n_p} \frac{\Delta A_{\text{mix}}}{k_B T} \right)_{T,V} = \frac{N}{n_{\text{site}}} \frac{\partial}{\partial \phi} \frac{\Delta A_{\text{mix}}}{k_B T} \quad (2.26)$$

because an increase in n_p (increase in ϕ) implies a decrease in n_s at constant V .

The plot of $\Delta\mu_{\text{rep}}/(k_B T)$ is shown in Figure 2.9 for $N = 100$. The three lines are for $\chi = 0.595$, 0.605 , and 0.615 . When the plot has a dip as for $\chi = 0.615$, the solution can be unstable. In the range of ϕ where the tangent to the plot of $\Delta\mu_{\text{rep}}$ has

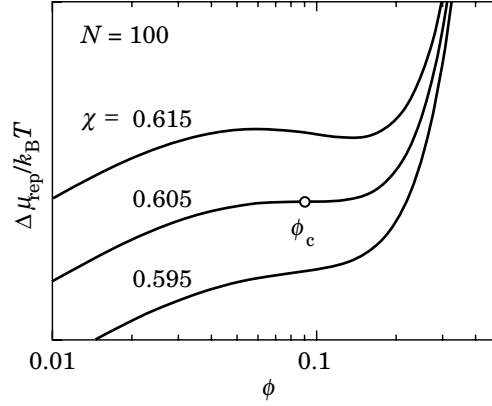


Figure 2.9. Replacement chemical potential $\Delta\mu_{\text{rep}}/(k_B T)$, plotted as a function of ϕ for $N = 100$ and $\chi = 0.595, 0.605,$ and 0.615 . At $\chi = 0.595$, the plot is an increasing function of ϕ . At $\chi = \chi_c = 0.605$, the plot has a stagnant point at $\phi = \phi_c$. At $\chi = 0.615$, the tangent to the plot is negative in $0.060 < \phi < 0.135$.

a negative slope, the solution is unstable; As a polymer chain is brought into the system, its chemical potential drops, thereby promoting further influx of the polymer. This situation is not physical, and, therefore, a negative slope in $\Delta\mu_{\text{rep}}$ indicates instability. In Figure 2.10, the system is stable in the range of a positive slope ($\phi < \phi_A$ or $\phi_B < \phi$ in the figure) and unstable in the other range ($\phi_A < \phi < \phi_B$).

2.2.4.2 Critical Point and Spinodal Line The boundaries to the instability, ϕ_A and ϕ_B , can be found from $\partial\Delta\mu_{\text{rep}}/\partial\phi = 0$. They are the two roots of the quadratic equation in the lattice model:

$$\frac{1}{\phi} + \frac{N}{1-\phi} = 2\chi N \quad (2.27)$$

The instability condition is given as

$$\frac{1}{\phi} + \frac{N}{1-\phi} < 2\chi N \quad (2.28)$$

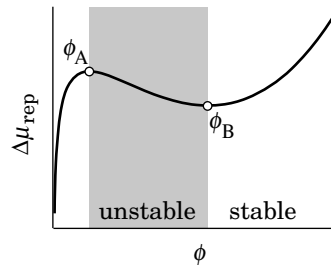


Figure 2.10. The solution is unstable between ϕ_A and ϕ_B , where $\Delta\mu_{\text{rep}}$ decreases on increasing ϕ .

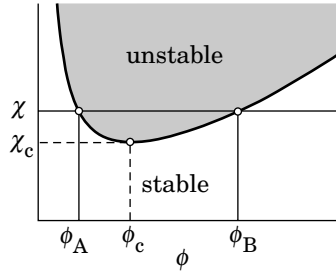


Figure 2.11. Plot of χ at $\partial\Delta\mu_{\text{rep}}/\partial\phi = 0$ as a function of ϕ . The curve minimizes to χ_c at ϕ_c . When $\chi > \chi_c$, the derivative is zero at ϕ_A and ϕ_B . The solution is unstable in the shaded region above the curve and stable in the other region.

The same condition can be obtained from the stability of an open system that allows n_p and n_s to change independently (Problem 2.10).

We can regard Eq. 2.27 as expressing χ at the stability–instability boundary as a function of ϕ . The dependence is indicated by a curve in Figure 2.11. The curve is asymmetric because $N \gg 1$. The unstable region (Inequality 2.28) is indicated by the shaded area. The curve that separates the stable region from the unstable region minimizes to χ_c at $\phi = \phi_c$. This point is called the **critical point**. When $\chi > \chi_c$, Eq. 2.27 has two roots, ϕ_A and ϕ_B , given as the intersections of the curve with the horizontal line at χ , and the plot of $\Delta\mu_{\text{rep}}(\phi)$ has a dip, as seen in the curve of $\chi = 0.615$ in Figure 2.9. When $\chi = \chi_c$, there is only one root: $\phi = \phi_c$. The horizontal is tangential to the curve at $\phi = \phi_c$. The plot of $\Delta\mu_{\text{rep}}(\phi)$ has a stagnant point at $\phi = \phi_c$ indicated by a circle on the curve of $\chi = 0.605$ in Figure 2.9 and has a positive slope everywhere else. When $\chi < \chi_c$, Eq. 2.27 does not have real roots, and $\Delta\mu_{\text{rep}}$ is an increasing function of ϕ in the entire range, as for the curve of $\chi = 0.595$ in Figure 2.9. The solution is stable in the whole range of ϕ . The line that separates the stable region from the unstable region is called the **spinodal line**. It is represented by Eq. 2.27. Table 2.5 summarizes the behavior of $\Delta\mu_{\text{rep}}(\phi)$ and stability of the solution.

2.2.4.3 Phase Separation When $\chi > \chi_c$ and $\phi_A < \phi < \phi_B$, the instability separates the solution spontaneously into two phases with different polymer volume fractions ϕ_1 and ϕ_2 ($\phi_1 < \phi_2$). The latter are determined from the condition that $\Delta\mu_p$ and $\Delta\mu_s$ be the same between the two phases. Both the polymer chain and the solvent molecule are free to leave one of the phases and enter the other phase (dynamic equilibrium). Figure 2.12 shows $\Delta\mu_{\text{rep}}$, $\Delta\mu_p$, and $\Delta\mu_s$ on a common ϕ axis. As proved in Problem 2.10, the region of the negative slope in $\Delta\mu_p$ and the region of the positive slope in $\Delta\mu_s$ (i.e., $(\partial\Delta\mu_s/\partial n_s)_{n_p} < 0$) coincide. Because

TABLE 2.5 χ parameter and stability

χ	$\Delta\mu_{\text{rep}}(\phi)$	Stable	Unstable
$\chi < \chi_c$	always increasing	everywhere	—
$\chi = \chi_c$	stagnant at $\phi = \phi_c$	$\phi \neq \phi_c$	$\phi = \phi_c$
$\chi > \chi_c$	having a dip	$\phi < \phi_A, \phi_B < \phi$	$\phi_A < \phi < \phi_B$

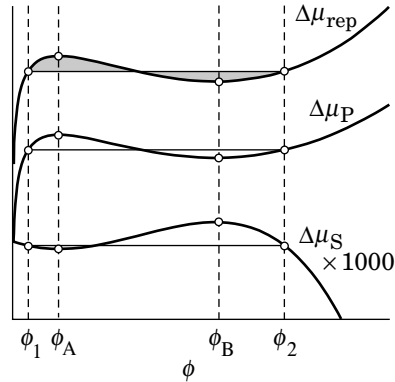


Figure 2.12. Plot of $\Delta\mu_{\text{rep}}$, $\Delta\mu_{\text{p}}$, and $\Delta\mu_{\text{s}} \times 1000$, vertically displaced for easy comparison, when $\Delta\mu_{\text{rep}}$ has a dip. The three curves share ϕ_{A} and ϕ_{B} , which give the local maximum and local minimum of each curve. The two parts in the shaded area have an equal area. The chemical potential is equal between ϕ_1 and ϕ_2 for each of $\Delta\mu_{\text{rep}}$, $\Delta\mu_{\text{p}}$, and $\Delta\mu_{\text{s}}$.

$\Delta\mu_{\text{p}}(\phi_1) = \Delta\mu_{\text{p}}(\phi_2)$ and $\Delta\mu_{\text{s}}(\phi_1) = \Delta\mu_{\text{s}}(\phi_2)$, the two phases have the same $\Delta\mu_{\text{rep}}$. At ϕ_1 and ϕ_2 , replacing N solvent molecules with a polymer chain or the other way around does not change the overall free energy. It can be shown that the average of $\Delta\mu_{\text{rep}}(\phi)$ for ϕ between ϕ_1 and ϕ_2 is equal to $\Delta\mu_{\text{rep}}(\phi_1) = \Delta\mu_{\text{rep}}(\phi_2)$ (Problem 2.11). Therefore, the two shaded parts in Figure 2.12 have an equal area. This situation is the same as the constant-pressure line for the vapor-liquid coexistence in the isothermal process of a single-component system (Maxwell construction). We can find ϕ_1 and ϕ_2 from this equality of the areas. It is, however, easier to find ϕ_1 and ϕ_2 from $\Delta\mu_{\text{p}}(\phi_1) = \Delta\mu_{\text{p}}(\phi_2)$ and $\Delta\mu_{\text{s}}(\phi_1) = \Delta\mu_{\text{s}}(\phi_2)$, although solving these two equations simultaneously requires numerical computation.

When $\chi > \chi_{\text{c}}$ and ϕ is either between ϕ_1 and ϕ_{A} or between ϕ_{B} and ϕ_2 , the solution is still stable ($\partial\Delta\mu_{\text{rep}}/\partial\phi > 0$). The chemical potential of either the polymer chain or the solvent molecule is, however, higher than the counterpart at ϕ_1 and ϕ_2 : In $\phi_1 < \phi < \phi_{\text{A}}$, $\Delta\mu_{\text{p}}(\phi) > \Delta\mu_{\text{p}}(\phi_1) = \Delta\mu_{\text{p}}(\phi_2)$, as seen in Figure 2.12. The polymer chain is ready to move into one of the two phases with ϕ_1 and ϕ_2 , if they exist, to lower its chemical potential. In $\phi_{\text{B}} < \phi < \phi_2$, $\Delta\mu_{\text{s}}(\phi) > \Delta\mu_{\text{s}}(\phi_1) = \Delta\mu_{\text{s}}(\phi_2)$. The solvent molecule is ready to move into one of the two phases. The solution will separate into two phases with ϕ_1 and ϕ_2 if the separation lowers the overall free energy of the system.

Now we examine whether the free energy decreases by the phase separation. For this purpose, we plot in Figure 2.13 the free energy ΔG_{mix} given by Eq. 2.7 with $\Delta G_{\text{mix}} = \Delta A_{\text{mix}}$ as a function of ϕ . We compare ΔG_{mix} for the single-phase solution at ϕ and a two-phase solution with ϕ_1 and ϕ_2 . Equation 2.26 tells that the slope of the curve is essentially $\Delta\mu_{\text{rep}}$. Together with the result of Problem 2.11, we find that the curve has a cotangent line at ϕ_1 and ϕ_2 (Problem 2.12). The inflexion points of the curve are at ϕ_{A} and ϕ_{B} where $\partial\Delta\mu_{\text{rep}}/\partial\phi = 0$ or $\partial^2\Delta G_{\text{mix}}/\partial\phi^2 = 0$. Between ϕ_1 and ϕ_2 , the curve is located higher than the cotangent line.

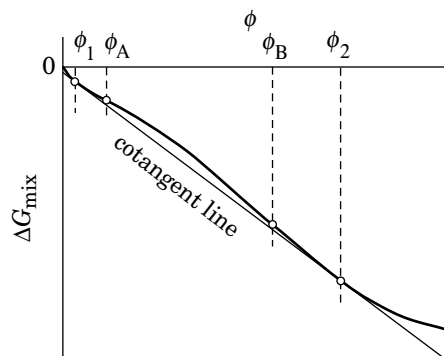


Figure 2.13. Free energy of mixing ΔG_{mix} , plotted as a function of ϕ when $\Delta\mu_{\text{rep}}$ has a dip. The difference between ΔG_{mix} and the cotangent at ϕ_1 and ϕ_2 is magnified.

In the two-phase solution, the volumes V_1 and V_2 of the two phases are determined by the distance of ϕ to ϕ_1 and ϕ_2 (lever rule):

$$\frac{V_1}{V_2} = \frac{\phi_2 - \phi}{\phi - \phi_1} \quad (2.29)$$

When $\phi = \phi_2$, V_1 is zero and the whole solution is in phase 2; When $\phi = \phi_1$, $V_2 = 0$. Adding the polymer to a single-phase solution of ϕ_1 creates a new phase with ϕ_2 . The lever rule requires that the two-phase solution with ϕ in the range of $\phi_1 < \phi < \phi_2$ have ΔG_{mix} on the cotangent line in Figure 2.13 (Problem 2.13). Therefore, the solution in that range, even if it is in the stable region of ϕ , can lower the total free energy by separating into two phases.

The phase separation in the stable region does not occur spontaneously, however. Therefore, we say that the solution with $\phi_1 < \phi < \phi_A$ or $\phi_B < \phi < \phi_2$ is **metastable**. The separation requires an external perturbation, such as stirring or the presence of dust particles. Fortunately, these perturbations are usually present in the solution. Therefore, a solution in the range of $\phi_1 < \phi < \phi_2$ separates into two phases spontaneously or not, as illustrated in Figure 2.14. Many domains in the two-phase solution coalesce into two macroscopic domains.

2.2.4.4 Phase Diagram Figure 2.15 shows the curve for ϕ_1 and ϕ_2 and the curve for ϕ_A and ϕ_B . The figure is essentially the **phase diagram** of the solution in

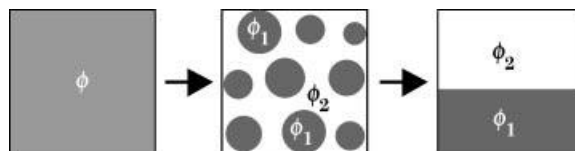


Figure 2.14. Polymer solution with ϕ between ϕ_1 and ϕ_2 separates into two phases with ϕ_1 and ϕ_2 . The multiple domains coalesce into two macroscopic phases.

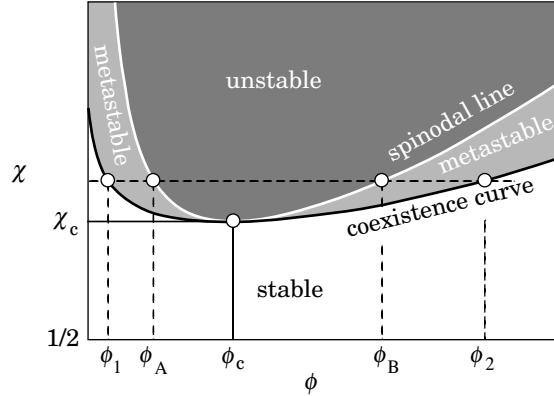


Figure 2.15. Spinodal line and the coexistence curve in the mean-field theory. The solution is unstable in the darkly shaded region, metastable in lightly shaded region, and stable in the other region.

the Flory–Huggins mean–field theory. The two curves share the apex at ϕ_c and χ_c . The lower curve for ϕ_1 and ϕ_2 demarcates the **single-phase regime** from the **two-phase regime** and therefore is called the **coexistence curve** (or a **binodal line**). The upper curve (spinodal line) is for ϕ_A and ϕ_B . Above the spinodal line, the system is unstable and spontaneously separates into two phases. Above the coexistence curve, the phase-separated state is thermodynamically more stable than the single-phase state is. Solutions in the two regions between the two curves are metastable.

A solution with $\chi < \chi_c$ is in a single phase in the entire range of concentrations. When $\chi > \chi_c$, the solution has a **miscibility gap**. Usually we cannot prepare a single-phase solution with ϕ between ϕ_1 and ϕ_2 . The phase with ϕ_1 is a solution saturated with the polymer (the concentration of polymer cannot be higher), and the phase with ϕ_2 is a solution saturated with the solvent (the concentration of solvent cannot be higher).

Now we look at how χ_c and ϕ_c change with N . From Eq. 2.27 and $\partial\chi/\partial\phi = 0$, we obtain

$$\chi_c = \frac{(1 + N^{1/2})^2}{2N} \cong \frac{1}{2} + N^{-1/2} \quad (2.30)$$

at

$$\phi_c = \frac{1}{1 + N^{1/2}} \cong N^{-1/2} \quad (2.31)$$

Figure 2.16 shows how χ_c approaches $1/2$ with an increasing N and how ϕ_c approaches zero. Both of them decrease in $N^{-1/2}$.

Solid lines in Figure 2.17a are the spinodal lines for $N = 32, 100, 316,$ and $1,000$. The critical point on each spinodal line is on the curve given by $\chi_c = 1/[2(1 - \phi_c)^2]$

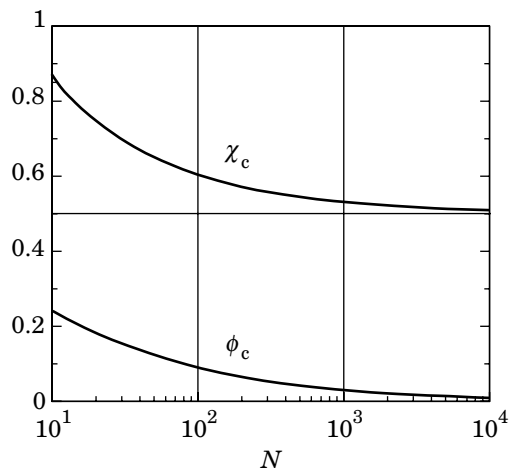


Figure 2.16. As N increases, χ_c approaches $1/2$, and ϕ_c decreases to zero.

(dashed line). As N increases, the spinodal line approaches the ordinate and the horizontal at $\chi = 1/2$. Figure 2.17b shows corresponding coexistence curves. Both the spinodal lines and the coexistence curves are skewed toward $\phi_c \ll 1$ because $N \gg 1$. For $N = 1$ (mixture of two small-molecule liquids), $\phi_c = 1/2$ and $\chi_c = 2$. The spinodal line and the coexistence curve are symmetric with respect to $\phi_c = 1/2$.

The **theta condition** refers to the critical condition in the long-chain limit, $N \rightarrow \infty$. A solvent that gives the theta condition to a given polymer is called a **theta solvent**. In the mean-field theory, a solvent that provides the polymer with $\chi = 1/2$ is the theta solvent. In general, theta condition is determined from $A_2 = 0$ (see

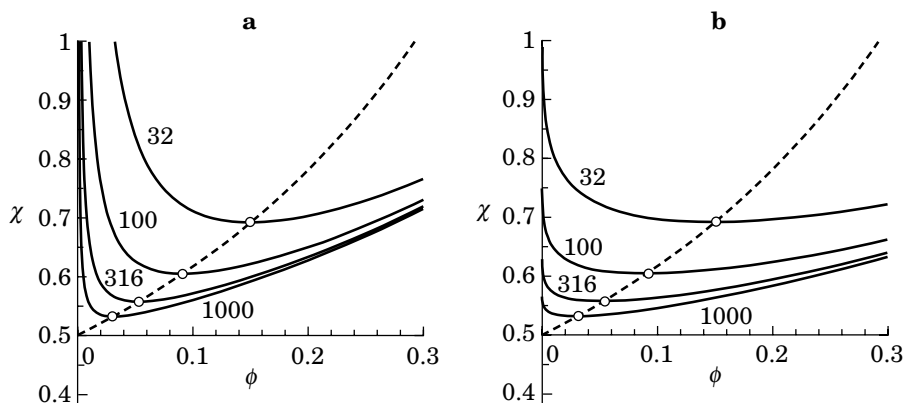


Figure 2.17. Spinodal lines (a) and coexistence curves (b) for $N = 32, 100, 316,$ and $1,000$. The open circles indicate the critical point for each N . It approaches $\chi = 1/2$ and $\phi = 0$ along the dashed line as N increases.

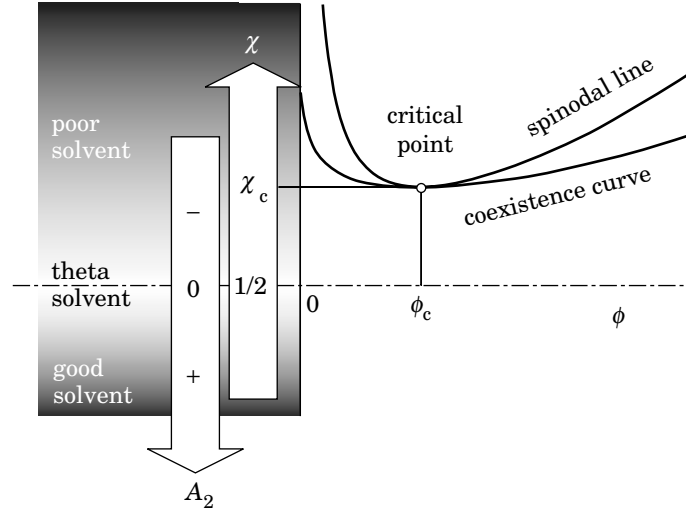


Figure 2.18. Good solvent ($A_2 > 0$, $\chi < 1/2$), theta solvent ($A_2 = 0$, $\chi = 1/2$), and poor solvent ($A_2 < 0$, $\chi > 1/2$).

Eq. 2.21). When it has a molecular weight dependence, its high molecular weight limit gives the theta condition. In the mean-field theory, the condition is independent of the molecular weight.

A solvent with χ sufficiently smaller than $1/2$ (A_2 is positive and sufficiently large), including negative χ , is called a **good solvent**. A solvent with $\chi > 1/2$ ($A_2 < 0$) is called a **poor solvent**. As χ increases, the solvent becomes unable to dissolve the polymer. Then, it is called a **nonsolvent**. Figure 2.18 illustrates the ranges of these solvents together with the phase diagram. Along the horizontal line of $\chi = 1/2$, $A_2 = 0$. Note that, in the theta solvent, polymer chains with a finite length (all polymers have a finite length) are still dissolved in the solvent in the entire range of concentrations. For a polymer solution to separate into two phases, A_2 has to be sufficiently negative, especially when its molecular weight is low.

2.2.5 Polydisperse Polymer

Almost all the polymer is polydisperse. We consider here the osmotic pressure of the solution of a polydisperse polymer.

Before mixing the polymer with the solvent, the polymer is already a mixture consisting of n_i chains of N_i beads for component i . This mixture is further mixed with n_s solvent molecules. The entropy of mixing of the polydisperse polymer with n_s solvent molecules is obtained as

$$-\Delta S_{\text{mix}}/(k_B n_{\text{site}}) = \sum_i \frac{\phi_i}{N_i} \ln \phi_i + (1 - \phi) \ln(1 - \phi) \quad (2.32)$$

where $\phi_i = n_i N_i / n_{\text{site}}$, $\phi = \sum_i \phi_i$ (the sum is with respect to i), and $n_{\text{site}} = n_s + \sum_i (n_i N_i)$. The energy of mixing is the same; we can naturally assume that P–P interactions are the same between chains of different lengths. Then, the free energy of mixing per site is

$$\Delta A_{\text{mix}} / (n_{\text{site}} k_B T) = \sum_i \frac{\phi_i}{N_i} \ln \phi_i + (1 - \phi) \ln(1 - \phi) + \chi \phi (1 - \phi) \text{ polydisperse} \quad (2.33)$$

Following the method we used in Section 2.2.2, the chemical potential of the solvent molecule, $\Delta \mu_s$, is calculated, from which we obtain the osmotic pressure (Problem 2.14):

$$\frac{\Pi V}{n_{\text{site}} k_B T} = \sum_i \frac{\phi_i}{N_i} - \ln(1 - \phi) - \phi - \chi \phi^2 \text{ polydisperse} \quad (2.34)$$

In the dilute solution limit, the solution is ideal:

$$\frac{\Pi_{\text{ideal}} V}{n_{\text{site}} k_B T} = \sum_i \frac{\phi_i}{N_i} \quad (2.35)$$

It is now apparent that the osmotic pressure counts the total number of polymer chains. Colligative properties such as the osmotic pressure give, in general, a measure for the number of independently moving species per unit volume of the solution.

If we force the ideal solution of the polydisperse polymer to have the osmotic pressure of a solution of a monodisperse polymer consisting of $\langle N \rangle$ beads dissolved at volume fraction ϕ , then

$$\sum_i \frac{\phi_i}{N_i} = \frac{\phi}{\langle N \rangle} \quad (2.36)$$

which leads to

$$\langle N \rangle = \frac{\sum_i \phi_i}{\sum_i \phi_i / N_i} = \frac{\sum_i N_i n_i}{\sum_i n_i} \quad (2.37)$$

Thus we find that $\langle N \rangle$ is the number average of N_i . The molecular weight estimated from the measurement of the osmotic pressure and Eq. 2.20 in the dilute solution limit is therefore the number-average molecular weight.

In Eq. 2.35, the nonideal terms depend on ϕ only. Then polydispersity affects the ideal solution part, but not the nonideal part, in the Flory–Huggins mean–field theory.

2.2.6 PROBLEMS

Problem 2.1: Calculate the entropy of mixing $\Delta S_{\text{mix,id}}$ for an ideal solution that consists of $n_p = n_{\text{site}}\phi/N$ solute molecules and $n_s = n_{\text{site}}(1 - \phi)$ solvent molecules. Compare it with ΔS_{mix} given by Eq. 2.3. [Note: the entropy of mixing for a rigid-chain polymer and a solvent is given approximately by $\Delta S_{\text{mix,id}}$, because dissolution does not provide the polymer molecule with an additional freedom in the conformation compared with the state without solvent, except for the orientational freedom. The latter is negligible compared with the freedom a flexible chain would acquire when mixed with solvent molecules.]

Solution 2.1: The entropy of mixing is given as

$$-\Delta S_{\text{mix,id}}/k_B = n_p \ln x_p + n_s \ln x_s = (n_{\text{site}}\phi/N) \ln x_p + n_{\text{site}}(1 - \phi) \ln x_s$$

where $x_p = (\phi/N)/(1 - \phi + \phi/N)$ and $x_s = (1 - \phi)/(1 - \phi + \phi/N)$ are the mole fractions of the polymer and solvent, respectively. Then,

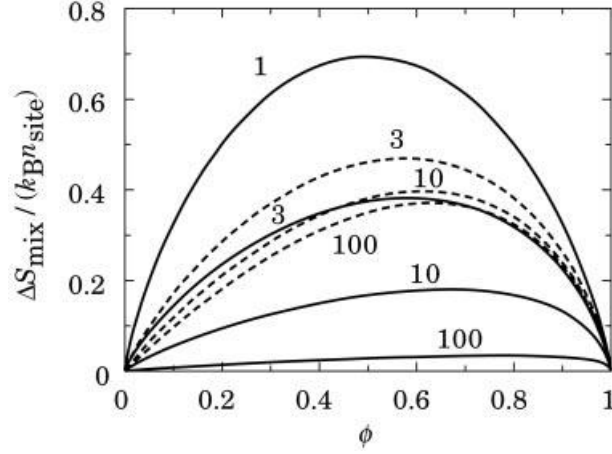
$$\begin{aligned} -\Delta S_{\text{mix,id}}/(k_B n_{\text{site}}) &= \frac{\phi}{N} \ln \frac{\phi/N}{1 - \phi + \phi/N} \\ &\quad + (1 - \phi) \ln \frac{1 - \phi}{1 - \phi + \phi/N} \\ &= (\phi/N) \ln(\phi/N) + (1 - \phi) \ln(1 - \phi) \\ &\quad - (1 - \phi + \phi/N) \ln(1 - \phi + \phi/N) \\ &= (\phi/N) \ln \phi + (1 - \phi) \ln(1 - \phi) - (\phi/N) \ln N \\ &\quad - (1 - \phi + \phi/N) \ln(1 - \phi + \phi/N) \end{aligned}$$

With Eq. 2.3,

$$\begin{aligned} \Delta S_{\text{mix,id}}/(k_B n_{\text{site}}) &= \Delta S_{\text{mix}}/(k_B n_{\text{site}}) + (\phi/N) \ln N \\ &\quad + (1 - \phi + \phi/N) \ln(1 - \phi + \phi/N) \end{aligned}$$

Let $F(x) \equiv x \ln(\phi/x) + (1 - \phi + x) \ln(1 - \phi + x)$, where $x \equiv \phi/N$ ranges between 0 ($N = \infty$) and ϕ ($N = 1$). Simple algebra shows that $dF/dx = \ln[\phi/(x(1 - \phi + x))]$ is always positive. Then, with $F(\phi) = 0$, $F(x) < 0$ for all $0 < x < \phi$. Therefore, $\Delta S_{\text{mix,id}} < \Delta S_{\text{mix}}$.

Solid lines in the figure below show the plot of $\Delta S_{\text{mix,id}}$ for $N = 1, 3, 10$, and 100. Dashed lines are ΔS_{mix} for $N = 1, 3, 10$, and 100. For $N = 1$, $\Delta S_{\text{mix,id}} = \Delta S_{\text{mix}}$. For the other values of N , $\Delta S_{\text{mix,id}}$ is smaller compared with ΔS_{mix} . As N increases, the plot of $\Delta S_{\text{mix,id}}$ approaches zero in the entire range of ϕ . In contrast, ΔS_{mix} for flexible chains remains finite in the limit of $N \rightarrow \infty$. For the rodlike molecule with a large N to dissolve (to make ΔA_{mix} negative), ΔH_{mix} must be negative.



Problem 2.2: We used Table 2.3 to calculate ΔU_{mix} of a homopolymer with a solvent. Use the same method to show that Eq. 2.6 holds for a binary solution of an A–B copolymer (its volume fraction is ϕ) and a solvent S in the mean-field approximation with the effective χ parameter given as $x_a\chi_{as} + x_b\chi_{bs} - x_ax_b\chi_{ab}$. Here x_a and x_b are the mole fractions of monomers A and B in the copolymer ($x_a + x_b = 1$), respectively, χ_{js} is the χ parameter for a binary solution of a homopolymer of j and solvent S, and χ_{ab} is the χ parameter for a binary mixture of the two homopolymers.

Solution 2.2:

Probability of Nearest-Neighbor Contacts

Contact	Energy	Probability before mixing	Probability after mixing
A–A	ε_{aa}	ϕx_a^2	$\phi^2 x_a^2$
A–B	ε_{ab}	$2\phi x_a x_b$	$2\phi^2 x_a x_b$
B–B	ε_{bb}	ϕx_b^2	$\phi^2 x_b^2$
A–S	ε_{as}	0	$2\phi(1 - \phi)x_a$
B–S	ε_{bs}	0	$2\phi(1 - \phi)x_b$
S–S	ε_{ss}	$1 - \phi$	$(1 - \phi)^2$

The change in the average energy per bond is

$$\begin{aligned}
 & \varepsilon_{aa}(\phi^2 - \phi)x_a^2 + \varepsilon_{ab}(\phi^2 - \phi)2x_ax_b + \varepsilon_{bb}(\phi^2 - \phi)x_b^2 \\
 & + \varepsilon_{as}2\phi(1 - \phi)x_a + \varepsilon_{bs}2\phi(1 - \phi)x_b + \varepsilon_{ss}[(1 - \phi)^2 - (1 - \phi)] \\
 & = \phi(1 - \phi)[x_a(2\varepsilon_{as} - \varepsilon_{aa} - \varepsilon_{ss}) + x_b(2\varepsilon_{bs} - \varepsilon_{bb} - \varepsilon_{ss}) \\
 & - x_ax_b(2\varepsilon_{ab} - \varepsilon_{aa} - \varepsilon_{bb})]
 \end{aligned}$$

Then,

$$\begin{aligned}\Delta U_{\text{mix}} = & \frac{Zn_{\text{site}}}{2}\phi(1-\phi)[x_a(2\varepsilon_{\text{as}} - \varepsilon_{\text{aa}} - \varepsilon_{\text{ss}}) \\ & + x_b(2\varepsilon_{\text{bs}} - \varepsilon_{\text{bb}} - \varepsilon_{\text{ss}}) - x_ax_b(2\varepsilon_{\text{ab}} - \varepsilon_{\text{aa}} - \varepsilon_{\text{bb}})]\end{aligned}$$

In terms of χ parameter,

$$\frac{\Delta U_{\text{mix}}}{n_{\text{site}}k_{\text{B}}T} = \phi(1-\phi)(x_a\chi_{\text{as}} + x_b\chi_{\text{bs}} - x_ax_b\chi_{\text{ab}})$$

Comparison with Eq. 2.6 leads to $\chi = x_a\chi_{\text{as}} + x_b\chi_{\text{bs}} - x_ax_b\chi_{\text{ab}}$.

Problem 2.3: Verify that Eq. 2.7 with $\Delta A_{\text{mix}} = \Delta G_{\text{mix}}$ and Eqs. 2.12 and 2.13 satisfy $\Delta G_{\text{mix}} = n_{\text{p}}\Delta\mu_{\text{p}} + n_{\text{s}}\Delta\mu_{\text{s}}$.

Solution 2.3:

$$\begin{aligned}\frac{n_{\text{p}}\Delta\mu_{\text{p}} + n_{\text{s}}\Delta\mu_{\text{s}}}{k_{\text{B}}T} &= n_{\text{p}}[\ln\phi - (N-1)(1-\phi) + \chi N(1-\phi)^2] \\ &+ n_{\text{s}}[\ln(1-\phi) + (1-1/N)\phi + \chi\phi^2] \\ &= n_{\text{site}}\left[\frac{\phi}{N}(\ln\phi - (N-1)(1-\phi) + \chi N(1-\phi)^2) \right. \\ &\quad \left. + (1-\phi)(\ln(1-\phi) + (1-1/N)\phi + \chi\phi^2)\right] \\ &= n_{\text{site}}\left[\frac{\phi}{N}\ln\phi + (1-\phi)\ln(1-\phi) + \chi\phi(1-\phi)\right]\end{aligned}$$

Problem 2.4: The osmotic pressure of the polymer solution can also be obtained by using the formula (see Appendix 2.B):

$$\frac{\Pi}{k_{\text{B}}T} = -\left(\frac{\partial}{\partial V}\frac{\Delta A_{\text{mix}}}{k_{\text{B}}T}\right)_{T,n_{\text{p}}} = -\frac{1}{v_{\text{site}}}\left(\frac{\partial}{\partial n_{\text{site}}}\frac{\Delta A_{\text{mix}}}{k_{\text{B}}T}\right)_{T,n_{\text{p}}}$$

Use the identity $\partial/\partial n_{\text{site}} = -(\phi/n_{\text{site}})\partial/\partial\phi$ that applies to changes at a fixed number of solute molecules to derive Eq. 2.14.

Solution 2.4: Use Eq. 2.7. At a fixed n_{p} ,

$$\frac{\Pi}{k_{\text{B}}T} = -\frac{1}{v_{\text{site}}}\left(-\frac{\phi}{n_{\text{site}}}\right)\frac{\partial}{\partial\phi}\frac{n_{\text{p}}N}{\phi}\frac{\Delta A_{\text{mix}}}{n_{\text{site}}k_{\text{B}}T} = \frac{\phi^2}{v_{\text{site}}}\frac{\partial}{\partial\phi}\frac{1}{\phi}\frac{\Delta A_{\text{mix}}}{n_{\text{site}}k_{\text{B}}T}$$

$$\begin{aligned}
&= \frac{\phi^2}{v_{\text{site}}} \frac{\partial}{\partial \phi} \left[\frac{1}{N} \ln \phi + (\phi^{-1} - 1) \ln(1 - \phi) + \chi(1 - \phi) \right] \\
&= \frac{1}{v_{\text{site}}} \left[\frac{\phi}{N} - \ln(1 - \phi) - \phi - \chi\phi^2 \right]
\end{aligned}$$

Problem 2.5: Show that $\Delta A_{\text{mix}} + \Pi V(1 - \phi) = n_p \Delta \mu_p$. The left-hand side is the Gibbs free energy change in the process that “vaporizes” the polymer in the condensed amorphous state into a total volume of V ($\Delta V_{\text{mix}} = V(1 - \phi)$).

Solution 2.5: From Eqs. 2.7 and 2.14,

$$\begin{aligned}
\frac{\Delta A_{\text{mix}} + \Pi V(1 - \phi)}{n_{\text{site}} k_B T} &= \frac{\phi}{N} \ln \phi + (1 - \phi) \ln(1 - \phi) + \chi \phi(1 - \phi) \\
&\quad + (1 - \phi) \left[\frac{\phi}{N} - \ln(1 - \phi) - \phi - \chi\phi^2 \right] \\
&= \frac{\phi}{N} \left[\ln \phi - (N - 1)(1 - \phi) \right. \\
&\quad \left. + \chi N(1 - \phi)^2 \right] = \frac{n_p \Delta \mu_p}{n_{\text{site}} k_B T}
\end{aligned}$$

In the last equality, Eq. 2.12 was used.

Problem 2.6: Equation 2.18 tells that $\Pi > \Pi_{\text{ideal}}$ when $\chi < 1/2$ in the dilute solution ($\phi \ll 1$). Use Eq. 2.14 to verify that it is also the case in the whole range of ϕ .

Solution 2.6: From Eq. 2.14,

$$\frac{(\Pi - \Pi_{\text{ideal}})V}{n_{\text{site}} k_B T} = -\ln(1 - \phi) - \phi - \chi\phi^2 \equiv f(\phi)$$

Since $f(0) = 0$ and

$$\frac{df}{d\phi} = \frac{1}{1 - \phi} - 1 - 2\chi\phi = \frac{\phi[1 - 2\chi(1 - \phi)]}{1 - \phi} > 0$$

in the whole range of ϕ when $\chi < 1/2$, we find that $f(\phi) > 0$ for $0 \leq \phi < 1$.

Problem 2.7: What is the free energy of mixing that corresponds to the virial expansion of the osmotic pressure given by Eq. 2.20? Also show that the ΔA_{mix} you obtained reproduces Eq. 2.7 with A_2 and A_3 given by Eqs. 2.21 and 2.22.

Solution 2.7: At a constant cV , that is, at a constant n_p ,

$$\frac{\Pi}{k_B T} = - \left(\frac{\partial}{\partial V} \frac{\Delta A_{\text{mix}}}{k_B T} \right)_{T,cV} = \frac{c}{V} \left(\frac{\partial}{\partial c} \frac{\Delta A_{\text{mix}}}{k_B T} \right)_{T,cV}$$

With Eq. 2.20,

$$\left(\frac{\partial}{\partial c} \frac{\Delta A_{\text{mix}}}{k_B T} \right)_{T,cV} = \frac{V}{c} \frac{\Pi}{k_B T} = N_A c V \left(\frac{1}{cM} + A_2 + A_3 c + \dots \right)$$

Integration with respect to c at constant cV yields

$$\frac{\Delta A_{\text{mix}}}{k_B T} = N_A c V \left(\text{const.} + \frac{1}{M} \ln c + A_2 c + \frac{1}{2} A_3 c^2 + \dots \right)$$

With Eqs. 2.19, 2.21, and 2.22, and neglecting the constant terms,

$$\frac{\Delta A_{\text{mix}}}{n_{\text{site}} k_B T} = \frac{\phi}{N} \ln \phi + \left(\frac{1}{2} - \chi \right) \phi^2 + \frac{1}{6} \phi^3 + \dots$$

Equation 2.7 is expanded with respect to ϕ as

$$\begin{aligned} \frac{\Delta A_{\text{mix}}}{n_{\text{site}} k_B T} &= \frac{\phi}{N} \ln \phi + (1 - \phi) \left(-\phi - \frac{1}{2} \phi^2 - \frac{1}{3} \phi^3 - \dots \right) + \chi \phi (1 - \phi) \\ &= \frac{\phi}{N} \ln \phi + (\chi - 1) \phi + \left(\frac{1}{2} - \chi \right) \phi^2 + \frac{1}{6} \phi^3 + \dots \end{aligned}$$

The above two equations are identical except for the linear term that becomes a constant term upon differentiation.

Problem 2.8: Show that $A_2 M = \left(\frac{1}{2} - \chi \right) N v_{\text{sp}}$ and $A_3 M = \frac{1}{3} N v_{\text{sp}}^2$ in the lattice chain model, where v_{sp} is the specific volume of the polymer in solution.

Solution 2.8: From Eq. 2.21,

$$A_2 M = \left(\frac{1}{2} - \chi \right) \frac{N_A v_{\text{site}} N}{M} N$$

where $N_A v_{\text{site}} N$ is the molar volume of the polymer chain, and M is the molar mass of the polymer. The ratio, $N_A v_{\text{site}} N / M$, is the reciprocal of the density of the polymer. In the solution, it is the specific volume (v_{sp}), that is, the increment in the solution volume when a unit mass of the polymer is added.

Likewise,

$$A_3M = \frac{1}{3} \frac{(N_A v_{\text{site}} N)^2}{M^2} N = \frac{1}{3} N v_{\text{sp}}^2$$

Problem 2.9: Use the Gibbs-Duhem theorem

$$n_p d\Delta\mu_p + n_s d\Delta\mu_s = 0$$

to find $\Delta\mu_p$ for the virial expansion of Π given by Eq. 2.20.

Solution 2.9: The Gibbs-Duhem theorem is rewritten to

$$n_p \frac{d\Delta\mu_p}{dc} + n_s \frac{d\Delta\mu_s}{dc} = 0$$

From Eq. 2.A.4,

$$\frac{\Delta\mu_s}{k_B T} = -N_A v^* \left(\frac{c}{M} + A_2 c^2 + A_3 c^3 + \dots \right)$$

Combining the two equations yields

$$\frac{d}{dc} \frac{\Delta\mu_p}{k_B T} = \frac{n_s v^*}{n_p M / N_A} (1 + 2A_2 M c + 3A_3 M c^2 + \dots)$$

Here, $n_s v^* / (n_p M / N_A)$ is the ratio of the total volume of the solvent to the total mass of the polymer. Assuming that the volume V of the solution is given by

$$V = n_s v^* + (n_p M / N_A) v_{\text{sp}}$$

with v_{sp} being the specific volume of the polymer in solution (see Problem 2.8), we find

$$\frac{n_s v^*}{n_p M / N_A} = \frac{1}{c} - v_{\text{sp}}$$

where $c = (n_p M / N_A) / V$ is the mass concentration of the polymer. Thus,

$$\frac{d}{dc} \frac{\Delta\mu_p}{k_B T} = \frac{1}{c} + (2A_2 M - v_{\text{sp}}) + (3A_3 M - 2A_2 M v_{\text{sp}})c + \dots$$

Upon integration,

$$\frac{\Delta\mu_p}{k_B T} = \ln c + (2A_2 M - v_{\text{sp}})c + (3A_3 M / 2 - A_2 M v_{\text{sp}})c^2 + \dots$$

Problem 2.10: For a lattice fluid system that allows n_p and n_s to change independently (total volume is not fixed),

$$\frac{\partial \Delta \mu_p}{\partial n_p} = 0 \quad \text{and} \quad \frac{\partial \Delta \mu_p}{\partial n_p} \frac{\partial \Delta \mu_s}{\partial n_s} = \frac{\partial \Delta \mu_p}{\partial n_s} \frac{\partial \Delta \mu_s}{\partial n_p}$$

gives the boundary of the stable state. Show that this condition is equivalent to Eq. 2.27. Show also that $\partial \Delta \mu_p / \partial n_p$ and $\partial \Delta \mu_s / \partial n_s$ share the sign.

Solution 2.10: Because

$$\frac{\partial \Delta \mu_p}{\partial n_p} = \frac{\partial \Delta \mu_p}{\partial \phi} \frac{\partial \phi}{\partial n_p}, \text{ etc.}$$

the second part of the condition always holds when the first part holds. From Eq. 2.12, the first part is calculated as

$$\frac{\partial(\Delta \mu_p / k_B T)}{\partial n_p} = \frac{\partial \phi}{\partial n_p} \left[\frac{1}{\phi} + (N - 1) - 2\chi N(1 - \phi) \right] = 0$$

Rearrangement gives Eq. 2.27. Likewise,

$$\frac{\partial(\Delta \mu_s / k_B T)}{\partial n_s} = \frac{\partial \phi}{\partial n_s} \left[-\frac{1}{1 - \phi} + 1 - \frac{1}{N} + 2\chi \phi \right] = 0$$

is equivalent to Eq. 2.27.

Comparison of the above two equations yields

$$\frac{\partial(\Delta \mu_p / k_B T)}{\partial n_p} \bigg/ \frac{\partial \phi}{\partial n_p} = -\frac{N(1 - \phi)}{\phi} \frac{\partial(\Delta \mu_s / k_B T)}{\partial n_s} \bigg/ \frac{\partial \phi}{\partial n_s}$$

Because $\partial \phi / \partial n_p$ and $\partial \phi / \partial n_s$ have the opposite sign, $\partial \Delta \mu_p / \partial n_p$ and $\partial \Delta \mu_s / \partial n_s$ have the same sign.

Problem 2.11: Use Gibbs-Duhem equation (in Problem 2.9) to show that

$$\int_{\phi_1}^{\phi_2} \Delta \mu_{\text{rep}}(\phi) d\phi = (\phi_2 - \phi_1) \Delta \mu_{\text{rep}}(\phi_1)$$

where $\Delta \mu_p(\phi_1) = \Delta \mu_p(\phi_2)$ and $\Delta \mu_s(\phi_1) = \Delta \mu_s(\phi_2)$.

Solution 2.11: The Gibbs-Duhem equation

$$\frac{\phi}{N} \frac{\partial \Delta \mu_p}{\partial \phi} + (1 - \phi) \frac{\partial \Delta \mu_s}{\partial \phi} = 0$$

leads to

$$\phi \frac{\partial \Delta \mu_{\text{rep}}}{\partial \phi} = -N \frac{\partial \Delta \mu_{\text{S}}}{\partial \phi}$$

Using integral by parts,

$$\begin{aligned} \int_{\phi_1}^{\phi_2} \Delta \mu_{\text{rep}} d\phi &= \left[\phi \Delta \mu_{\text{rep}} \right]_{\phi_1}^{\phi_2} - \int_{\phi_1}^{\phi_2} \phi \frac{\partial \Delta \mu_{\text{rep}}}{\partial \phi} d\phi \\ &= (\phi_2 - \phi_1) \Delta \mu_{\text{rep}}(\phi_1) + N \int_{\phi_1}^{\phi_2} \frac{\partial \Delta \mu_{\text{S}}}{\partial \phi} d\phi = (\phi_2 - \phi_1) \Delta \mu_{\text{rep}}(\phi_1) \end{aligned}$$

Problem 2.12: Use the result of Problem 2.11 to show that the plot of ΔG_{mix} has a cotangent line at ϕ_1 and ϕ_2 (see Fig. 2.13).

Solution 2.12: The slope of the line that connects the two points on $\Delta G_{\text{mix}}/(n_{\text{site}} k_{\text{B}} T)$ at ϕ_1 and ϕ_2 is

$$\begin{aligned} \frac{[\Delta G_{\text{mix}}(\phi_2) - \Delta G_{\text{mix}}(\phi_1)]/(n_{\text{site}} k_{\text{B}} T)}{\phi_2 - \phi_1} &= \frac{1}{\phi_2 - \phi_1} \frac{1}{N} \int_{\phi_1}^{\phi_2} \frac{\Delta \mu_{\text{rep}}(\phi)}{k_{\text{B}} T} d\phi \\ &= \frac{1}{N} \frac{\Delta \mu_{\text{rep}}(\phi_1)}{k_{\text{B}} T} = \frac{1}{N} \frac{\Delta \mu_{\text{rep}}(\phi_2)}{k_{\text{B}} T} \end{aligned}$$

where Eq. 2.26 and the result of Problem 2.11 were used. The last part of the above equation is the slope of the $\Delta G_{\text{mix}}/(n_{\text{site}} k_{\text{B}} T)$ at ϕ_1 and ϕ_2 according to Eq. 2.26.

Problem 2.13: Use the lever rule to show that the two-phase solution has its ΔG_{mix} on the cotangent line (see Fig. 2.13).

Solution 2.13: From Eq. 2.29, the total free energy of the two-phase solution is given as

$$\begin{aligned} \frac{V_1}{v_{\text{site}}} \frac{\Delta G_{\text{mix}}(\phi_1)}{n_{\text{site}}} + \frac{V_2}{v_{\text{site}}} \frac{\Delta G_{\text{mix}}(\phi_2)}{n_{\text{site}}} &= \frac{V_1 + V_2}{v_{\text{site}} n_{\text{site}}} \\ &\left(\frac{\phi_2 - \phi}{\phi_2 - \phi_1} \Delta G_{\text{mix}}(\phi_1) + \frac{\phi - \phi_1}{\phi_2 - \phi_1} \Delta G_{\text{mix}}(\phi_2) \right) \end{aligned}$$

which represents a straight line through the two points $[\phi_1, \Delta G_{\text{mix}}(\phi_1)]$ and $[\phi_2, \Delta G_{\text{mix}}(\phi_2)]$ in the figure.

Problem 2.14: Derive Eq. 2.34 from Eq. 2.33.

Solution 2.14: For a total n_{site} sites,

$$\Delta A_{\text{mix}}/(k_{\text{B}}T) = \sum_i n_i \ln \phi_i + n_{\text{S}} \ln(1 - \phi) + \chi(1 - \phi) \sum_i N_i n_i$$

Using the identities

$$\left(\frac{\partial \phi}{\partial n_{\text{S}}} \right)_{n_i} = - \frac{\phi}{n_{\text{site}}}, \quad \left(\frac{\partial \phi_j}{\partial n_{\text{S}}} \right)_{n_i \neq j} = - \frac{\phi_j}{n_{\text{site}}}$$

the chemical potential of the solvent molecule is calculated as

$$\begin{aligned} \frac{\Delta \mu_{\text{S}}}{k_{\text{B}}T} &= \left(\frac{\partial}{\partial n_{\text{S}}} \frac{\Delta G_{\text{mix}}}{k_{\text{B}}T} \right)_{T,p,n_i} = \sum_i n_i \frac{1}{\phi_i} \frac{\partial \phi_i}{\partial n_{\text{S}}} + \ln(1 - \phi) \\ &\quad - n_{\text{S}} \frac{\partial \phi}{\partial n_{\text{S}}} \frac{1}{1 - \phi} - \chi \frac{\partial \phi}{\partial n_{\text{S}}} \sum_i N_i n_i \\ &= \ln(1 - \phi) + \phi - \sum_i \frac{\phi_i}{N_i} + \chi \phi^2 \end{aligned}$$

Then, with Eq. 2.A.4, the osmotic pressure is obtained as

$$\frac{\Pi V}{n_{\text{site}} k_{\text{B}}T} = \sum_i \frac{\phi_i}{N_i} - \ln(1 - \phi) - \phi - \chi \phi^2$$

Problem 2.15: Show that the chemical potential of component i of the poly-disperse polymer in the solution is given as

$$\frac{\Delta \mu_i}{k_{\text{B}}T} = \ln \phi_i + 1 + N_i \left[-1 + \phi - \sum_k \frac{\phi_k}{N_k} + \chi(1 - \phi)^2 \right]$$

Solution 2.15: First, we rewrite Eq. 2.33 into

$$\frac{\Delta A_{\text{mix}}}{k_{\text{B}}T} = \sum_k n_k \ln \phi_k + n_{\text{S}} \ln(1 - \phi) + \chi n_{\text{S}} \phi$$

Using the identities

$$\left(\frac{\partial \phi_k}{\partial n_i} \right)_{n_{\text{S}}, n_{j \neq i}} = \frac{\partial}{\partial n_i} \frac{N_k n_k}{n_{\text{S}} + \sum_k N_k n_k} = \frac{\phi_i}{n_i} \delta_{ik} - \frac{\phi_i \phi_k}{n_i}$$

and

$$\left(\frac{\partial \phi}{\partial n_i}\right)_{n_s, n_j \neq i} = \sum_k \left(\frac{\phi_i}{n_i} \delta_{ik} - \frac{\phi_i \phi_k}{n_i} \right) = \frac{\phi_i}{n_i} (1 - \phi)$$

$\Delta \mu_i$ is calculated as

$$\begin{aligned} \frac{\Delta \mu_i}{k_B T} &= \left(\frac{\partial}{\partial n_i} \frac{\Delta G_{\text{mix}}}{k_B T} \right)_{n_s, n_j \neq i} = \frac{\partial}{\partial n_i} \left(\sum_k n_k \ln \phi_k + n_s \ln(1 - \phi) + \chi n_s \phi \right) \\ &= \ln \phi_i + \sum_k \frac{n_k}{\phi_k} \left(\frac{\phi_i}{n_i} \delta_{ik} - \frac{\phi_i}{n_i} \phi_k \right) + \left(\chi - \frac{1}{1 - \phi} \right) n_s \frac{\phi_i}{n_i} (1 - \phi) \\ &= \ln \phi_i + 1 + N_i \left[-1 + \phi - \sum_k \frac{\phi_k}{N_k} + \chi(1 - \phi)^2 \right] \end{aligned}$$

Problem 2.16: The osmotic pressure of the lattice polymer solution is, in general, given in the virial expansion with respect to ϕ :

$$\frac{\Pi V}{n_{\text{site}} k_B T} = \frac{\phi}{N} + B_2 \phi^2 + B_3 \phi^3 + B_4 \phi^4 + \dots$$

Assume that the second virial coefficient B_2 is susceptible to the environmental change but its effect on the higher-order coefficients (B_3, B_4, \dots) is weak. What are the values of B_2 and ϕ at the critical condition?

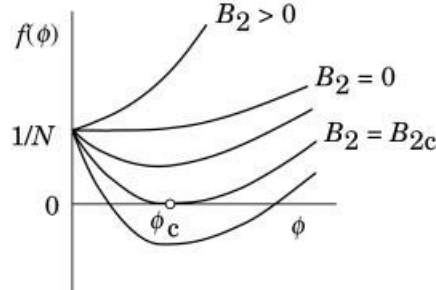
Solution 2.16: From Eq. 2.A.4,

$$\frac{\Delta \mu_s}{k_B T} = -\frac{\Pi V}{n_{\text{site}} k_B T} = -\left(\frac{\phi}{N} + B_2 \phi^2 + B_3 \phi^3 + B_4 \phi^4 + \dots \right)$$

As we have seen in Problem 2.10, the spinodal line is given by

$$\frac{\partial}{\partial \phi} \frac{\Delta \mu_s}{k_B T} = -\left(\frac{1}{N} + 2B_2 \phi + 3B_3 \phi^2 + 4B_4 \phi^3 + \dots \right) = 0$$

Let $f(\phi) \equiv 1/N + 2B_2 \phi + 3B_3 \phi^2 + 4B_4 \phi^3 + \dots$. The plot of $f(\phi)$ depends on B_2 . The system is stable if $f(\phi) > 0$ for all $\phi > 0$. At $B_2 = B_{2c}$, the plot of $f(\phi)$ is tangent on the ϕ axis at $\phi = \phi_c$. The critical condition is therefore



given as

$$f(\phi_c) = 1/N + 2B_{2c}\phi_c + 3B_3\phi_c^2 + 4B_4\phi_c^3 + \dots = 0$$

$$f'(\phi_c) = 2B_{2c} + 6B_3\phi_c + 12B_4\phi_c^2 + \dots = 0$$

which leads to

$$\phi_c = (3B_3N)^{-1/2} - \frac{4}{9} \frac{B_4}{B_3^2N} + \dots, B_{2c} = -(3B_3/N)^{1/2} - \frac{2}{3} \frac{B_4}{B_3N} + \dots$$

2.3 PHASE DIAGRAM AND THETA SOLUTIONS

2.3.1 Phase Diagram

2.3.1.1 Upper and Lower Critical Solution Temperatures The quality of the solvent for a given polymer can be changed either by changing the temperature or by changing the mixing ratio of a good solvent to a poor solvent. When the temperature is changed, it is customary to draw a coexistence curve on a temperature–composition plane. We use the temperature for the ordinate in place of χ , because of convenience. Any scale can be used to represent the composition: mass concentration, volume fraction, molar fraction, mass fraction, and so forth.

There are different types of phase diagram. Figure 2.19a shows the most commonly observed diagram. The parabolic coexistence curve is inverted from the one on the $\chi - \phi$ plane in the figures in Section 2.2 because increasing T decreases χ in general. The temperature at the critical condition is called the **critical temperature**. The phase diagram has the critical temperature (T_c) at the highest point on the coexistence curve. Therefore, the critical temperature is referred to as the **upper critical solution temperature (UCST)**. The phase diagram shown in Figure 2.19a is called a UCST-type phase diagram. At high temperatures, the solution is uniform and therefore transparent. At $T < T_c$ the system has a miscibility gap. When cooled to temperatures below the coexistence curve, the solution separates into two phases. Each of the two phases is uniform, but they have different compositions. A polymer–solvent system with a near-constant and positive $\Delta\varepsilon = \varepsilon_{PS} - (\varepsilon_{PP} + \varepsilon_{SS})/2$ will yield a UCST. Note $\chi = Z\Delta\varepsilon/k_B T$ in Eq. 2.4.

An inverted phase diagram shown in Figure 2.19b is observed in some polymer–solvent systems. Because T_c is at the lowest point on the coexistence

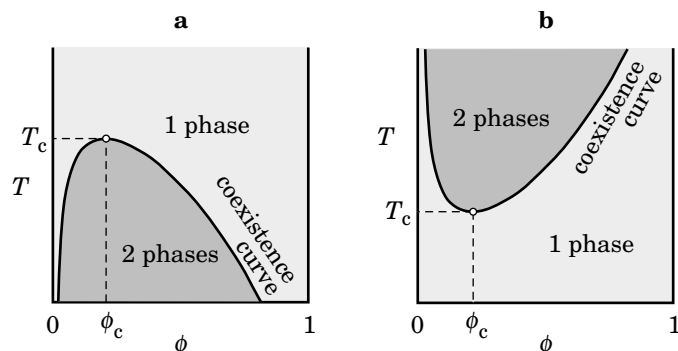


Figure 2.19. Phase diagram of polymer solution on temperature–composition plane. a: UCST-type phase diagram. b: LCST-type phase diagram. The critical point is at the apex of the coexistence curve and is specified by the critical temperature T_c and the critical composition ϕ_c .

curve, this T_c is called the **lower critical solution temperature (LCST)**. The phase diagram shown in Figure 2.19b is called a LCST-type phase diagram. A polymer soluble in water due to hydrogen bonding usually has an LCST-type phase diagram because the hydrogen bonding disrupts at higher temperatures.

It can happen that the coexistence curve is closed and has both UCST and LCST, as shown in Figure 2.20. The solution is in a single phase exterior to the loop but in two phases within the loop.

It is common to all three types of the phase diagram that the system is in a single phase at compositions close to the vertical line at $\phi = 0$ or the other vertical line at $\phi = 1$. The majority component can always accommodate a small amount of the minority component with a help from the entropy of mixing.

2.3.1.2 Experimental Methods The **cloud-point method** is commonly used to determine the phase diagram. Let us consider a solution that has a UCST-type phase diagram. We prepare solutions at different concentrations and bring them into a single phase by heating. The solutions are then cooled slowly. In Figure 2.21, the

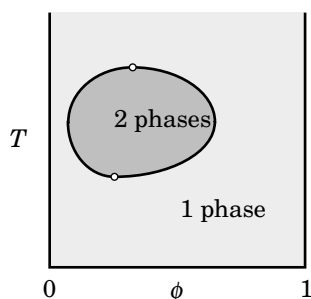


Figure 2.20. A phase diagram can show both upper and lower critical solution temperatures.

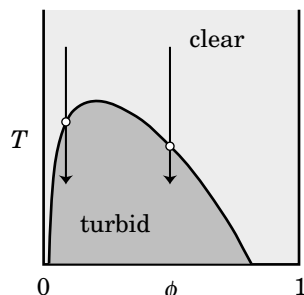


Figure 2.21. Cloud point is defined as the temperature at which the solution becomes turbid as the solution in a single phase is brought into the two-phase regime. Illustration is given for the UCST-type phase diagram.

polymer–solvent system changes its state along a vertical line. As the temperature crosses the coexistence curve, the solution becomes turbid, indicating microscopic heterogeneity. The point is called the **cloud point**. The turbidity is due to scattering of light by a difference in the refractive index between the two phases. When left for a sufficiently long time, the polymer–solvent system separates into two macroscopic phases, each of which is uniform and therefore transparent. The lighter phase is now on top of the heavier phase. In some solutions, crystallization of the polymer occurs simultaneously as the polymer-rich phase separates. The crystallite that has grown from a solution may be clear. By connecting the cloud points measured for solutions of different concentrations, we can obtain the coexistence curve and construct the phase diagram.

Naked eyes can easily detect the cloudiness. A more sophisticated method will use a photodetector. A polymer solution in a single phase is prepared in a cuvette. The intensity of the light transmitted through the solution, or the intensity of light scattered, typically at 90° , is continuously monitored as the temperature is lowered across the coexistence curve. The scattering intensity shoots up and the transmission drops as the solution becomes turbid.

Atactic polystyrene in cyclohexane is the most famous example of polymer solutions that exhibit a UCST-type phase diagram. Figure 2.22 shows the phase diagrams for different molecular weights of polystyrene.¹⁵ For each molecular weight, the critical point is at the highest point of the curve. As the molecular weight increases, the critical temperature (T_c) becomes higher and the critical volume fraction ϕ_c decreases. The extrapolate of T_c to infinite molecular weight is about 35.4°C .

2.3.2 Theta Solutions

2.3.2.1 Theta Temperature For a given polymer–solvent system, the light-scattering experiment at different concentrations gives an estimate of A_2 at the temperature of the measurement, as we will learn in the following section. In a system that has a UCST-type phase diagram (Fig. 2.23a), the sign of A_2 changes from

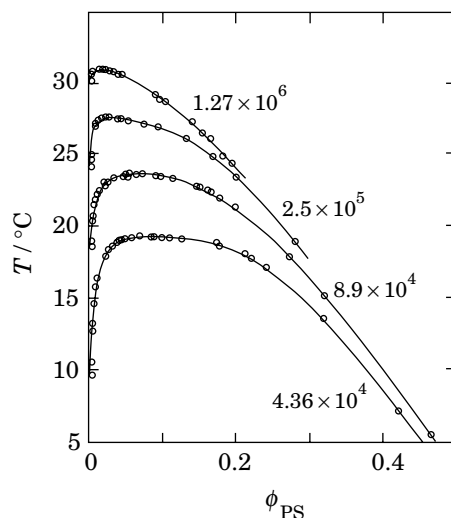


Figure 2.22. Coexistence curves determined from the cloud-point method (circles) for solutions of polystyrene of different molecular weights in cyclohexane. The abscissa is the volume fraction of polystyrene. The molecular weight of the polymer in g/mol is indicated adjacent to each curve. (From Ref. 15.)

positive to negative as the temperature drops below a certain level. The temperature at which $A_2 = 0$ is called the **theta temperature** and expressed by T_θ or Θ . The solvent at T_θ is a theta solvent for the polymer. The theta temperature thus defined is identical to the extrapolate of T_c to infinite molecular weight of the polymer. The latter is another definition of T_θ . In a solution of a polymer in g/mol of a finite molecular weight with UCST, $T_c < T_\theta$.

In polymer solutions with LCST, the critical temperature T_c is higher than T_θ (Fig. 2.23b). The sign of A_2 changes from positive to negative as the temperature exceeds T_θ .

The theta temperature is different for each combination of polymer and solvent. Table 2.6 lists T_θ for some polymer solutions.¹¹ Each system has its own theta temperature, although it may not be reached in the liquid phase of the solvent or below the decomposition temperature of the polymer.

There is a slight molecular weight dependence of the temperature that renders $A_2 = 0$ when the molecular weight is not sufficiently high. The dependence is much

TABLE 2.6 Theta Conditions

Polymer	Solvent	Temperature	Type
polystyrene	cyclohexane	~35°C	UCST
polystyrene	<i>trans</i> -decahydronaphthalene	~21°C	UCST
poly(methyl methacrylate)	acetonitrile	~44°C	UCST
poly(<i>N</i> -isopropyl acrylamide)	water	~30°C	LCST

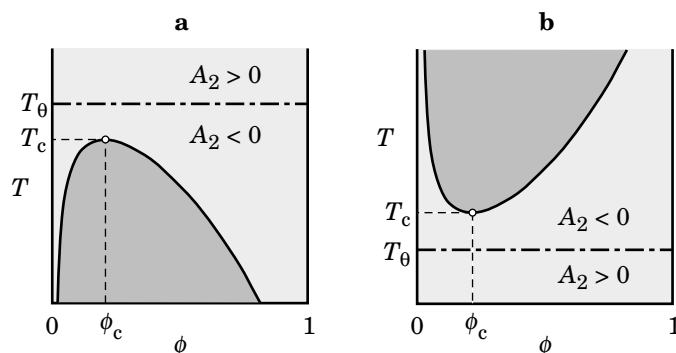


Figure 2.23. Relationship between the theta temperature T_θ with the critical temperature T_c . a: UCST-type phase diagram. b: LCST-type phase diagram. The second virial coefficient A_2 changes its sign at $T = T_\theta$.

smaller compared with the dependence of T_c on the molecular weight. Therefore, the light-scattering experiments do not need to be repeated on polymer fractions of different molecular weights to find T_θ . Measurement of A_2 on a single fraction of the polymer should suffice.

Figure 2.24 shows an example of A_2 obtained in the light-scattering experiments at several different temperatures near T_θ for a solution of polystyrene in cyclohexane.¹⁶ Apparently, $A_2 \cong 0$ at around 35.7°C for the solution. The temperature agrees with the extrapolate of T_c within experimental errors.

2.3.2.2 Properties of Theta Solutions Solutions in the theta condition have $A_2 = 0$. When $A_2 = 0$, the second-order term in $\Pi/\Pi_{\text{ideal}} = 1 + A_2Mc + A_3Mc^2 + \dots$ (Eq. 2.20) is absent. The nonideality of the solution does not become apparent until the third-order term A_3Mc^2 becomes sufficiently large. The osmotic pressure is

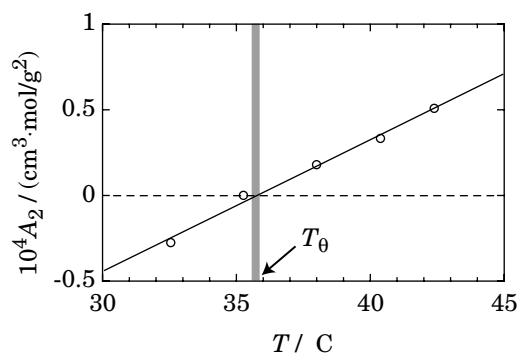


Figure 2.24. Second virial coefficient A_2 for polystyrene in cyclohexane at different temperatures near the theta temperature. (From Ref. 16.)

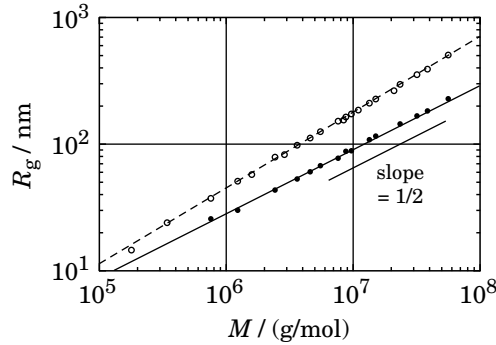


Figure 2.25. Radius of gyration R_g of polystyrene in cyclohexane at the theta temperature (35.4°C), plotted as filled circles as a function of molecular weight. Open symbols indicate R_g of polystyrene in toluene and benzene (good solvents) and are the same as those in Figure 1.37. A slope of 1/2 is indicated in the figure. (From Ref. 2.)

close to that of the ideal solution in a wide range of concentrations. The near ideality of the theta solution is not limited to the osmotic pressure.

The chain dimension such as R_g and R_F in theta solution increases with the molecular weight M just as the ideal chains do. Figure 2.25 shows an example obtained for polystyrene in cyclohexane at 35.4°C.² The data for R_g are plotted as solid circles. For reference, R_g in the good solvent is plotted as open circles (same as Fig. 1.37). The polymer chain in the theta solvent is shrunk compared with the good solvent. The curve fitting (for $M < 10^7$ g/mol) gives

$$R_g/\text{nm} = 0.02675 \times (M/(\text{g/mol}))^{0.5040} \quad \text{polystyrene in cyclohexane, } 35.4^\circ\text{C} \quad (2.28)$$

close to the predicted $R_g \propto M^{1/2}$.

In Section 1.4.2, we derived $R_F \cong bN^{3/5}$ for an excluded-volume chain using Flory's method. Here, we use a similar method to derive $R_F \cong bN^{1/2}$ for theta chains. The difference in the free energy A_{ch} of the chain is in the second term of Eq. 1.63. For the theta chains, binary interaction is effectively absent ($A_2 = 0$) and therefore the leading term in the polymer-polymer interaction is $b^6 R^3 (N/R^3)^3 = b^6 N^3 / R^6$, which is due to the ternary interactions. Then, A_{ch} is given as

$$\frac{A_{\text{ch}}}{k_B T} \cong \frac{R^2}{Nb^2} + b^6 \frac{N^3}{R^6} \quad (2.39)$$

A_{ch} minimizes when $\partial(A_{\text{ch}}/k_B T)/\partial R|_{R=R_F} = 0$, that is, $R_F \cong bN^{1/2}$, reproducing the experimental results. The relationship becomes questionable when N is large, however. See Problem 2.17.

The nature of the theta solvent can be better understood in the lattice chain model. We choose the interaction with a solvent to be zero: $\varepsilon_{\text{PS}} = \varepsilon_{\text{PP}} = 0$. Then $\chi = -(Z/2)\varepsilon_{\text{PP}}/k_B T$. The theta condition, $\chi = 1/2$, is realized by $\varepsilon_{\text{PP}}/k_B T = -1/Z$.

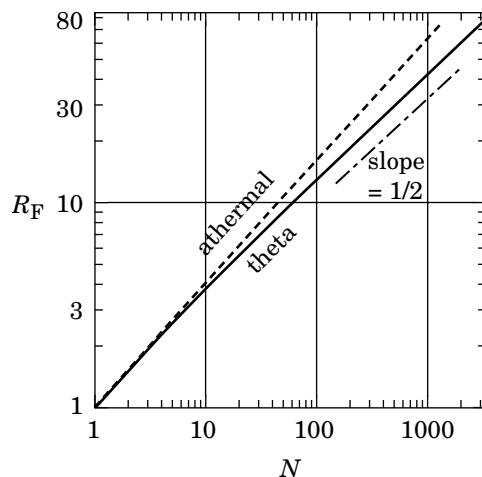


Figure 2.26. End-to-end distance R_F of self-avoiding walks on the cubic lattice, plotted as a function of the number of bonds, N , of the chain. The solid line and the dashed line represent the theta chains and athermal chains, respectively. The dash-dotted line has a slope of $1/2$. (From Ref. 18.)

This negative interaction in the monomer–monomer contact promotes association between monomers and contracts the polymer chain. The repulsive interaction due to the excluded volume is compensated by the attractive ε_{pp} .

However, the Flory–Huggins theory is an approximate theory based on random mixing of monomers. The interaction for the theta condition is slightly different in the computer simulation on the cubic lattice:¹⁷

$$\varepsilon_{pp}/k_B T = -0.2693 \quad \text{theta condition, cubic lattice simulation} \quad (2.40)$$

Figure 2.26 compares a plot of the root mean square end-to-end distance R_F for polymer chains on the cubic lattice for the theta chains with a plot for athermal chains.¹⁸ The chain contraction in the theta condition is evident. The data for the theta solution follow a power law of $R_F \sim N^{1/2}$ when $N \gg 1$.

2.3.3 Coil-Globule Transition

As the solvent quality turns poorer to the polymer from the theta condition, polymer–solvent contacts become more unfavorable, and the chain contracts even more. Eventually, the random-coil conformation changes to a globular shape to minimize the polymer–solvent contacts and maximize the contacts between monomers. The chain dimension should be now proportional to $N^{1/3}$, as expected for a packed sphere. When N is sufficiently large, the change from $R_g \cong bN^{1/2}$ to $bN^{1/3}$ is rather abrupt; therefore, it is called **coil-globule transition**. Figure 2.27 summarizes how

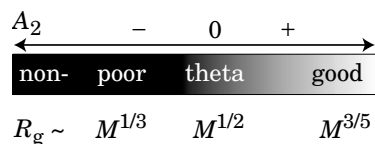


Figure 2.27. Molecular-weight (M) dependence of the radius of gyration R_g changes as the solvent quality, and therefore the second virial coefficient A_2 , change.

the chain dimension changes with A_2 . It is not easy to observe the transition in experiments because, as the intrachain attraction becomes stronger, the interchain attraction becomes stronger as well, leading to formation of aggregates. Then, the light-scattering measurements give the size of the aggregate, not a single chain dimension.

Figure 2.28 is a rare example of a successful observation.¹⁹ It shows how R_g of poly(*N*-isopropyl acrylamide) in water changes with the solvent quality. The solution exhibits an LCST-type phase diagram with $T_\theta \cong 30.5^\circ\text{C}$. At $T \ll T_\theta$, the solvent is good to the polymer and the chains are swollen. As T rises, the solvent quality becomes poorer and R_g decreases. At $T > T_c \cong 32^\circ\text{C}$, R_g is nearly independent of temperature. A slight hysteresis was observed.

Most protein molecules are globular. Strong interactions due to hydrogen bonding and S–S linkage force the protein to take a specific structure close to a globule.

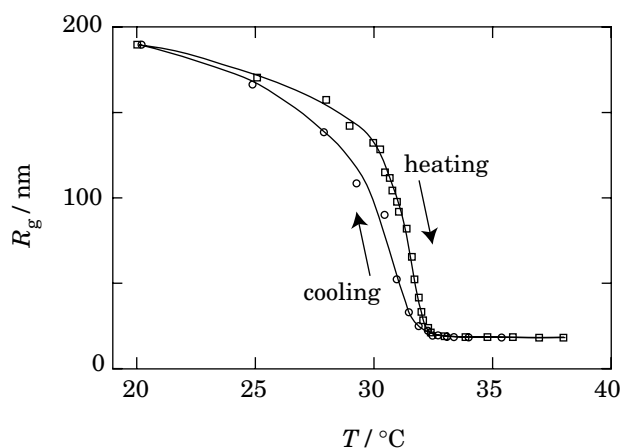


Figure 2.28. Contraction and swelling of linear poly(*N*-isopropyl acrylamide) chains in water by cooling and heating. The radius of gyration R_g is plotted as a function of temperature T . (From Ref. 19.)

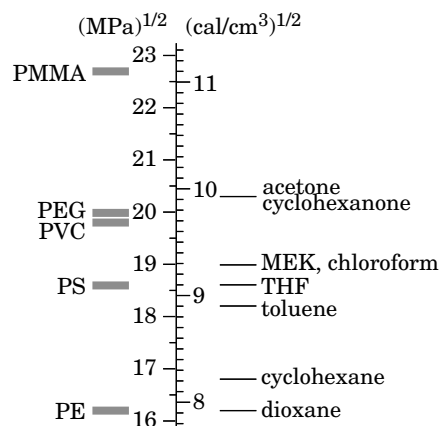


Figure 2.29. Solubility parameters of some solvents and polymers, given in (MPa)^{1/2} and (cal/cm³)^{1/2}.

2.3.4 Solubility Parameter

The interaction between a polymer and a solvent is often expressed by a **solubility parameter**. The solubility parameter δ_i of substance i is defined as

$$\delta_i \equiv (\Delta E_i^{\text{vap}}/V_i)^{1/2} \quad (2.41)$$

where ΔE_i^{vap} is the molar energy of vaporization and V_i is the molar volume of substance i . Figure 2.29 shows a partial list of the solubility parameter expressed in (MPa)^{1/2} and (cal/cm³)^{1/2}.¹¹ Simple thermodynamics on the binary mixture gives the χ parameter expressed by the solubility parameters:

$$\chi = \frac{V_S}{N_A k_B T} (\delta_S - \delta_P)^2 + 0.34 \quad (2.42)$$

where subscripts S and P stand for solvent and polymer, respectively.

Equation 2.42 illustrates that the polymer and the solvent mix when their solubility parameters are close and do not when they differ a lot. However, this is not always the case. For instance, polyethylene and 1,4-dioxane have similar solubility parameters but do not mix partly because of crystallinity of polyethylene. Poly(methyl methacrylate) dissolves well in tetrahydrofuran, although the solubility parameters are greatly different. Furthermore, Eq. 2.42 is always positive. It fails to describe specific interactions that may make χ negative such as the hydrogen bonding. We should regard Eq. 2.42 as one of the possible ways to describe χ for some polymer–solvent systems.

2.3.5 PROBLEMS

Problem 2.17: We apply Flory's method (Section 1.4) to find how much a small deviation from the theta condition changes the end-to-end distance. For this purpose, we express the free energy per chain that has an end-to-end distance R by

$$\frac{A_{\text{ch}}}{k_{\text{B}}T} \cong \frac{R^2}{Nb^2} + b^6 \frac{N^3}{R^6} + \beta b^3 \frac{N^2}{R^3}$$

where $\beta = 0$ at theta. Treat the last term as a perturbation and evaluate its effect on R_{F} .

Solution 2.17: At $R = R_{\text{F}}$,

$$\frac{\partial}{\partial R} \frac{A_{\text{ch}}}{k_{\text{B}}T} = \frac{2R}{Nb^2} - 6b^6 \frac{N^3}{R^7} - 3\beta b^3 \frac{N^2}{R^4} = 0$$

which leads to

$$R_{\text{F}}^8 = 3b^8 N^4 + \frac{3}{2} \beta b^5 N^3 R^3$$

Treat the second term as a perturbation:

$$R_{\text{F}} \cong bN^{1/2} \left(1 + \beta \frac{R^3}{Nb^3} \right)^{1/8} \cong bN^{1/2} \left(1 + \frac{1}{8} \frac{\beta}{N} \frac{R^3}{b^3} \right) \cong bN^{1/2} \left(1 + \frac{\beta}{8} N^{1/2} \right)$$

where R was replaced by the unperturbed dimension, $bN^{1/2}$. Even when β is close to zero, R_{F} may deviate from $bN^{1/2}$ as N increases. The deviation is more serious for high-molecular-weight fractions.

2.4 STATIC LIGHT SCATTERING

2.4.1 Sample Geometry in Light-Scattering Measurements

Light scattering has been widely used to characterize polymer chains in a solution. We can find the weight-average molecular weight (M_w), the radius of gyration (R_g), and the second virial coefficient (A_2). We can also learn about the shape of the polymer molecule—whether it is spherical, random-coiled, or rodlike. These quantities are difficult to obtain with other methods. Commercial instruments are available.

Figure 2.30 shows a sample geometry. A cylindrical test tube containing a clear polymer solution is immersed in a glass vat filled with a fluid that has a refractive index close to that of the glass. The fluid is called an index-matching liquid and is thermostatted. A coherent, collimated laser beam enters the index-matching liquid through the vat and then into the test tube. Nearly all of the incoming photons travel

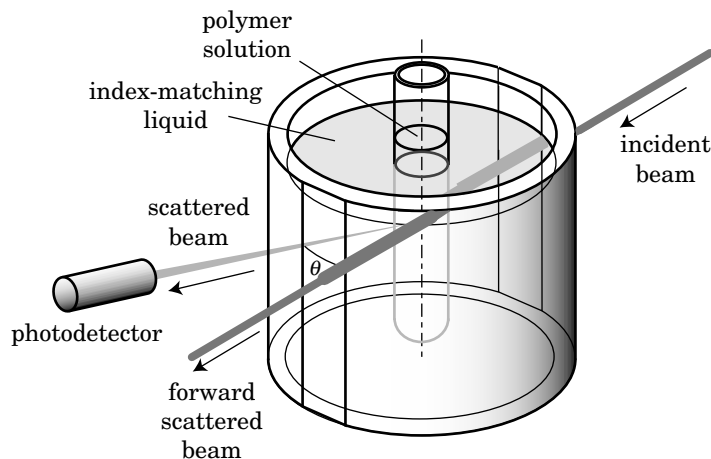


Figure 2.30. Schematic of the geometry around a sample cell in a light-scattering measurement system. A photodetector detects the light scattered by a polymer solution in the beam path into a direction at angle θ from the forward direction. The vat is filled with an index-matching liquid.

straight through the index-matching liquid and the polymer solution, forming a strong, unscattered (or forward-scattered) beam. The molecules in the beam path scatter a tiny fraction of the photons in all directions. The intensity of the scattered beam is detected by a photodetector, typically a photomultiplier, placed horizontally at an angle θ (**scattering angle**) from the forward-scattering direction. To prevent streak scattering at the air-glass interface, the glass vat has a planar cut at each side of the path of the direct beam.

Figure 2.31 is a top view of the sample geometry. The incident beam has a wave vector \mathbf{k}_i . The **wave vector** is parallel to the propagation direction of the beam and has a magnitude of $2\pi/(\lambda/n_{\text{sol}})$, where λ/n_{sol} is the wavelength of light in the solvent of refractive index n_{sol} , with λ being the wavelength of light in vacuum. The wave vector \mathbf{k}_s of the scattered beam has nearly the same magnitude as that of \mathbf{k}_i . In the **static light scattering** (often abbreviated as **SLS**) in which the molecules are assumed to be motionless, the two magnitudes are exactly equal. In reality, motions of the molecules make \mathbf{k}_s different from \mathbf{k}_i , but the change is so small (typically less than 0.01 ppm) that we can regard $|\mathbf{k}_i| = |\mathbf{k}_s|$. The change in the wave vector upon scattering is called the **scattering vector**. The scattering vector \mathbf{k} is defined as

$$\mathbf{k} \equiv \mathbf{k}_s - \mathbf{k}_i \quad (2.43)$$

The inset of Figure 2.31 allows the magnitude of $|\mathbf{k}| = k$ to be conveniently calculated as

$$k = \frac{4\pi n_{\text{sol}}}{\lambda} \sin \frac{\theta}{2} \quad \text{scattering wave vector} \quad (2.44)$$

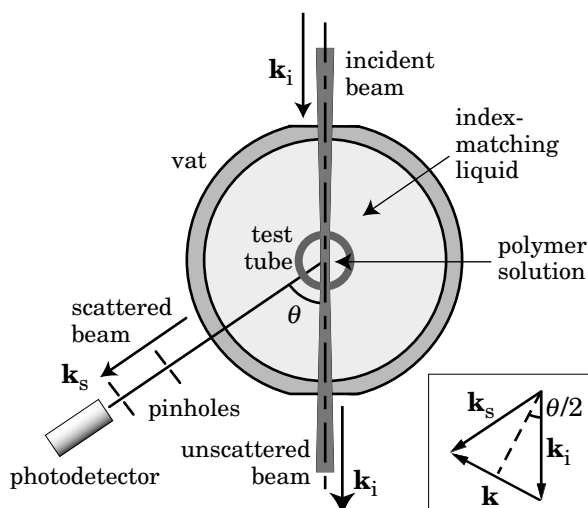


Figure 2.31. Top view of the geometry around the sample cell. The wave vector \mathbf{k}_i of the incident beam changes to \mathbf{k}_s when scattered. Two pinholes or two slits specify the scattering angle. The inset defines the scattering wave vector \mathbf{k} .

For the forward-scattered beam, $k = 0$. With an increasing θ , k increases. Figure 2.32 shows how k changes with θ for water ($n_{\text{sol}} = 1.331$) at 25°C and He-Ne laser ($\lambda = 632.8$ nm) as a light source and for toluene ($n_{\text{sol}} = 1.499$) at 25°C and Ar^+ laser ($\lambda = 488.0$ nm; there is another strong beam at 514.5 nm). For the first system, k spans from $3.46 \times 10^6 \text{ m}^{-1}$ at $\theta = 15^\circ$ to $2.56 \times 10^7 \text{ m}^{-1}$ at $\theta = 150^\circ$.

Two pinholes or two vertical slits are placed along the path of the scattered beam to restrict the photons reaching the detector to those scattered by the molecules in a small part of the solution called the **scattering volume**. The scattering volume is an intersection of the laser beam with the solid angle subtended by the two pinholes (Fig. 2.33).

Polymer molecules, especially those with a high molecular weight, scatter the light strongly. In the following subsections, we will first learn the scattering by small particles and then find why it is strong for the polymer molecules. We will also learn what characteristics of the polymer molecules can be obtained from the scattering pattern.

2.4.2 Scattering by a Small Particle

Small particles (solvent molecules and monomers constituting the polymer) suspended in vacuum can scatter the light. They are called **scatterers**. An electromagnetic wave, also called radiation, enters the isotropic particle to cause polarization in the direction of the electric field of the incident wave (Fig. 2.34). The polarization is a displacement of the spatial average of the positively charged nuclei with

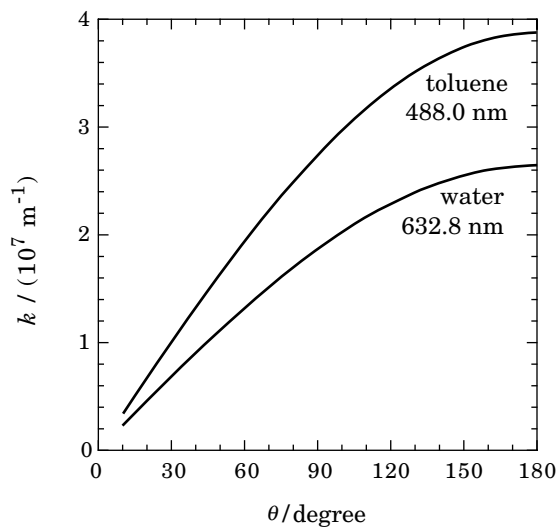


Figure 2.32. The magnitude k of the scattering wave vector plotted as a function of the scattering angle θ for water at 25°C and $\lambda = 632.8 \text{ nm}$ and for toluene at 25°C and $\lambda = 488.0 \text{ nm}$.

respect to the negatively charged electrons. The polarization, oscillating with the frequency of the radiation, serves as a broadcasting station that emits a weak radiation in all directions. The scattered radiation has the same frequency as that of the incident radiation. This mechanism of scattering is called **Rayleigh scattering**.

Figure 2.34 shows the relationship between the vertically polarized incident beam of intensity I_0 and the radiation scattered by the vertically polarized particle.

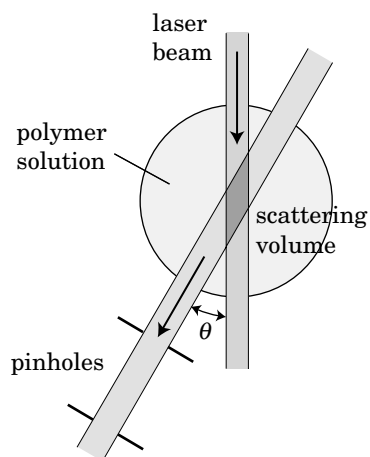


Figure 2.33. Scattering volume is an intersection of the laser beam with the solid angle subtended by the two pinholes.

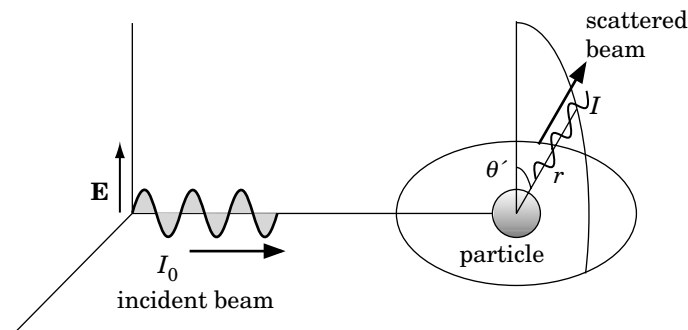


Figure 2.34. Vertically polarized beam causes polarization in the particle, which radiates into different directions. Angle θ' is defined as the angle between the electric field of the incident beam and the scattering direction. The particle size is drawn much larger than it is relative to the wavelength of light.

At a distance r from the particle and at angle θ' from the vertical, the intensity I of the scattered light is given by

$$\frac{I}{I_0} = \frac{\pi^2}{\lambda^4} \frac{\alpha^2}{\epsilon_0^2} \frac{\sin^2 \theta'}{r^2} \quad \text{Rayleigh scattering, vacuum} \quad (2.45)$$

where α is the polarizability of the particle in SI unit and $\epsilon_0 = 8.854 \times 10^{-12}$ F/m is the electric permittivity of vacuum. Most measurement systems detect the light scattered horizontally and therefore $\theta' = \pi/2$.

The polarizability α is proportional to the volume of the particle. The light scattered by a single atom or a small molecule is too weak to be detected in the visible range of light, even if the volume has many of these particles. A strong scattering by these small particles can occur in the X-ray range, where λ is sufficiently small. To have a strong scattering in the visible range, the volume of the scatterer must be sufficiently large. Then, it is necessary to take into account the interference between the beams scattered by different parts of the scatterer. We will see this effect first for a single polymer chain. The scatterer does not have to be filled like a solid sphere to cause the strong scattering. A string of monomers can also scatter the light strongly.

In Eq. 2.45, $I/I_0 \propto \lambda^{-4}$. The Rayleigh scattering is a lot stronger for light of a shorter wavelength. The sky is blue because the scattering is stronger toward the short-wavelength end of the visible spectrum. Each molecule of the atmosphere is too small to scatter the visible light effectively. What we see as the blue sky is due to density fluctuations in the atmosphere.

2.4.3 Scattering by a Polymer Chain

Scattering by a larger molecule is stronger, because beams scattered by different parts of the molecule can interfere constructively. We consider here how the

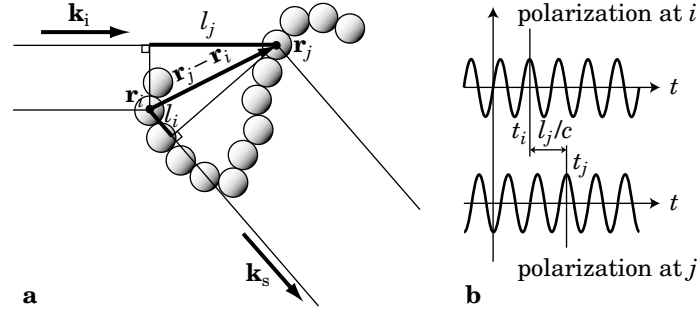


Figure 2.35. A polymer chain, on exposure to an incoming plane wave of radiation, scatters light. (a) A beam path for the incoming light and a beam path for the scattered light are drawn for two monomers i and j at \mathbf{r}_i and \mathbf{r}_j on the chain. The difference in the path length is $l_j - l_i$. b: Polarizations at monomers i and j as a function of time t . The phase difference is $k_i l_j$ in the geometry in a.

interference affects the overall scattering intensity for a single polymer chain. We model the chain as a sequence of N motionless monomers each of which scatters the radiation. Figure 2.35a is a two-dimensional rendering of the polymer chain. The incident light is a plane wave with a wave vector \mathbf{k}_i and an electric field \mathbf{E}_i oscillating with an angular frequency ω in the direction perpendicular to \mathbf{k}_i (any direction in the plane perpendicular to \mathbf{k}_i). At position \mathbf{r} and time t , \mathbf{E}_i is given by

$$\mathbf{E}_i = \mathbf{E}_{i0} \exp [i(\mathbf{k}_i \cdot \mathbf{r} - \omega t)] \quad (2.46)$$

where \mathbf{E}_{i0} is the complex amplitude of the field. The intensity of the light is calculated as the product of \mathbf{E}_{i0} and its complex conjugate. The photons on a plane perpendicular to \mathbf{k}_i are assumed to be all in phase (**coherent**). It means that their electric fields oscillate without a delay to each other. A laser beam has a large area of coherence.

These photons enter the monomers to cause polarization on each of them. Because monomers are located at different positions along the beam path, the \mathbf{E}_i that causes the polarization at a given time is different from monomer to monomer. Therefore, compared at the same time, the phase of the oscillating polarization is different for each monomer. The scattered radiation \mathbf{E}_{si} caused by the polarization on the i th monomer at \mathbf{r}_i at time t_i and traveling with a wave vector \mathbf{k}_s is given by

$$\mathbf{E}_{si} = \mathbf{E}_{sm} \exp [i(\mathbf{k}_s \cdot (\mathbf{r} - \mathbf{r}_i) - \omega(t - t_i))] \quad (2.47)$$

where \mathbf{E}_{sm} is the complex amplitude of the beam scattered by a single monomer and propagating in the direction of \mathbf{k}_s . Note that \mathbf{E}_{si} is one of many radiations emanating from the i th monomer. The same phase of the plane wave that has caused \mathbf{E}_{si} travels further and causes \mathbf{E}_{sj} in the same propagation direction as \mathbf{E}_{si} by polarization of the

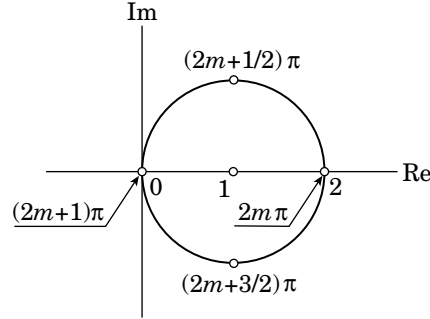


Figure 2.36. Real and imaginary parts of $1 + \exp(i\phi_{ij})$ are shown for ϕ_{ij} as a parameter. When $\phi_{ij} = 2m\pi$ ($m = 0, \pm 1, \pm 2, \dots$), $1 + \exp(i\phi_{ij}) = 2$, and the interference is constructive.

j th monomer at \mathbf{r}_j at time t_j :

$$\mathbf{E}_{sj} = \mathbf{E}_{sm} \exp[i(\mathbf{k}_s \cdot (\mathbf{r} - \mathbf{r}_j) - \omega(t - t_j))] \quad (2.48)$$

Figure 2.35b compares the change of the polarizations with time on monomers i and j .

The photodetector detects the total amplitude of the radiation scattered by different monomers. The total electric field of the scattered light is $\mathbf{E}_{s1} + \mathbf{E}_{s2} + \dots + \mathbf{E}_{sN}$. Before adding all of them, we first consider the sum of \mathbf{E}_{si} and \mathbf{E}_{sj} :

$$\mathbf{E}_{si} + \mathbf{E}_{sj} = \mathbf{E}_{sm}[1 + \exp(i\phi_{ij})] \exp[i(\mathbf{k}_s \cdot (\mathbf{r} - \mathbf{r}_i) - \omega(t - t_i))] \quad (2.49)$$

where ϕ_{ij} is the phase difference between the two beams and given as

$$\phi_{ij} \equiv \mathbf{k}_s \cdot (\mathbf{r}_i - \mathbf{r}_j) - \omega(t_i - t_j) \quad (2.50)$$

Now $\mathbf{E}_{sm}[1 + \exp(i\phi_{ij})]$ is the complex amplitude for $\mathbf{E}_{si} + \mathbf{E}_{sj}$. Depending on ϕ_{ij} , $1 + \exp(i\phi_{ij})$ can vary widely. This phenomenon is called interference. Figure 2.36 shows how the real and imaginary parts of $1 + \exp(i\phi_{ij})$ change with ϕ_{ij} . When $\phi_{ij} = 0, \pm 2\pi, \pm 4\pi, \dots$, we have $1 + \exp(i\phi_{ij}) = 2$, and the amplitude maximizes (constructive interference). When $\phi_{ij} = \pm\pi, \pm 3\pi, \dots$, in contrast, $1 + \exp(i\phi_{ij}) = 0$, and the amplitude is zero (destructive interference). The interference is in-between at other angles of ϕ_{ij} .

For the chain configuration in Figure 2.35a,

$$\omega(t_j - t_i) = \omega l_j / c = k l_j = k \hat{\mathbf{k}}_i \cdot (\mathbf{r}_j - \mathbf{r}_i) = -\mathbf{k}_i \cdot (\mathbf{r}_i - \mathbf{r}_j) \quad (2.51)$$

where c is the velocity of light, l_j is defined in the figure, and $\hat{\mathbf{k}}_i$ is the unit vector parallel to \mathbf{k}_i . Thus,

$$\phi_{ij} \equiv (\mathbf{k}_s - \mathbf{k}_i) \cdot (\mathbf{r}_i - \mathbf{r}_j) = \mathbf{k} \cdot (\mathbf{r}_i - \mathbf{r}_j) \quad (2.52)$$

The ϕ_{ij} can also be calculated from the difference in the path length between the two beams reaching the detector. The difference is $l_j - l_i$ as seen in Figure 2.35a. The corresponding phase difference is $\phi_{ij} = (\omega/c)(l_j - l_i)$, which is equal to Eq. 2.52.

For 1 through N monomers,

$$\sum_{i=1}^N \mathbf{E}_{si} = \mathbf{E}_{sm} \exp[i(\mathbf{k}_s \cdot (\mathbf{r} - \mathbf{r}_1) - \omega(t - t_1))] \sum_{i=1}^N \exp(i\phi_{1i}) \quad (2.53)$$

Thus we find that the complex amplitude of the light scattered by the whole chain is modified by a factor of $\sum_{i=1}^N \exp(i\phi_{1i})$. The square of the magnitude of the factor determines how the beams scattered by the N monomers interfere. Thus the intensity of the light scattered by the whole chain is proportional to

$$\begin{aligned} \left| \sum_{i=1}^N \exp(i\phi_{1i}) \right|^2 &= \sum_{i=1}^N \exp[-i\mathbf{k} \cdot (\mathbf{r}_1 - \mathbf{r}_i)] \sum_{j=1}^N \exp[i\mathbf{k} \cdot (\mathbf{r}_1 - \mathbf{r}_j)] \\ &= \sum_{i,j=1}^N \exp[i\mathbf{k} \cdot (\mathbf{r}_i - \mathbf{r}_j)] \end{aligned} \quad (2.54)$$

If the monomers are isotropic particles with the same polarizability α , the intensity I of horizontally scattered light ($\theta' = \pi/2$ in Eq. 2.45) is

$$\frac{I}{I_0} = \frac{\pi^2}{\lambda^4} \frac{\alpha^2}{\epsilon_0^2} \frac{1}{r^2} \sum_{i,j=1}^N \exp[i\mathbf{k} \cdot (\mathbf{r}_i - \mathbf{r}_j)] \quad (2.55)$$

At low angles, $\exp[i\mathbf{k} \cdot (\mathbf{r}_i - \mathbf{r}_j)] \cong 1$ and I/I_0 is increased by a factor of N^2 compared with a single monomer. The constructive interference between photons scattered by different parts of the polymer chain causes this N^2 dependence. If each part scatters the light independently, then I/I_0 would increase only by a factor of N .

2.4.4 Scattering by Many Polymer Chains

The scattering volume contains many polymer chains. We consider here how these chains collectively contribute to the total scattering intensity. We forget for now the presence of solvent molecules as we did in the preceding section and assume that the polymer chains are suspended in vacuum to scatter the light. To obtain the formula for the scattering intensity by a single polymer chain, we did not invoke connectivity of monomers. The formula, Eq. 2.55, can easily be extended to a system of n_p chains ($n_p \gg 1$), each consisting of N monomers. We denote by \mathbf{r}_{mi} the position of the i th monomer of the m th chain. Equation 2.54 now reads

$$\begin{aligned} &\sum_{m,n=1}^{n_p} \sum_{i,j=1}^N \exp[i\mathbf{k} \cdot (\mathbf{r}_{mi} - \mathbf{r}_{nj})] \\ &= \sum_{m=1}^{n_p} \sum_{i,j=1}^N \exp[i\mathbf{k} \cdot (\mathbf{r}_{mi} - \mathbf{r}_{mj})] + \sum_{m \neq n=1}^{n_p} \sum_{i,j=1}^N \exp[i\mathbf{k} \cdot (\mathbf{r}_{mi} - \mathbf{r}_{nj})] \end{aligned} \quad (2.56)$$

The first term is a contribution from two monomers on the same chain, and the second term is a contribution from two monomers on different chains. There are various chain configurations occurring simultaneously on different chains. The summations in Eq. 2.56 can therefore be replaced by statistical averages:

$$\begin{aligned} & \sum_{m,n=1}^{n_p} \sum_{i,j=1}^N \exp[\mathbf{i}\mathbf{k} \cdot (\mathbf{r}_{mi} - \mathbf{r}_{nj})] \\ &= n_p \sum_{i,j=1}^N \langle \exp[\mathbf{i}\mathbf{k} \cdot (\mathbf{r}_{1i} - \mathbf{r}_{1j})] \rangle + n_p^2 \sum_{i,j=1}^N \langle \exp[\mathbf{i}\mathbf{k} \cdot (\mathbf{r}_{1i} - \mathbf{r}_{2j})] \rangle \end{aligned} \quad (2.57)$$

where $n_p(n_p - 1)$ was approximated by n_p^2 in the second term. The average in the first term is taken with a statistical weight of a configuration for a single chain. The average in the second term is taken with a weight of configurations for the two chains. The latter configurations refer to the relative position of the two chains and the monomer arrangement of each chain.

At low concentrations, polymer chains are sufficiently separated from each other. Interference by monomers on different chains are cancelled out on the average; therefore, the second term is negligible compared with the first term. Thus, the scattering intensity $I(\mathbf{k})$ is given by

$$\frac{I(\mathbf{k})}{I_0} = \frac{\pi^2}{\lambda^4} \frac{\alpha^2}{\varepsilon_0^2} \frac{1}{r^2} n_p \sum_{i,j=1}^N \langle \exp[\mathbf{i}\mathbf{k} \cdot (\mathbf{r}_i - \mathbf{r}_j)] \rangle \quad (2.58)$$

where the index “1” was dropped in \mathbf{r}_{1i} . The summation factor in Eq. 2.58 divided by N is called the (single-chain) **static structure factor** $S_1(\mathbf{k})$:

$$S_1(\mathbf{k}) = \frac{1}{N} \sum_{i,j=1}^N \langle \exp[\mathbf{i}\mathbf{k} \cdot (\mathbf{r}_i - \mathbf{r}_j)] \rangle \quad \text{single-chain static structure factor} \quad (2.59)$$

In the absence of constructive interference between different monomers, only terms with $i = j$ would survive and therefore $S_1(\mathbf{k})$ would be equal to 1. The interference makes $S_1(\mathbf{k})$ and $I(\mathbf{k})$ depend on \mathbf{k} . With $S_1(\mathbf{k})$, Eq. 2.58 becomes to $I(\mathbf{k})/I_0 = (\pi^2/\lambda^4)(\alpha/\varepsilon_0)^2 r^{-2} n_p N S_1(\mathbf{k})$. Note that uncorrelated $n_p N$ monomers in solution have $I(\mathbf{k})/I_0 = (\pi^2/\lambda^4)(\alpha/\varepsilon_0)^2 r^{-2} n_p N$. Thus we find that $S_1(\mathbf{k})$ indicates how much the interference from different parts of the chain increases $I(\mathbf{k})$.

The static structure factor (also called **scattering function**) that applies also to finite concentrations is obtained from Eq. 2.57 as

$$\begin{aligned} S(\mathbf{k}) &= \frac{1}{n_p N} \sum_{m,n=1}^{n_p} \sum_{i,j=1}^N \langle \exp[\mathbf{i}\mathbf{k} \cdot (\mathbf{r}_{mi} - \mathbf{r}_{nj})] \rangle \\ &= S_1(\mathbf{k}) + \frac{n_p}{N} \sum_{i,j=1}^N \langle \exp[\mathbf{i}\mathbf{k} \cdot (\mathbf{r}_{1i} - \mathbf{r}_{2j})] \rangle \end{aligned} \quad (2.60)$$

The second term is due to correlations between different chains. Note that chains 1 and 2 have to be nearby to scatter beams that interfere constructively. At low

concentrations, the statistical average for different chains is mostly zero, and $S(\mathbf{k})$ becomes identical to $S_1(\mathbf{k})$. The interference between different chains becomes more significant with an increasing concentration.

2.4.5 Correlation Function and Structure Factor

2.4.5.1 Correlation Function We now find how the structure factor is related to the local **segment density** $\rho(\mathbf{r})$ defined by

$$\rho(\mathbf{r}) = \sum_{m,i} \delta(\mathbf{r} - \mathbf{r}_{mi}) \quad (2.61)$$

The segment density (monomer density) counts the number of monomers per unit volume locally. Integration of the right-hand side over the entire volume gives $n_p N$, which is the total number of monomers in volume V , as it should be. Thus $\rho = \langle \rho(\mathbf{r}) \rangle = n_p N / V$ is the global segment density. Mathematically, $\rho(\mathbf{r})$ itself can be a continuous distribution, although the definition given here is for a discrete distribution of the monomers.

The **pair distribution function** is the statistical average of the product of the densities at \mathbf{r}_1 and \mathbf{r}_2 :

$$\langle \rho(\mathbf{r}_1) \rho(\mathbf{r}_2) \rangle = \sum_{m,n=1}^{n_p} \sum_{i,j=1}^N \left\langle \sum_{m,i} \delta(\mathbf{r}_1 - \mathbf{r}_{mi}) \sum_{n,j} \delta(\mathbf{r}_2 - \mathbf{r}_{nj}) \right\rangle = \langle \rho(\mathbf{r}_1 - \mathbf{r}_2) \rho(0) \rangle \quad (2.62)$$

where the last equality holds for a macroscopically homogeneous solution (the system can be microscopically heterogeneous, but after taking statistical average, the system gains a translational symmetry). The pair distribution function depends on $\mathbf{r}_1 - \mathbf{r}_2$. Then, $\langle \rho(\mathbf{r}) \rho(0) \rangle$ is called the **autocorrelation function** (or **correlation function**) of the segment density.

When the solution is isotropic in addition, $\langle \rho(\mathbf{r}) \rho(0) \rangle = \langle \rho(r) \rho(0) \rangle$ is a function of the distance $r = |\mathbf{r}|$ only.

2.4.5.2 Relationship Between the Correlation Function and Structure Factor

The statistical average in the definition of the structure factor $S(\mathbf{k})$ in Eq. 2.60 is taken with respect to the pair distribution. With Eq. 2.62, Eq. 2.60 is rewritten to

$$\begin{aligned} S(\mathbf{k}) &= \frac{1}{n_p N} \int_V d\mathbf{r}_1 \int_V d\mathbf{r}_2 \sum_{m,n=1}^{n_p} \sum_{i,j=1}^N \left\langle \sum_{m,i} \delta(\mathbf{r}_1 - \mathbf{r}_{mi}) \sum_{n,j} \delta(\mathbf{r}_2 - \mathbf{r}_{nj}) \right\rangle \exp[i\mathbf{k} \cdot (\mathbf{r}_1 - \mathbf{r}_2)] \\ &= \frac{1}{n_p N} \int_V d\mathbf{r}_1 \int_V d\mathbf{r}_2 \langle \rho(\mathbf{r}_1) \rho(\mathbf{r}_2) \rangle \exp[i\mathbf{k} \cdot (\mathbf{r}_1 - \mathbf{r}_2)] \\ &= \frac{V}{n_p N} \int_V \langle \rho(\mathbf{r}) \rho(0) \rangle \exp(i\mathbf{k} \cdot \mathbf{r}) d\mathbf{r} \end{aligned} \quad (2.63)$$

With the average density $\rho = n_p N/V$, Eq. 2.63 leads to

$$S(\mathbf{k}) = \frac{1}{\rho} \int_V \langle \rho(\mathbf{r})\rho(0) \rangle \exp(i\mathbf{k} \cdot \mathbf{r}) d\mathbf{r} \quad \begin{array}{l} \text{static structure factor} \\ \text{by segment correlation} \end{array} \quad (2.64)$$

Note that $\rho(0)/\rho$ is the segment density at $\mathbf{r} = 0$ normalized by the average. We can therefore interpret $\langle \rho(\mathbf{r})\rho(0) \rangle/\rho$ as measuring the average number of monomers per volume at \mathbf{r} when there is already a monomer at $\mathbf{r} = 0$.

Equation 2.64 illustrates that the static structure factor, and hence the scattering pattern obtained in the light-scattering experiments, is the **Fourier transform** (see Appendix A2) of the autocorrelation function of the local segment density. $S(\mathbf{k})$ indicates which wave vector components are present in the correlation function.

If the local segment density were continuously distributed at a uniform density ρ , then $\langle \rho(\mathbf{r})\rho(0) \rangle/\rho = \rho$ and $S(\mathbf{k}) = (2\pi)^3 \rho \delta(\mathbf{k})$. A uniform medium does not scatter the light at all (or forward scattering only). Another view is that $S(\mathbf{k})$ is essentially the average of $\exp[i\mathbf{k} \cdot (\mathbf{r}_1 - \mathbf{r}_2)]$ weighted with the pair distribution function $\langle \rho(\mathbf{r}_1)\rho(\mathbf{r}_2) \rangle$.

If $N = 1$ (only nonbonded small particles are present) and correlation between scatterers is absent, that is, $\langle \rho(\mathbf{r})\rho(0) \rangle/\rho = \delta(\mathbf{r})$, then $S(\mathbf{k}) = 1$. The scattering is uniform at all angles. This pattern is observed in the scattering by a solvent. The wavelength λ of visible light is too long to detect any correlations among small particles. On the length scale of λ , $\langle \rho(\mathbf{r})\rho(0) \rangle/\rho = \delta(\mathbf{r})$.

From Eq. A2.7, we find that the inverse-Fourier transform of $S(\mathbf{k})$ gives the correlation function of the segment density:

$$\langle \rho(\mathbf{r})\rho(0) \rangle = \frac{\rho}{(2\pi)^3} \int S(\mathbf{k}) \exp(-i\mathbf{k} \cdot \mathbf{r}) d\mathbf{k} \quad \text{segment density correlation} \quad (2.65)$$

In the isotropic solution, the above Fourier transform and inverse-Fourier transform are

$$S(\mathbf{k}) = \frac{4\pi}{\rho} \int_0^\infty \langle \rho(r)\rho(0) \rangle \frac{\sin kr}{kr} r^2 dr \quad \text{isotropic} \quad (2.66)$$

$$\langle \rho(r)\rho(0) \rangle = \frac{\rho}{2\pi^2} \int_0^\infty S(k) \frac{\sin kr}{kr} k^2 dk \quad \text{isotropic} \quad (2.67)$$

In practice, the relationships between the structure factor and the local monomer concentration $c(\mathbf{r})$ are more useful. The local concentration is related to $\rho(\mathbf{r})$ by

$$c(\mathbf{r}) = \frac{M}{N_A N} \sum_{m,i} \delta(\mathbf{r} - \mathbf{r}_{mi}) = \frac{M}{N_A N} \rho(\mathbf{r}) \quad (2.68)$$

where M is the molecular weight of the polymer chain. The relationships between $S(\mathbf{k})$ and $c(\mathbf{r})$ are

$$S(\mathbf{k}) = \frac{N_A N}{cM} \int_V \langle c(\mathbf{r})c(0) \rangle \exp(i\mathbf{k} \cdot \mathbf{r}) d\mathbf{r} \quad (2.69)$$

where $c = \langle c \rangle = Mn_p/(N_A V)$ is the average concentration, and

$$\langle c(\mathbf{r})c(0) \rangle = \frac{cM}{(2\pi)^3 N_A N} \int S(\mathbf{k}) \exp(-i\mathbf{k} \cdot \mathbf{r}) d\mathbf{k} \quad (2.70)$$

2.4.5.3 Examples in One Dimension Before leaving this subsection, we look at the relationship between the density autocorrelation function and the structure factor for some examples in one-dimensional isotropic systems. Figure 2.37 shows four pairs of $\langle \rho(x)\rho(0) \rangle$ and $S(k)$. Isotropy makes the autocorrelation function an even function of x .

In panel a, $\langle \rho(x)\rho(0) \rangle$ is a constant plus a cosine function with a period of a . This correlation function is observed when $\rho(x)$ changes sinusoidally. The Fourier transform converts the constant into $\delta(k)$ and $\cos(2\pi x/a)$ into $\delta(k - 2\pi/a)$. In part b, $\langle \rho(x)\rho(0) \rangle$ has a harmonic at $k = 4\pi/a$. The density correlation is slightly distorted from the cosine function.

Panel c shows $\langle \rho(x)\rho(0) \rangle$ that consists of more harmonics with a fundamental wave vector being 1/4 of that shown in panels a and b. $\langle \rho(x)\rho(0) \rangle$ has a period equal to the window of x shown, but, within the period, it looks like a decaying

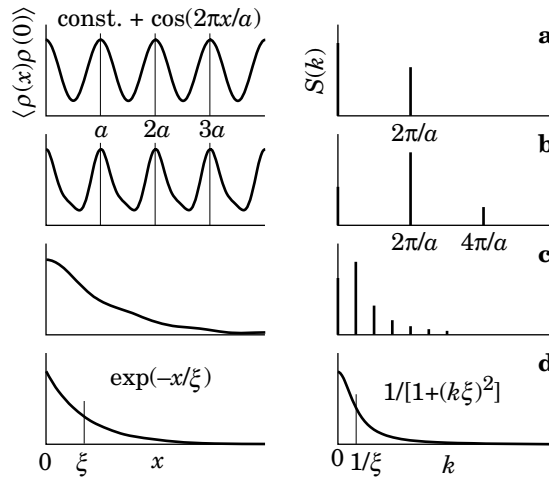


Figure 2.37. Segment density autocorrelation function $\langle \rho(x)\rho(0) \rangle$ and structure factor $S(k)$ for four examples of distribution in one dimension. The autocorrelation functions are cosine + constant (a), with a harmonic (b), with more harmonics (c), and exponential decay (d).

function. Panel d is for an exponentially decaying autocorrelation function with a **correlation length** ξ for all $x \geq 0$. Its Fourier transform is a Lorentzian: $1/[1 + (k\xi)^2]$. We notice that $\langle \rho(x)\rho(0) \rangle$ and $S(k)$ in panel c resemble the counterparts in panel d. In fact, we can construct $\exp(-x/\xi)$ by overlapping many cosine functions as in panel c. $S(k) \propto 1/[1 + (k\xi)^2]$ tells how to overlap these cosine functions of different k .

In the following subsections, we will examine the scattering from polymer chains in three dimensions. Chain connectivity gives rise to a specific pattern in the correlation and the scattering, depending on the conformation.

2.4.6 Structure Factor of a Polymer Chain

2.4.6.1 Low-Angle Scattering At low scattering angles, that is, when k is small,

$$\exp[i\mathbf{k} \cdot (\mathbf{r}_i - \mathbf{r}_j)] \cong 1 + i\mathbf{k} \cdot (\mathbf{r}_i - \mathbf{r}_j) - \frac{1}{2}[\mathbf{k} \cdot (\mathbf{r}_i - \mathbf{r}_j)]^2 + \cdots \quad (2.71)$$

Then, Eq. 2.59 is rewritten to

$$S_1(\mathbf{k}) = N - \frac{1}{2N} \sum_{i,j=1}^N \langle [\mathbf{k} \cdot (\mathbf{r}_i - \mathbf{r}_j)]^2 \rangle + \cdots \quad (2.72)$$

where $\langle \mathbf{r}_i - \mathbf{r}_j \rangle = 0$ was used. In this equation,

$$\langle [\mathbf{k} \cdot (\mathbf{r}_i - \mathbf{r}_j)]^2 \rangle = k^2 \langle [\hat{\mathbf{k}} \cdot (\mathbf{r}_i - \mathbf{r}_j)]^2 \rangle = k^2 \langle (x_i - x_j)^2 \rangle = \frac{1}{3} k^2 \langle (\mathbf{r}_i - \mathbf{r}_j)^2 \rangle \quad (2.73)$$

where $\hat{\mathbf{k}} = \mathbf{k}/k$, and the x direction is taken to be parallel to \mathbf{k} . The isotropy of the chain configuration [$\langle (x_i - x_j)^2 \rangle = \langle (y_i - y_j)^2 \rangle = \langle (z_i - z_j)^2 \rangle$] was used in the last equality. Thus $S_1(\mathbf{k})$ is further converted to

$$S_1(\mathbf{k}) = N - k^2 \frac{1}{6N} \sum_{i,j=1}^N \langle (\mathbf{r}_i - \mathbf{r}_j)^2 \rangle + \cdots = N(1 - k^2 R_g^2/3 + \cdots) \quad (2.74)$$

where Eq. 1.25 ($N \gg 1$) was used. It is usually rewritten to

$$S_1(\mathbf{k}) \cong \frac{N}{1 + k^2 R_g^2/3} \quad kR_g < 1, \text{ any conformation} \quad (2.75)$$

The last expression compensates the neglect of the higher-order terms in Eq. 2.72 to some extent.

We did not assume any specific chain conformation or a chain model to derive Eqs. 2.74 and 2.75. The formulas apply to any chain conformation. When the reciprocal of the light-scattering intensity is plotted as a function of k^2 , the slope in the small k limit is equal to $R_g^2/3$, as illustrated in Figure 2.38.

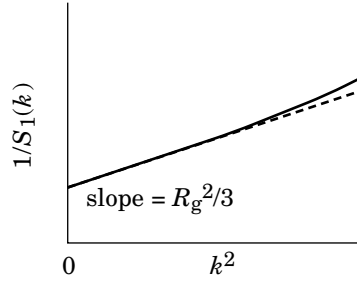


Figure 2.38. Reciprocal of the single-chain structure factor $S_1(k)$ plotted as a function of the square of the scattering vector k has a slope equal to $R_g^2/3$ at low angles.

2.4.6.2 Scattering by a Gaussian Chain It is possible to calculate $S_1(\mathbf{k})$ in the whole range of k for a Gaussian chain without approximations. A continuous version of Eq. 2.59 is needed for the definition of $S_1(\mathbf{k})$.

$$S_1(\mathbf{k}) = \frac{1}{N} \int_0^N dn \int_0^N dn' \langle \exp[i\mathbf{k} \cdot (\mathbf{r} - \mathbf{r}')] \rangle \quad (2.76)$$

where the statistical average in the integrand is taken with respect to \mathbf{r} and \mathbf{r}' , the spatial positions of the segments at distance n and n' , respectively, from the chain end (Fig. 2.39). Because a partial chain between the two segments is also a Gaussian chain (see Section 1.3 and Eq. 1.34),

$$\begin{aligned} \langle \exp[i\mathbf{k} \cdot (\mathbf{r} - \mathbf{r}')] \rangle &= \int d(\mathbf{r} - \mathbf{r}') \exp[i\mathbf{k} \cdot (\mathbf{r} - \mathbf{r}')] (2\pi|n - n'|b^2/3)^{-3/2} \\ &\quad \times \exp\left(-\frac{3(\mathbf{r} - \mathbf{r}')^2}{2|n - n'|b^2}\right) \\ &= \exp(-\frac{1}{6}\mathbf{k}^2|n - n'|b^2) \end{aligned} \quad (2.77)$$

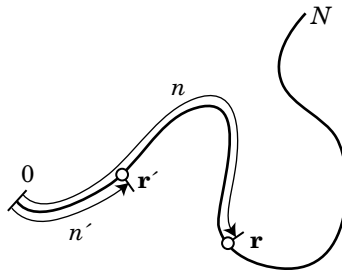


Figure 2.39. Scattering by two monomers at \mathbf{r}' and \mathbf{r} at distances n' and n along the chain from its end interferes.

which is essentially the Fourier-transform of the Gaussian probability density. Because the probability density is isotropic, its Fourier transform is also isotropic. The double integral with respect to n and n' leads to

$$S_1(\mathbf{k}) = \frac{1}{N} \int_0^N \mathrm{d}n \int_0^N \mathrm{d}n' \exp\left(-\frac{1}{6} \mathbf{k}^2 |n - n'| b^2\right) = N f_D(kR_g) \quad (2.78)$$

where $f_D(x)$ is called a Debye function and defined as

$$f_D(x) = 2x^{-2} \left[1 - x^{-2} \left(1 - \exp(-x^2) \right) \right] \quad \text{Debye function, Gaussian} \quad (2.79)$$

At $x \gg 1$, $f_D(x) \cong 2x^{-2}$. At $x \ll 1$, $f_D(x) \cong 1 - x^2/3$, in agreement with Eq. 2.74. Figure 2.40 shows $N/S_1(\mathbf{k}) = N/S_1(k) = [f_D(kR_g)]^{-1}$ as a function of kR_g . The slope is $1/3$ at low scattering angles and $1/2$ at high angles.

The density autocorrelation function for two segments on the Gaussian chain is given as

$$\frac{1}{\rho} \langle \rho(\mathbf{r}) \rho(\mathbf{r}') \rangle = \frac{1}{N} \int_0^N \mathrm{d}n \int_0^N \mathrm{d}n' (2\pi |n - n'| b^2/3)^{-3/2} \exp\left(-\frac{3(\mathbf{r} - \mathbf{r}')^2}{2|n - n'| b^2}\right) \quad (2.80)$$

After some calculations (see Appendix 2.C), Eq. 2.80 with $\mathbf{r}' = 0$ simplifies to

$$\frac{1}{\rho} \langle \rho(\mathbf{r}) \rho(0) \rangle = \frac{N}{\pi^{3/2}} \frac{1}{rR_g^2} \left[(1 + 2u) \text{Erfc}(u^{1/2}) - u^{1/2} \exp(-u) \right] \quad (2.81)$$

where $u = (r/2R_g)^2$ and the error function $\text{Erfc}(x)$ is defined by

$$\text{Erfc}(x) \equiv \int_x^\infty \exp(-t^2) \mathrm{d}t \quad (2.82)$$

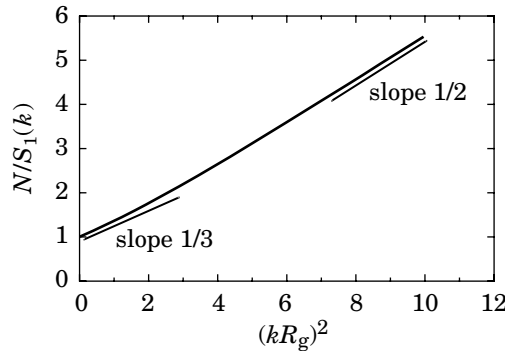


Figure 2.40. Reciprocal of the static structure factor $S_1(k)$ of a Gaussian chain. $N/S_1(k)$ is a linear function of k^2 at both $kR_g \ll 1$ and $kR_g \gg 1$ but with different slopes.

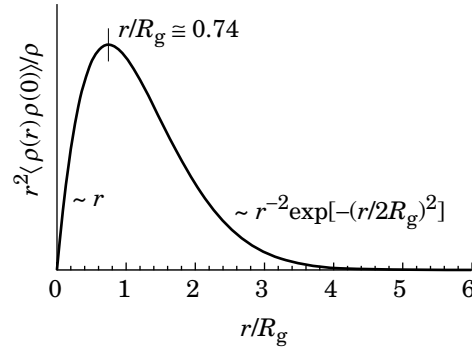


Figure 2.41. Probability distribution for the distance r of other segments from a given segment in a Gaussian chain. The segment density autocorrelation function $\langle \rho(r)\rho(0) \rangle / \rho$ multiplied by r^2 is plotted as a function of r/R_g . Short-distance and long-distance asymptotes are indicated.

Now we examine $\langle \rho(r)\rho(0) \rangle / \rho$ in the small r and large r asymptotes. When $x \ll 1$, $\text{Erfc}(x) \cong \pi^{1/2}/2 - x$. Then, at short distances,

$$\frac{1}{\rho} \langle \rho(r)\rho(0) \rangle = \frac{N}{2\pi} \frac{1}{rR_g^2} \quad (2.83)$$

This relationship can also be intuitively obtained in the following discussion. When $r < R_g$, a partial chain of n segments is contained in the sphere of a radius $r = bn^{1/2}/2$. The average segment density within the sphere is

$$\frac{1}{\rho} \langle \rho(r)\rho(0) \rangle = \frac{n}{(4\pi/3)r^3} = \frac{3}{\pi r b^2} = \frac{N}{2\pi} \frac{1}{rR_g^2} \quad (2.84)$$

When $x \gg 1$, $\text{Erfc}(x) \cong \exp(-x^2)[1/(2x) - 1/(4x^3) + 3/(8x^5)]$. Thus, over long distances, the correlation is lost exponentially:

$$\frac{1}{\rho} \langle \rho(\mathbf{r})\rho(0) \rangle = \frac{4N}{\pi^{3/2}} \frac{R_g}{r^4} \exp[-(r/2R_g)^2] \quad (2.85)$$

Figure 2.41 is a plot of $r^2 \langle \rho(r)\rho(0) \rangle / \rho$. The prefactor r^2 is for the surface area of the sphere of radius r . Note that $4\pi r^2 \langle \rho(r)\rho(0) \rangle / \rho dr$ is the probability of finding another segment at distance between r and $r + dr$ from a given segment for this isotropic autocorrelation function. When $r \ll R_g$, $r^2 \langle \rho(r)\rho(0) \rangle / \rho$ is proportional to r . When $r \gg R_g$, $r^2 \langle \rho(r)\rho(0) \rangle / \rho \sim r^{-2} \exp[-(r/2R_g)^2]$. The probability peaks at $r/R_g \cong 0.74$. The other segments can be most probably found at a distance of $r \cong 0.74 \times R_g$.

2.4.6.3 Scattering by a Real Chain At low-scattering angles, $S_1(\mathbf{k})$ of a real chain is essentially the same as that of the Gaussian chain when plotted as a function of R_g , as we have seen in Section 2.4.6.1. At high angles, however, $S_1(\mathbf{k})$ of the real chain does not follow k^{-2} dependence. Intuitively, $S_1(\mathbf{k})$ at large \mathbf{k} can be obtained from the pair distribution function of two segments within a sphere of radius R_g . For the real chain with $r \cong bn^\nu$, Eq. 2.84 changes to

$$\frac{1}{\rho} \langle \rho(\mathbf{r})\rho(0) \rangle \cong \frac{n}{r^3} = r^{1/\nu-3} b^{-1/\nu} \quad (r < R_g) \quad (2.86)$$

The correlation decays as $r^{-4/3}$ (or $r^{-1.31}$) with an increasing r at short distances in a real chain, as opposed to r^{-1} in the Gaussian chain. Figure 2.42 compares $r^2 \langle \rho(r)\rho(0) \rangle$ for the real chain obtained in the computer simulation²⁰ and the Gaussian chain. What is plotted here is $r^2 \langle \rho(r)\rho(0) \rangle$, which is proportional to the probability of finding a segment at r from another segment at $\mathbf{r} = 0$. At $r \ll R_g$, the real chain has a slightly higher value ($r^{0.69}$ vs. r^1). The peak position relative to R_g is greater for the real chain. The monomers are more spread in the real chain. However, the difference is small.

The Fourier transform of Eq. 2.86 by Eq. 2.66 gives

$$S_1(k) \cong \frac{4\pi}{k} b^{-1/\nu} \int r^{1/\nu-2} \sin kr \, dr \quad (2.87)$$

The integrand is valid only for $r < R_g$, but, at large k ($kR_g \gg 1$), $\sin kr$ is a rapidly varying function, especially for large r ($r > R_g$). Therefore, the contribution of the integral from $r > R_g$ is negligible, and we can use the same integrand from

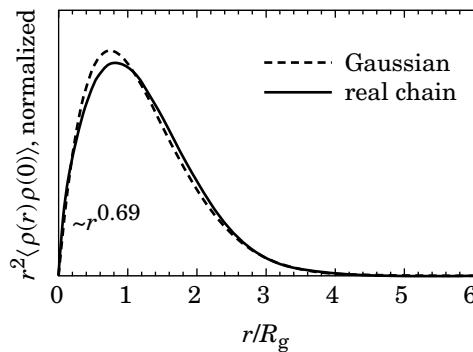


Figure 2.42. Comparison of $r^2 \langle \rho(r)\rho(0) \rangle$ for a real chain and a Gaussian chain. At short distance, the real chain follows a power law of $r^{0.69}$, as opposed to r^1 for the Gaussian chain.

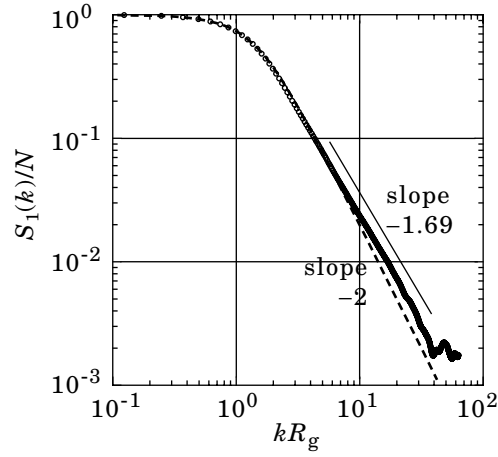


Figure 2.43. Comparison of $S_1(k)$ of a self-avoiding walk on a cubic lattice obtained in computer simulation with a Debye function. When $S_1(k)/N$ is plotted as a function of kR_g , the Debye function describes $S_1(k)$ of a self-avoiding walk at low angles, but they have different dependences at high angles. The self-avoiding walk follows the power law of $S_1 \sim k^{-1.69}$ as predicted by the theory. (From Ref. 5.)

$r = 0$ to ∞ :

$$\begin{aligned} S_1(k) &= \frac{4\pi}{k} b^{-1/\nu} \int_0^\infty r^{1/\nu-2} \sin kr dr \\ &= \frac{4\pi}{k} b^{-1/\nu} \frac{\Gamma(1/\nu-1)}{k^{1/\nu-1}} \sin \frac{(1/\nu-1)\pi}{2} \cong \frac{1}{(kb)^{1/\nu}} \end{aligned} \quad (2.88)$$

See Appendix A3. At high angles, $S_1(\mathbf{k}) \sim k^{-1/\nu} \cong k^{-5/3}$.

Figure 2.43 compares $S_1(\mathbf{k})/N = S_1(k)/N$ obtained in the cubic lattice Monte Carlo simulations for a real chain and the Debye function.⁵ At $kR_g < 1$, $S_1(k)/N$ of the real chain follows the Debye function, but, at large kR_g , $S_1(k)/N$ deviates from the Debye function (slope -2) and follows $\sim k^{-1.69}$ as predicted.

2.4.6.4 Form Factors The plot of $S_1(\mathbf{k})$ as a function of k^2 at small k gives the radius of gyration for any conformation, but, beyond that range, $S_1(\mathbf{k})$ depends on the conformation. For a Gaussian chain, $S_1(\mathbf{k})$ follows the Debye function. Equations 2.59 and 2.76 allow us to calculate $S_1(\mathbf{k})$ for other conformations. Let us first define a **form factor** $P(\mathbf{k})$ by

$$P(\mathbf{k}) \equiv \frac{S_1(\mathbf{k})}{S(0)} = \frac{1}{N} S_1(\mathbf{k}) \quad \text{form factor} \quad (2.89)$$

It is also called a shape factor or an internal structure factor. For a Gaussian chain, it is

$$P_{\text{Gaussian}}(\mathbf{k}) = f_D(kR_g) \quad (2.90)$$

Let us calculate $P(\mathbf{k})$ for a spherical molecule of radius R_s stuffed uniformly with monomers that scatter light with the same intensity. Now we use Eq. 2.76 to directly integrate with respect to \mathbf{r} and \mathbf{r}' in the sphere:

$$P_{\text{sphere}}(\mathbf{k}) = \frac{1}{V_{\text{sp}}^2} \int_{V_{\text{sp}}} d\mathbf{r} \int_{V_{\text{sp}}} d\mathbf{r}' \exp[i\mathbf{k} \cdot (\mathbf{r} - \mathbf{r}')] = \left| \frac{1}{V_{\text{sp}}} \int_{V_{\text{sp}}} d\mathbf{r} \exp(i\mathbf{k} \cdot \mathbf{r}) \right|^2 \quad (2.91)$$

where the integral is carried out over the volume $V_{\text{sp}} = (4\pi/3)R_s^3$ of the sphere. After some calculations (Problem 2.19), we find that

$$P_{\text{sphere}}(\mathbf{k}) = [3x^{-3}(\sin x - x \cos x)]^2 \quad \text{with } x = kR_s \quad (2.92)$$

For a rodlike molecule with length L , it can be shown that (Problem 2.20)

$$P_{\text{rod}}(\mathbf{k}) = x^{-1} \int_0^{2x} \frac{\sin z}{z} dz - \left(\frac{\sin x}{x} \right)^2 \quad \text{with } x = kL/2 \quad (2.93)$$

Figure 2.44 summarizes $P(\mathbf{k}) = P(k)$ for three polymer conformations of a simple geometry. Figure 2.45 compares $P_{\text{Gaussian}}(k)$, $P_{\text{sphere}}(k)$, and $P_{\text{rod}}(k)$ plotted as a function of kR_g . The three factors are identical for $kR_g \ll 1$ as required. At higher kR_g , the three curves are different.

We now calculate the form factor $P_{\text{star}}(k)$ for an n_A -arm star polymer with a uniform arm length N_1 . When calculating the average of $\exp[i\mathbf{k} \cdot (\mathbf{r} - \mathbf{r}')]$, it is necessary to distinguish two cases for \mathbf{r} and \mathbf{r}' : (1) being on the same arm and (2) being on different arms. The former takes place with a probability of $1/n_A$. Then,

$$P_{\text{star}}(\mathbf{k}) = \frac{1}{n_A} \langle\langle \exp[i\mathbf{k} \cdot (\mathbf{r} - \mathbf{r}')] \rangle\rangle_1 + \left(1 - \frac{1}{n_A} \right) \langle\langle \exp[i\mathbf{k} \cdot (\mathbf{r} - \mathbf{r}')] \rangle\rangle_2 \quad (2.94)$$

where the subscripts 1 and 2 correspond to the two cases, and $\langle\langle \exp[i\mathbf{k} \cdot (\mathbf{r} - \mathbf{r}')] \rangle\rangle$ stands for the average of $\langle \exp[i\mathbf{k} \cdot (\mathbf{r} - \mathbf{r}')] \rangle$ with respect to the two monomers over

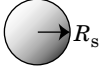
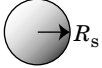
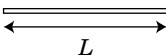
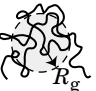
shape		R_g^2	x	$P(\mathbf{k})$
spherical		$(3/5)R_s^2$	kR_s	$[3x^{-3}(\sin x - x \cos x)]^2$
rodlike		$L^2/12$	$kL/2$	$x^{-1} \int_0^{2x} z^{-1} \sin z dz - (x^{-1} \sin x)^2$
Gaussian		$b^2 N/6$	kR_g	$2x^{-2}[1 - x^{-2}(1 - \exp(-x^2))]$

Figure 2.44. Polymers with a simple geometry and their form factors.

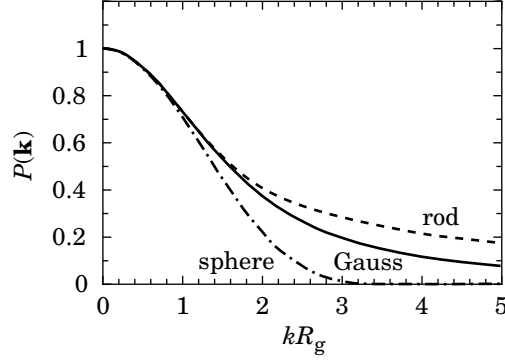


Figure 2.45. Form factor $P(k)$ for a spherical molecule, a rodlike molecule, and a Gaussian chain, plotted as a function of kR_g .

the length of the arm(s). Using, Eq. 2.78, we have

$$\langle\langle \exp[i\mathbf{k} \cdot (\mathbf{r} - \mathbf{r}')]] \rangle\rangle_1 = f_D(kR_{g1}) \quad (2.95)$$

where $R_{g1}^2 = N_1 b^2 / 6 = R_g^2 / (3 - 2/n_A)$ is the mean square radius of gyration of the arm, with R_g being the radius of gyration of the whole star polymer (see Eq. 1.84). In the second average,

$$\begin{aligned} \langle\langle \exp[i\mathbf{k} \cdot (\mathbf{r} - \mathbf{r}')]] \rangle\rangle_2 &= \langle\langle \exp[i\mathbf{k} \cdot (\mathbf{r} - \mathbf{r}_0) + i\mathbf{k} \cdot (\mathbf{r}_0 - \mathbf{r}')]] \rangle\rangle \\ &= \langle\langle \exp[i\mathbf{k} \cdot (\mathbf{r} - \mathbf{r}_0)] \rangle\rangle \langle\langle \exp[i\mathbf{k} \cdot (\mathbf{r}_0 - \mathbf{r}')]] \rangle\rangle = |\langle\langle \exp[i\mathbf{k} \cdot (\mathbf{r} - \mathbf{r}_0)] \rangle\rangle|^2 \end{aligned} \quad (2.96)$$

where \mathbf{r}_0 is the position of the core of the star polymer, and the average in the last equation is calculated for a single arm as

$$\begin{aligned} \langle\langle \exp[i\mathbf{k} \cdot (\mathbf{r} - \mathbf{r}_0)] \rangle\rangle &= \frac{1}{N_1} \int_0^{N_1} dn \langle \exp[i\mathbf{k} \cdot (\mathbf{r} - \mathbf{r}_0)] \rangle \\ &= \frac{1}{N_1} \int_0^{N_1} dn \exp(-\frac{1}{6} k^2 n b^2) = (kR_{g1})^{-2} [1 - \exp(-(kR_{g1})^2)] \end{aligned} \quad (2.97)$$

Thus,

$$P_{\text{star}}(k) = \frac{1}{n_A} f_D(kR_{g1}) + \left(1 - \frac{1}{n_A}\right) \left((kR_{g1})^{-2} [1 - \exp(-(kR_{g1})^2)] \right)^2 \quad (2.98)$$

The difference in $P_{\text{star}}(k)$ between a 2-arm star (= linear chain) and a 6-arm star is not as striking as the difference between a Gaussian chain and a rodlike molecule. At low kR_g , all the curves overlap (not shown), as required. At $kR_{g1} \gg 1$, the second term becomes negligible, and the scattering comes mostly from two nearby monomers on the same arm. The difference in $P_{\text{star}}(k)$ is, however, clearly seen in the plot of $(kR_g)^2 P_{\text{star}}(k)$ as a function of kR_g . Figure 2.46 compares the form factor

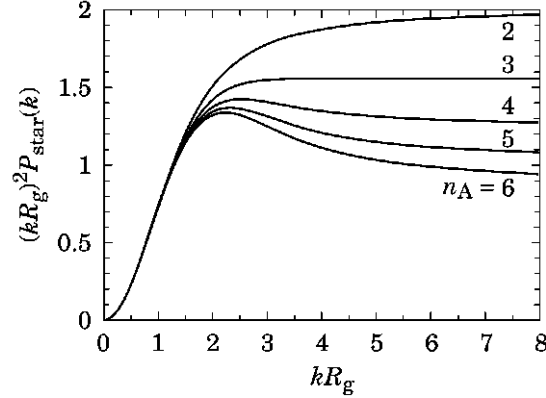


Figure 2.46. Plot of $(kR_g)^2 P_{\text{star}}(k)$ of an n_A -arm star polymer as a function of kR_g . The number adjacent to each curve indicates n_A .

for star polymers with $n_A = 2, 3, 4, 5,$ and 6 . For $n_A = 3$, $(kR_g)^2 P_{\text{star}}(k)$ approaches the asymptote of $14/9$ at high kR_g . For $n_A \geq 4$, there is a peaking at around $kR_g \cong 2$. The peaking, also observed in a spherical molecule, indicates the compactness of the polymer molecule.

2.4.7 Light Scattering of a Polymer Solution

2.4.7.1 Scattering in a Solvent We have assumed so far that polymer chains and particles are suspended in vacuum. Now we consider the light scattered by a fluid or, in general, a continuous dielectric medium of scattering volume V . Scattering by particles suspended in a solvent is obtained from the Rayleigh scattering formula for particles in vacuum. In a medium with a refractive index n , the wavelength is λ/n and the electric permittivity is $\epsilon_0 n^2$. In Eq. 2.45, we change λ to λ/n , ϵ_0 to $\epsilon = \epsilon_0 n^2$, and α to α_{ex} , where α_{ex} is the excess polarizability of the suspended particle relative to the surrounding medium. The result is

$$\frac{I}{I_0} = \frac{\pi^2}{(\lambda/n)^4} \frac{\alpha_{\text{ex}}^2}{(\epsilon_0 n^2)^2} \frac{\sin^2 \theta'}{r^2} = \frac{\pi^2}{\lambda^4} \frac{\alpha_{\text{ex}}^2}{\epsilon_0^2} \frac{\sin^2 \theta'}{r^2} \quad (2.99)$$

In effect, α is replaced by α_{ex} , but no other changes. The wavelength λ refers to the one in vacuum. The other equations (Eqs. 2.55 and 2.58) are rewritten in the same way.

It is more convenient to extend Eq. 2.99 to include spatial fluctuations in α_{ex} . Every part of the scattering volume has naturally occurring fluctuations in the density and, for solutions, also in the concentration, as illustrated in Figure 2.47. The density and concentration are slightly different from place to place. The density fluctuations and concentration fluctuations cause fluctuations in α_{ex} through fluctuations $\Delta \epsilon_r$ in the relative electric permittivity $\epsilon_r = \epsilon/\epsilon_0$ (also called dielectric

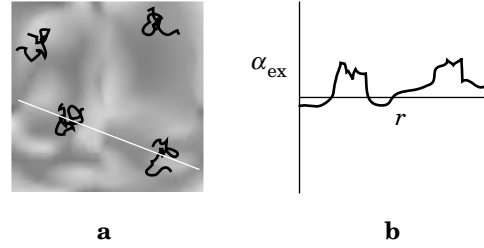


Figure 2.47. Spatial variations of the local solvent density and the polymer concentration lead to fluctuation in the excess polarizability α_{ex} . The plot in b shows α_{ex} along the white line in a.

constant) because the latter is determined by the number of charges (electrons and protons) in a unit volume. The Clausius-Mossotti equation gives the extra polarizability $d\alpha_{\text{ex}}$ due to $\Delta\epsilon_r$ of a small volume $d\mathbf{r}$ at \mathbf{r} as $d\alpha_{\text{ex}} = \epsilon_0\Delta\epsilon_r d\mathbf{r}$, when ϵ_r is not too large (which is the case in water and most organic solvents; Problem 2.24). Note that $d\alpha_{\text{ex}}$ can be either positive or negative depending on the sign of $\Delta\epsilon_r$. Because $\epsilon_r = n^2$ in the visible range of the spectrum, $d\alpha_{\text{ex}}(\mathbf{r}) = 2\epsilon_0 n \Delta n(\mathbf{r}) d\mathbf{r}$. As the refractive index fluctuation Δn is different from place to place in the volume, $d\alpha$ also depends on \mathbf{r} . Similar to the calculation of interference of light scattered by different parts of a polymer chain in Section 2.4.3, we can calculate contributions from different parts of the volume. The extension of Eq. 2.55 gives the total scattering intensity I as

$$\begin{aligned} \frac{I}{I_0} &= \frac{\pi^2}{\lambda^4 r^2} \int \frac{d\alpha_{\text{ex}}(\mathbf{r}_1)}{\epsilon_0} \int \frac{d\alpha_{\text{ex}}(\mathbf{r}_2)}{\epsilon_0} \exp[i\mathbf{k} \cdot (\mathbf{r}_1 - \mathbf{r}_2)] \\ &= \frac{4\pi^2 n^2}{\lambda^4 r^2} \int_V d\mathbf{r}_1 \int_V d\mathbf{r}_2 \Delta n(\mathbf{r}_1) \Delta n(\mathbf{r}_2) \exp[i\mathbf{k} \cdot (\mathbf{r}_1 - \mathbf{r}_2)] \end{aligned} \quad (2.100)$$

where the integrals are calculated over the scattering volume V (Fig. 2.33).

2.4.7.2 Scattering by a Polymer Solution Light-scattering study of a polymer is usually carried out by first measuring the scattering intensity I_S of the pure solvent at different angles θ and then repeating the procedure on polymer solutions to obtain the scattering intensity I at different angles. The excess scattering (I_{ex}) is defined by $I_{\text{ex}} \equiv I - I_S$ (Fig. 2.48). Usually I_S is flat, if V is constant, by the reason explained in Section 2.4.5.

In Eq. 2.100, $\Delta n(\mathbf{r})$ has two components: $\Delta_d n(\mathbf{r})$ and $\Delta_c n(\mathbf{r})$. The former is due to density fluctuations of the fluid that appears also in I_S . The latter is caused by concentration fluctuations of the polymer and is unique to the solutions. The excess scattering I_{ex} is due to $\Delta_c n(\mathbf{r})$:

$$\frac{I_{\text{ex}}}{I_0} = \frac{4\pi^2 n^2}{\lambda^4 r^2} \int_V d\mathbf{r}_1 \int_V d\mathbf{r}_2 \langle \Delta_c n(\mathbf{r}_1) \Delta_c n(\mathbf{r}_2) \rangle \exp[i\mathbf{k} \cdot (\mathbf{r}_1 - \mathbf{r}_2)] \quad (2.101)$$

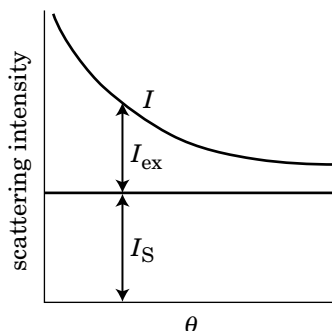


Figure 2.48. The excess scattering I_{ex} is the increment in the scattering intensity of the polymer solution, I , over that of the pure solvent, I_S .

where the statistical average is taken with respect to the concentration fluctuations. We set the reference for n to the refractive index of the solvent. The refractive index fluctuation $\Delta_c n(\mathbf{r})$ is related to the concentration fluctuation $\Delta c(\mathbf{r})$ by

$$\Delta_c n(\mathbf{r}) = \frac{dn}{dc} \Delta c(\mathbf{r}) \quad (2.102)$$

where dn/dc is called the **differential refractive index** (or **specific refractive index increment**). It expresses how much the refractive index of the polymer solution increases as the concentration c of the polymer increases. Each polymer–solvent pair has its own value of dn/dc . It also depends on the temperature and the wavelength. Roughly, dn/dc is approximated by

$$\frac{dn}{dc} \cong (n_{\text{polymer}} - n_{\text{solvent}})v_{\text{sp}} \quad (2.103)$$

where n_{polymer} and n_{solvent} are the refractive indices of the bulk polymer in the amorphous state and of the solvent, respectively, and v_{sp} is the specific volume of the polymer in the solution. If the volumes of the polymer and the solvent are additive, v_{sp} is the reciprocal of the density of the polymer.

Note that dn/dc can be positive or negative, depending on whether the polymer has a higher refractive index than the solvent does. As we will see below, the scattering intensity is proportional to $(dn/dc)^2$. A greater contrast in the refractive index between the polymer and the solvent gives a stronger scattering. In some polymer–solvent systems, dn/dc is near zero, making the excess scattering near zero. Then, the polymer is optically indistinguishable from the solvent. This condition is called **index matching**. A solvent **isorefractive** with the polymer makes the polymer invisible.

2.4.7.3 Concentration Fluctuations With Eq. 2.102, Eq. 2.101 is rewritten to

$$\frac{I_{\text{ex}}(\mathbf{k})}{I_0} = \frac{4\pi^2 n^2}{\lambda^4 r^2} \left(\frac{dn}{dc} \right)^2 \psi_{\text{cc}}(\mathbf{k}) \quad (2.104)$$

with $\psi_{\text{cc}}(\mathbf{k})$ being the Fourier transform for the correlation function of the concentration fluctuations:

$$\psi_{\text{cc}}(\mathbf{k}) \equiv \int_V d\mathbf{r}_1 \int_V d\mathbf{r}_2 \langle \Delta c(\mathbf{r}_1) \Delta c(\mathbf{r}_2) \rangle \exp[i\mathbf{k} \cdot (\mathbf{r}_1 - \mathbf{r}_2)] \quad (2.105)$$

We consider $\psi_{\text{cc}}(\mathbf{k})$ in the limit of $\mathbf{k} = 0$ and in the low concentration limit separately. First, at $\mathbf{k} = 0$,

$$\psi_{\text{cc}}(0) = \left\langle \left[\int_V d\mathbf{r}_1 \Delta c(\mathbf{r}_1) \right]^2 \right\rangle = V^2 \langle \Delta c_{\text{tot}}^2 \rangle \quad (2.106)$$

where Δc_{tot} is the fluctuation in the overall concentration in the scattering volume. It is not the local concentration fluctuation $\Delta c(\mathbf{r}) = c(\mathbf{r}) - \langle c \rangle$ with $\langle c \rangle = Mn_p / (N_A V)$ defined in Eq. 2.68. The scattering volume is not in any container, and the solvent and solid molecules are free to leave the volume and enter the volume from the surroundings. The system is open to exchange of matter. Now we use the osmotic compressibility requirement for an open system in general:

$$\boxed{\langle \Delta c_{\text{tot}}^2 \rangle = \frac{ck_B T}{V} \frac{\partial c}{\partial \Pi} \quad \text{osmotic compressibility requirement}} \quad (2.107)$$

The relationship can be obtained from the statistical mechanics for the open system (Problem 2.25). From the virial expansion of Π given in Eq. 2.20,

$$\frac{\partial \Pi}{\partial c} = N_A k_B T \left[\frac{1}{M} + 2A_2 c + \dots \right] \quad (2.108)$$

From Eqs. 2.106–2.108, we find

$$\psi_{\text{cc}}(0) = \frac{cV}{N_A} \left[\frac{1}{M} + 2A_2 c + \dots \right]^{-1} \quad (2.109)$$

Next, we consider $\psi_{\text{cc}}(\mathbf{k})$ for a small \mathbf{k} in the low-concentration limit. Because $\langle \Delta c(\mathbf{r}_1) \Delta c(\mathbf{r}_2) \rangle = \langle c(\mathbf{r}_1) c(\mathbf{r}_2) \rangle - c^2$, Eq. 2.70 leads to

$$\langle \Delta c(\mathbf{r}_1) \Delta c(\mathbf{r}_2) \rangle = \frac{cM}{(2\pi)^3 N_A N} \int S(\mathbf{k}') \exp[-i\mathbf{k}' \cdot (\mathbf{r}_1 - \mathbf{r}_2)] d\mathbf{k}' - c^2 \quad (2.110)$$

Then, Eq. 2.105 leads to

$$\begin{aligned}\psi_{cc}(\mathbf{k}) &= \frac{cM}{(2\pi)^3 N_A N} \int S(\mathbf{k}') d\mathbf{k}' \int_V d\mathbf{r}_1 \int_V d\mathbf{r}_2 \exp[i(\mathbf{k} - \mathbf{k}') \cdot (\mathbf{r}_1 - \mathbf{r}_2)] \\ &\quad - c^2 \int_V d\mathbf{r}_1 \int_V d\mathbf{r}_2 \exp[i\mathbf{k} \cdot (\mathbf{r}_1 - \mathbf{r}_2)] \\ &= \frac{cMV}{N_A N} S(\mathbf{k}) - (2\pi)^3 c^2 V \delta(\mathbf{k})\end{aligned}\quad (2.111)$$

where Eq. A1.8 was used. The second term is nonzero only at $\mathbf{k} = 0$ (forward scattering). Because $I_{ex}(\mathbf{k})/I_0 \propto \psi_{cc}(\mathbf{k})$, the negative sign for this term indicates how the concentration fluctuations decrease the intensity of unscattered light. We neglect this second term because it is not what is detected by the photodetector in the static light scattering experiments. We thus find from Eq. 2.75 that, at small \mathbf{k} ,

$$\psi_{cc}(k) = \frac{cMV}{N_A N} \frac{N}{1 + k^2 R_g^2/3} = \frac{cV}{N_A} M(1 + k^2 R_g^2/3)^{-1} \quad (2.112)$$

Combining Eqs. 2.109 and 2.112, we obtain $\psi_{cc}(k)$ as

$$\psi_{cc}(k) = \frac{cV}{N_A} (1 + k^2 R_g^2/3)^{-1} \left[\frac{1}{M} + 2A_2c + \dots \right]^{-1} \quad (2.113)$$

This expression applies to small scattering angles and low concentrations.

2.4.7.4 Light-Scattering Experiments From Eqs. (2.104) and (2.113), we finally obtain

$$\boxed{\frac{I_{ex}(k)}{I_0} = \frac{1}{N_A} \frac{4\pi^2 n^2}{\lambda^4} \left(\frac{dn}{dc} \right)^2 \frac{cV}{r^2} (1 + k^2 R_g^2/3)^{-1} \left[\frac{1}{M} + 2A_2c + \dots \right]^{-1}} \quad (2.114)$$

Here we introduce the **Rayleigh ratio** R_θ according to

$$\frac{I_{ex}}{I_0} \equiv \frac{R_\theta V}{r^2} \quad (2.115)$$

The Rayleigh ratio eliminates the geometry-dependent factors in $I_{ex}(k)/I_0$ such as the scattering volume $V(\theta)$ and the detector-sample distance r and retains the factors related to the solution only. In the actual measurement system, I_0 and $V(\theta)$ cannot be measured correctly. Therefore, a pure solvent such as benzene and toluene is used as a calibration standard. See Refs. 21 and 22 for details. With R_θ , Eq. 2.114 is rewritten to

$$\boxed{\frac{Hc}{R_\theta} = \frac{1}{M} \left(1 + \frac{1}{3} k^2 R_g^2 + 2A_2Mc + \dots \right)} \quad \text{static light scattering, monodisperse} \quad (2.116)$$

where

$$H \equiv \frac{1}{N_A} \left(\frac{2\pi n}{\lambda^2} \frac{dn}{dc} \right)^2 \quad (2.117)$$

The equations we derived in the above assume that the polymer in solution is monodisperse. Usually, the polymer is polydisperse. M and R_g that we obtain in the static light-scattering experiments are then averages of M and R_g . Below we find what kind of averages they are.

For a monodisperse polymer, $I_{\text{ex}}/I_0 \propto cM - (1/3)k^2cMR_g^2$ in the low concentration limit. When the solution contains components of molecular weight M_i and radius of gyration R_{gi} at concentration c_i ($c = \sum c_i$), the total excess scattering intensity from all the components is

$$I_{\text{ex}}/I_0 \propto \sum_i c_i M_i - \frac{k^2}{3} \sum_i c_i M_i R_{gi}^2 = c \sum_i \frac{c_i}{c} M_i \left[1 - \frac{k^2}{3} \frac{\sum_i c_i M_i R_{gi}^2}{\sum_i c_i M_i} \right] \quad (2.118)$$

Because c_i/c is the weight fraction of component i , $\sum_i (c_i/c)M_i = M_w$ by definition. For R_g^2 , $c_i M_i$ is proportional to the product of the weight fraction and M_i . Thus, the average for R_g^2 is the z -average.

$$\boxed{\frac{Hc}{R_\theta} = \frac{1}{M_w} \left(1 + \frac{1}{3}k^2 \langle R_g^2 \rangle_z \tau 2A_2 M_w c + \dots \right)} \quad \text{static light scattering, polydisperse} \quad (2.119)$$

There is also an effect of the polydispersity on A_2 , but the effect is usually weak, as we have seen in Section 2.2.3.

2.4.7.5 Zimm Plot Here we learn how M_w , $\langle R_g^2 \rangle_z$, and A_2 are evaluated in the light-scattering experiments conducted on solutions of finite concentrations and at finite scattering angles. The excess scattering intensity is recorded at different scattering angles. The measurement is repeated for several concentrations of the polymer at the same set of angles for a given polymer solution. The intensity data are converted into Hc/R_θ and plotted as a function of $\sin^2(\theta/2) + \text{const.} \times c$. The constant is arbitrary. The plot is called a **Zimm plot**. Open circles in Figure 2.49 illustrate the ideal data. Each dashed line represents a series of measurements at a constant angle. Each solid gray line is for those at a constant concentration. The plot looks like a lattice deformed by a shear. The data obtained at nonzero angles and nonzero concentrations are extrapolated to $\theta = 0$ and $c = 0$, represented by two solid dark lines with a common intercept. The intercept gives M_w^{-1} . The slope of the $c = 0$ line is equal to $(1/3)(4\pi n/\lambda)^2 R_g^2/M_w$, where we write R_g^2 for $\langle R_g^2 \rangle_z$ here. The slope of the $\theta = 0$ line is equal to $2A_2/\text{const.}$ Thus, the Zimm plot gives estimates of M_w , R_g , and A_2 with no need of other references. If the constant coefficient on c is large, the sheared lattice can be inverted with the $\theta = 0$ line lying below the $c = 0$ line. A negative A_2 inverts the plot vertically (Problem 2.32).

An example of the actual data is shown in Figure 2.50. The data were obtained for polyguanidine in tetrahydrofuran.²³ The intercept gives $M_w = 6.73 \times 10^5$ g/mol.

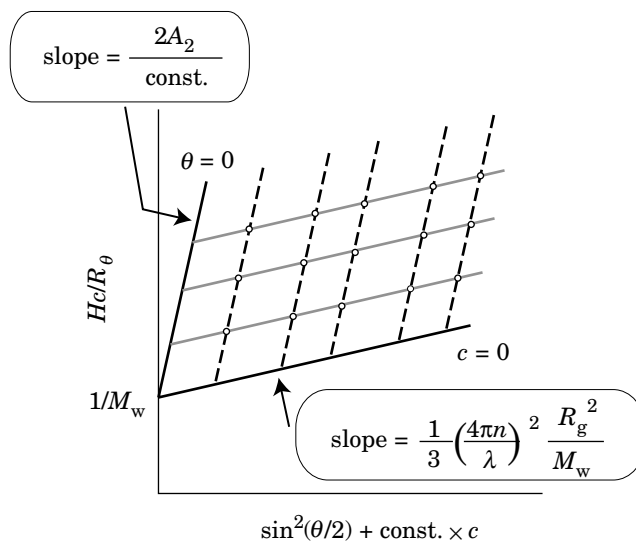


Figure 2.49. Schematic of the Zimm plot. Results obtained for solutions of different concentrations c at different scattering angles θ are converted to Hc/R_θ and plotted as a function of $\sin^2(\theta/2) + \text{const.} \times c$. The extrapolate to $c = 0$ has a slope of $(1/3)(4\pi n/\lambda)^2 R_g^2/M_w$. The extrapolate to $\theta = 0$ has a slope of $2A_2/\text{const.}$ The two extrapolates have a common intercept of $1/M_w$.

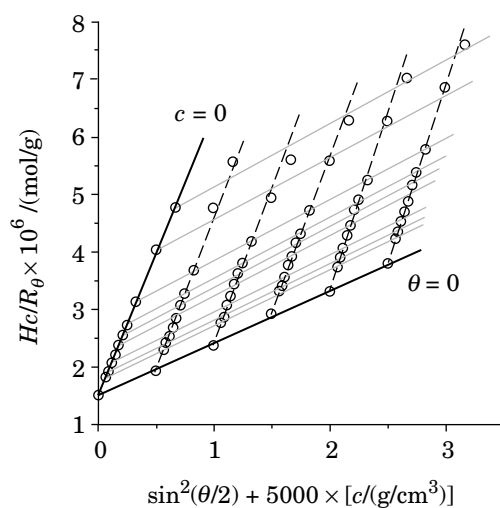


Figure 2.50. Example of the Zimm plot. Data were obtained for polyguanidine in tetrahydrofuran. (From Ref. 23.)

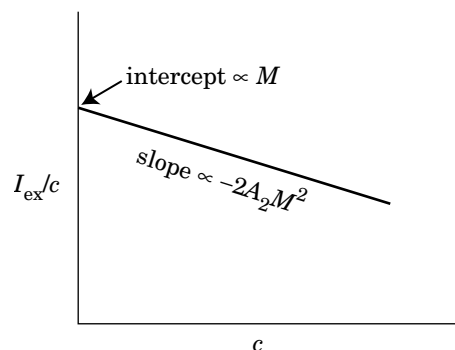


Figure 2.51. A plot of I_{ex}/c as a function of c at sufficiently low scattering angles has an intercept proportional to M and a slope proportional to $-2A_2M^2$. The ratio gives an estimate of A_2M .

The slope of the $c = 0$ line gives $R_g = 99$ nm, and the slope of the $\theta = 0$ lines gives $A_2 = 2.59 \times 10^{-3}$ (mol·cm³)/g².

When the light-scattering data are available only for one concentration, but the concentration is sufficiently low, we can regard that the line connecting the measured data as the $c = 0$ line in the Zimm plot. The intercept of the line gives M_w and the slope gives R_g .

A simpler alternative to estimate A_2M is to measure I_{ex} at a sufficiently low angle ($kR_g \leq 1$) for solutions of different concentrations and plot I_{ex}/c as a function of c . The plot is schematically explained in Figure 2.51. The data for low concentrations ($c < c^*$) will lie on a straight line. The ratio of the slope to the intercept is equal to $-2A_2M$.

2.4.7.6 Measurement of dn/dc To have a good accuracy in the estimates of M_w , $\langle R_g^2 \rangle_z$, and A_2 , dn/dc must be evaluated with a high accuracy because the relative error in dn/dc is doubled in the errors in M_w , $\langle R_g^2 \rangle_z$, and A_2 . The dn/dc is usually measured by using a differential refractometer for solutions of the polymer at different concentrations in the dilute regime. Fitting the plot of Δn as a function of c by a straight line through the origin gives the estimate of dn/dc . The measurement of dn/dc must be done at the same temperature and wavelength as those in the light-scattering measurements.

Commercial instruments based on two different principles are available. One uses a vertically divided cell.²⁴ The top view is shown in Figure 2.52a. One of the chambers contains a reference fluid, typically the pure solvent, and the other chamber contains the sample solution. A laser beam passes the divided cell twice before reaching a two-part photodetector. The detector is placed so that the beam hits the two parts equally when the two chambers of the cell have the same refractive index. A difference in the refractive index in the chambers deflects the beam, resulting in unequal intensities on the two parts of the detector. Thus the imbalance of the two intensities gives the refractive index difference Δn .

A variant of this scheme is also used. A mirror is on a rotation stage. The mirror is rotated so that the beam hits the two parts of the detector with the same intensity. The angle of rotation gives the refractive index difference Δn .

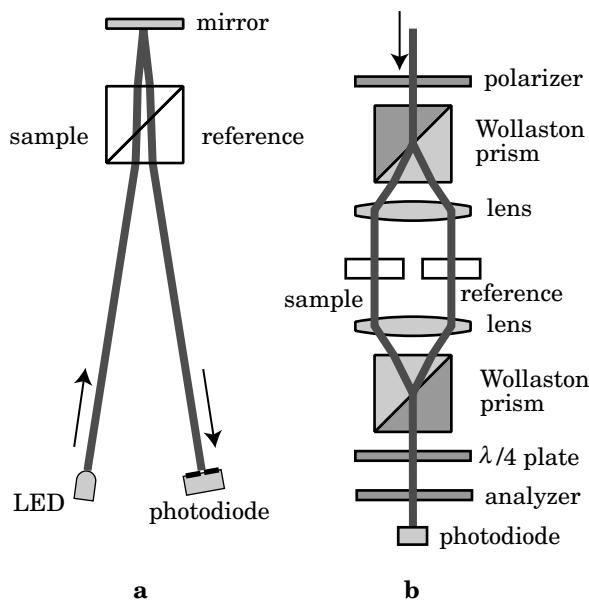


Figure 2.52. Differential refractive index dn/dc is measured usually in one of two methods: refraction (a) and interferometer (b).

The other method uses an interferometer.²⁵ In Figure 2.52b, a beam linearly polarized at 45° from vertical is split into two beams by a Wollaston prism. One of the two beams passes a sample cell, and the other beam passes a reference cell. When there is a difference in the refractive index between the two fluids, one of the beams is delayed compared with the other, resulting in a phase shift. When the two beams are coupled by another prism, they form a circularly polarized light. A quarterwave plate converts it into a linearly polarized beam. With the analyzer (another polarizer) adjusted to be extinct when there is no phase shift, the intensity of light though the analyzer is proportional to the phase shift. The latter is proportional to Δn .

As an alternative, we can use a regular Abbe refractometer that reads the refractive index of a liquid for a typical light source of a sodium lamp (D line; $\lambda = 589.3$ nm) at a given temperature. Unlike the differential refractometer, the fluid is exposed to the atmosphere; therefore, this method is not suitable for a solution dissolved in a volatile solvent.

2.4.8 Other Scattering Techniques

2.4.8.1 Small-Angle Neutron Scattering (SANS) Small-angle neutron scattering (SANS) has become a preferred tool of research for a variety of polymer systems, including pure and blend bulk polymers, phase-separated systems, micellar suspensions, and solutions, especially concentrated ones. Unlike light scattering, it is

available only in a limited number of facilities around the globe. Labeling of polymer by deuterium, that is, straight synthesis of the polymer using deuterated compounds, is often required. SANS is therefore best suited where light-scattering measurements fail, for instance, for opaque systems such as micellar suspensions in which multiple light-scattering complicates the scattering pattern.

As in light scattering, SANS provides information on static structures of the system, but the length scale is smaller. The range of the scattering vector is typically from 0.02 to 3 nm⁻¹, overlapping with the high end of the scattering vectors in the light scattering (see Fig. 2.32). It is customary to use symbol \mathbf{q} to denote the scattering vector whose magnitude q is given by

$$q = \frac{4\pi}{\lambda} \sin \frac{\theta}{2} \quad (2.120)$$

where λ is the de Broglie wavelength of neutrons and θ is the scattering angle. The particles that scatter neutrons are nuclei. The scattering intensity by each nucleus is proportional to a **scattering length** b , which is different from nucleus to nucleus. For a proton ¹H, $b < 0$ and there is no change in phase upon scattering. With a deuterium D = ²H and most other nuclei that constitute polymers, $b > 0$ and the phase shifts by π upon scattering.

We can imagine that each atom has a shield of area $4\pi b^2$ to block the incident neutrons and scatter them in all directions. This area is called a **scattering cross section**. The cross section of the entire sample is denoted by Σ . The coherent part of the scattering intensity I_{coh} per unit solid angle $d\Omega$ at \mathbf{q} is related to the position \mathbf{r}_i and the scattering length b_i of the i th nucleus by

$$I_{\text{coh}}(\mathbf{q}) = \frac{d\Sigma^{\text{coh}}(\mathbf{q})}{d\Omega} = \left\langle \sum_{i,j} b_i b_j \exp[i\mathbf{q} \cdot (\mathbf{r}_i - \mathbf{r}_j)] \right\rangle \quad (2.121)$$

where Σ^{coh} is the coherent component of the scattering cross section. Incoherent component does not interfere to take part in the structure factor. Equation 2.121 is similar to the structure factor we obtained in the static light scattering. The contrast factor dn/dc is now replaced by b_i .

Now we apply the general formula to a solution of polymer. We consider that the polymer consists of hydrogenated chains (regular chains) and deuterated chains, both having the same distribution in the chain length. The coherent scattering by the solution of total concentration c is given as

$$\frac{d\Sigma^{\text{coh}}(\mathbf{q})}{d\Omega} = \frac{M_w c N_A}{m_0^2} [(a_H - a_D)^2 x_H x_D S_1(\mathbf{q}) + (a_p - a_s)^2 S(\mathbf{q})] \quad (2.122)$$

where m_0 is the mass of a monomer, a_H and a_D are the scattering lengths per monomer for hydrogenated and deuterated polymers, respectively, x_H and x_D are their mole fractions in the polymer sample (without solvent), and $S_1(\mathbf{q})$ and $S(\mathbf{q})$ are the single-chain and total structure factors, respectively, as we defined earlier in

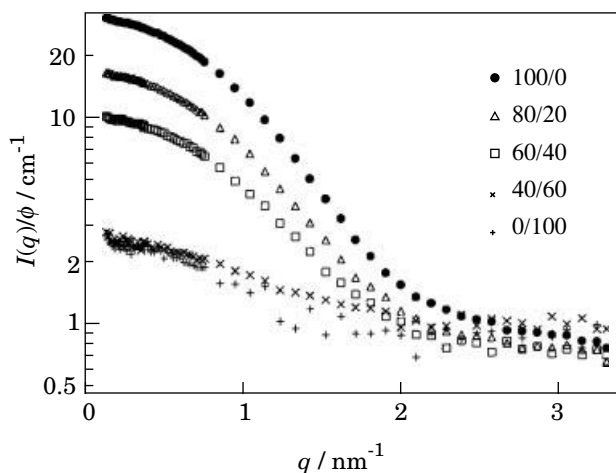


Figure 2.53. Scattering intensity I in SANS divided by the polymer volume fraction ϕ , plotted as a function of the scattering vector q . The sample was a hydrogenated dendrimer in a mixture of deuterated (D) and hydrogenated (H) solvents. The D-to-H mixing ratio is indicated in the legend. (From Ref. 26.)

the sections on light scattering. The a_p and a_s are defined as

$$a_p = x_H a_H + x_D a_D, \quad a_s = x_{sH} a_{sH} + x_{sD} a_{sD} \quad (2.123)$$

where a_{sH} and a_{sD} are the scattering lengths of hydrogenated and deuterated solvent molecules, respectively, and x_{sH} and x_{sD} are their mole fractions in the solvent mixture (without polymer). Note that $M_w c / m_0^2$ in Eq. 2.122 is the same between hydrogenated and deuterated chains, as long as the molar concentration is common.

Extraction of $S_1(\mathbf{q})$ from $I(\mathbf{q})$ is facilitated by contrast matching in which a_p and a_s are brought to be equal by choosing an appropriate isotopic mixture of the solvents for a given isotopic mixture of the polymer samples. Because of the factor $x_H x_D$, the scattering intensity maximizes for a 50:50 mixture of the isotopes. Once we obtain $S_1(\mathbf{q})$, the methods used in the analysis of SLS data can be applied, including the Zimm plot.

Example of SANS experiments is shown in Figure 2.53.²⁶ The scattering intensity from a hydrogenated dendrimer ($x_H = 1$, $x_D = 0$) normalized by its volume fraction ϕ is plotted as a function of the scattering vector. At high q , $I(q)$ levels off to a constant due to incoherent scattering. Mixtures of deuterated (D) and hydrogenated (H) solvents with different mixing ratios were used as a solvent. Apparently, the contrast matching is reached at around 20% of the hydrogenated solvent in this example. The concentration was sufficiently low for this compact molecule; thus $S_1(\mathbf{q}) \cong S(\mathbf{q})$. The coherent part of the scattering is close to $1/(1 + q^2 R_g^2/3)$ dependence.

2.4.8.2 Small-Angle X-Ray Scattering (SAXS) Small-angle X-ray scattering (SAXS) is, in principle, the same as wide-angle X-ray diffraction (WAXD), broadly used in crystallography. In SAXS, the scattering angles are low to allow investigation of structures over the length much longer than 1 Å. The mechanism of scattering discussed in Section 2.4.2 applies as it is. Unlike WAXD, the intensity of scattered X-ray is weak. Therefore, a synchrotron radiation source that provides a strong monochromatic beam is usually used. The scattering vector is given by the same formula as the one used for SANS, with λ being the wavelength of the X-ray. Note that the relative electric permittivity is nearly equal to unity in the relevant range of wavelength (to be precise, it is slightly smaller than 1). The magnitude of the scattering vector is typically 0.2 to 4 nm⁻¹, much greater than the range available in static light scattering. Therefore, SAXS is suitable to study local structures of polymer molecules. The form factor studied at a high q range gives, for instance, an estimate for the diameter of a rodlike molecule.

2.4.9 PROBLEMS

Problem 2.18: A copolymer chain consisting of N_a beads of monomer a and N_b beads of monomer b has three single-chain structure factors: $S_{aa}(\mathbf{k})$, $S_{ab}(\mathbf{k})$, and $S_{bb}(\mathbf{k})$. They are defined as

$$S_{ll'}(\mathbf{k}) = \frac{1}{N} \sum_{i,j=1}^N \langle \exp[i\mathbf{k} \cdot (\mathbf{r}_i - \mathbf{r}_j)] \delta_i^l \delta_j^{l'} \rangle \quad (l, l' = a, b)$$

where $N = N_a + N_b$ is the total number of beads in the chain and δ_i^l specifies the monomer type:

$$\delta_i^l = \begin{cases} 1 & \text{(the } i\text{th bead is } l) \\ 0 & \text{(otherwise)} \end{cases}$$

By definition, $\delta_i^a + \delta_i^b = 1$. Assume that the copolymer chain follows the Gaussian statistics and has a common segment length b . Find $S_{aa}(\mathbf{k})$, $S_{ab}(\mathbf{k})$, and $S_{bb}(\mathbf{k})$ for (1) a diblock copolymer and (2) a random copolymer in which the two monomers are placed without correlation to the neighboring monomers. Also evaluate each of $S_{aa}(\mathbf{k})$, $S_{ab}(\mathbf{k})$, and $S_{bb}(\mathbf{k})$ in the small \mathbf{k} limit up to the order of \mathbf{k}^2 .

Solution 2.18 (1):

$$\delta_i^a = 1 \text{ for } i = 1, \dots, N_a \quad \text{and} \quad \delta_i^b = 1 \text{ for } i = N_a + 1, \dots, N_a + N_b$$

$$S_{aa}(\mathbf{k}) = \frac{1}{N} \sum_{i,j=1}^N \langle \exp[i\mathbf{k} \cdot (\mathbf{r}_i - \mathbf{r}_j)] \delta_i^a \delta_j^a \rangle = \frac{1}{N} \sum_{i,j=1}^{N_a} \langle \exp[i\mathbf{k} \cdot (\mathbf{r}_i - \mathbf{r}_j)] \rangle = \frac{N_a^2}{N} f_D(kR_{ga})$$

$$\begin{aligned}
S_{bb}(\mathbf{k}) &= \frac{1}{N} \sum_{i,j=1}^N \langle \exp[i\mathbf{k} \cdot (\mathbf{r}_i - \mathbf{r}_j)] \delta_i^b \delta_j^b \rangle = \frac{1}{N} \sum_{i,j=N_a+1}^{N_a+N_b} \langle \exp[i\mathbf{k} \cdot (\mathbf{r}_i - \mathbf{r}_j)] \rangle \\
&= \frac{N_b^2}{N} f_D(kR_{gb})
\end{aligned}$$

where $R_{gl}^2 = b^2 N_l / 6$ ($l = a, b$) is the mean square radius of gyration of block l .

$$\begin{aligned}
S_{ab}(\mathbf{k}) &= \frac{1}{N} \sum_{i,j=1}^N \langle \exp[i\mathbf{k} \cdot (\mathbf{r}_i - \mathbf{r}_j)] \delta_i^a \delta_j^b \rangle = \frac{1}{N} \sum_{i=1}^{N_a} \sum_{j=N_a+1}^{N_a+N_b} \langle \exp[i\mathbf{k} \cdot (\mathbf{r}_i - \mathbf{r}_j)] \rangle \\
&= \frac{1}{N} \int_0^{N_a} dn \int_{N_a}^{N_a+N_b} dn' \exp\left(-\frac{1}{6}k^2(n' - n)b^2\right) \\
&= \frac{1}{N} \int_0^{N_a} dn \exp\left(\frac{1}{6}k^2 nb^2\right) \int_{N_a}^{N_a+N_b} dn' \exp\left(-\frac{1}{6}k^2 n' b^2\right) \\
&= \frac{N_a N_b}{N} \left(\frac{1 - \exp(-k^2 R_{ga}^2)}{k^2 R_{ga}^2} \right) \left(\frac{1 - \exp(-k^2 R_{gb}^2)}{k^2 R_{gb}^2} \right)
\end{aligned}$$

In the small \mathbf{k} limit,

$$\begin{aligned}
S_{aa}(\mathbf{k}) &= \frac{N_a^2}{N} \left(1 - \frac{1}{3}k^2 R_{ga}^2 \right), \quad S_{bb}(\mathbf{k}) = \frac{N_b^2}{N} \left(1 - \frac{1}{3}k^2 R_{gb}^2 \right), \\
S_{ab}(\mathbf{k}) &= \frac{N_a N_b}{N} \left(1 - \frac{1}{2}k^2 (R_{ga}^2 + R_{gb}^2) \right)
\end{aligned}$$

Solution 2.18 (2): $\delta_i^a = 1$ with a probability of N_a/N for any i . Whether the bead i is monomer a or b is independent of other factors and $\langle \delta_i^a \rangle = N_a/N$. Therefore,

$$\begin{aligned}
S_{aa}(\mathbf{k}) &= \frac{1}{N} \sum_{i,j=1}^N \langle \exp[i\mathbf{k} \cdot (\mathbf{r}_i - \mathbf{r}_j)] \rangle \langle \delta_i^a \rangle \langle \delta_j^a \rangle \\
&= \frac{N_a^2}{N^3} \sum_{i,j=1}^N \langle \exp[i\mathbf{k} \cdot (\mathbf{r}_i - \mathbf{r}_j)] \rangle = \frac{N_a^2}{N} f_D(kR_g)
\end{aligned}$$

where R_g is the radius of gyration of the whole chain. Likewise,

$$S_{bb}(\mathbf{k}) = \frac{N_b^2}{N} f_D(kR_g), \quad S_{ab}(\mathbf{k}) = \frac{N_a N_b}{N} f_D(kR_g)$$

In the small \mathbf{K} limit,

$$S_{aa}(\mathbf{k}) = \frac{N_a^2}{N} \left(1 - \frac{1}{3}k^2 R_g^2\right), \quad S_{bb}(\mathbf{k}) = \frac{N_b^2}{N} \left(1 - \frac{1}{3}k^2 R_g^2\right),$$

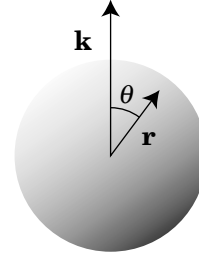
$$S_{ab}(\mathbf{k}) = \frac{N_a N_b}{N} \left(1 - \frac{1}{3}k^2 R_g^2\right)$$

Real random copolymers may have a correlation between δ_i' of different i .

Problem 2.19: Calculate the form factor for a spherical molecule.

Solution 2.19: Choose the polar axis along \mathbf{k} . Then,

$$\begin{aligned} \int_V \mathbf{dr} \exp(i\mathbf{k} \cdot \mathbf{r}) &= \int_0^{R_s} r^2 dr \int_0^\pi \sin\theta d\theta \int_0^{2\pi} d\phi \exp(ikr \cos\theta) \\ &= 2\pi \int_0^{R_s} r^2 dr \frac{2 \sin kr}{kr} \\ &= \frac{4\pi}{k} \operatorname{Im} \int_0^{R_s} r dr \exp(ikr) \\ &= \frac{4\pi}{k} \operatorname{Im} \left[\frac{R_s}{ik} \exp(ikR_s) + \frac{1}{k^2} (\exp(ikR_s) - 1) \right] \\ &= 4\pi k^{-3} (\sin kR_s - kR_s \cos kR_s) \end{aligned}$$



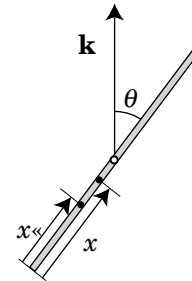
Then,

$$P_{\text{sphere}}(\mathbf{k}) = \left| V^{-1} \int_V \mathbf{dr} \exp(i\mathbf{k} \cdot \mathbf{r}) \right|^2 = [3(kR_s)^{-3} (\sin kR_s - kR_s \cos kR_s)]^2$$

Problem 2.20: Calculate the form factor for a rodlike molecule.

Solution 2.20: Let θ be the angle between \mathbf{k} and the molecule.

$$\begin{aligned} P_{\text{rod}} &= \frac{1}{2L^2} \int_0^L dx \int_0^L dx' \int_0^\pi \sin\theta d\theta \exp[ik(x-x')\cos\theta] \\ &= \frac{1}{L^2} \int_0^L dx \int_0^L dx' \frac{\sin k(x-x')}{k(x-x')} \\ &= \frac{2}{L^2} \int_0^L dx \int_0^x dx' \frac{\sin k(x-x')}{k(x-x')} \\ &[k(x-x') \equiv z, kx = y] \end{aligned}$$



$$\begin{aligned}
&= \frac{2}{k^2 L^2} \int_0^{kL} dy \int_0^y dz \frac{\sin z}{z} = \frac{2}{k^2 L^2} \int_0^{kL} dz \frac{\sin z}{z} (kL - z) \\
&= (kL/2)^{-1} \int_0^{kL} \frac{\sin z}{z} dz - \left(\frac{\sin(kL/2)}{kL/2} \right)^2
\end{aligned}$$

Problem 2.21: Verify that the form factor of a two-arm star polymer ($n_A = 2$ in Eq. 2.98) reproduces the form factor of a Gaussian chain.

Solution 2.21: When $n_A = 2$, with $x = kR_{g1}$,

$$\begin{aligned}
P_{\text{star}} &= \frac{1}{2} f_D(x) + \frac{1}{2} \left(x^{-2} [1 - \exp(-x^2)] \right)^2 \\
&= \frac{1}{2} \cdot 2x^{-2} \left[1 - x^{-2} (1 - \exp(-x^2)) \right] + \frac{1}{2} x^{-4} [1 - \exp(-x^2)]^2 \\
&= x^{-2} \left[1 - \frac{1}{2} x^{-2} (1 - \exp(-2x^2)) \right] \\
&= 2(2^{1/2}x)^{-2} \left[1 - (2^{1/2}x)^{-2} (1 - \exp(-(2^{1/2}x)^2)) \right] = f_D(2^{1/2}kR_{g1})
\end{aligned}$$

$2^{1/2}R_{g1}$ is the radius of gyration of the two-arm star polymer.

Problem 2.22: Show that Eq. 2.98 reduces to Eq. 2.74 when $kR_g \ll 1$.

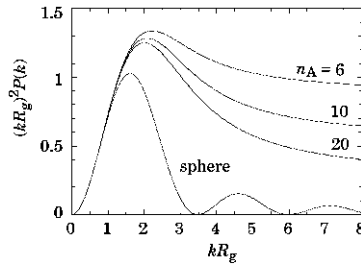
Solution 2.22: In Eq. 2.98, when k is small,

$$\begin{aligned}
P_{\text{star}}(k) &\cong \frac{1}{n_A} \left(1 - \frac{1}{3} (kR_{g1})^2 \right) + \left(1 - \frac{1}{n_A} \right) \left(1 - \frac{1}{2} (kR_{g1})^2 \right)^2 \\
&= 1 - \left(1 - \frac{2}{3n_A} \right) (kR_{g1})^2 = 1 - \frac{1}{3} (kR_g)^2
\end{aligned}$$

where Eq. 1.84 or Eq. 1.85 was used.

Problem 2.23: Compare the form factor of a sphere and that of a star polymer by plotting $(kR_g)^2 P_{\text{sphere}}(k)$ and $(kR_g)^2 P_{\text{star}}(k)$ as a function of kR_g . Consider $n_A = 6, 10,$ and 20 for the number of arms of the star polymer.

Solution 2.23:



Problem 2.24: Clausius-Mossotti formula is given as

$$\frac{\epsilon_r - 1}{\epsilon_r + 2} \nu = \frac{\alpha}{3\epsilon_0}$$

where ν is the volume per molecule. Use this formula to derive $d\alpha_{\text{ex}} = \epsilon_0 \Delta\epsilon_r d\mathbf{r}$.

Solution 2.24: The contribution to α from a small volume $d\mathbf{r}$ is given as

$$d\alpha = 3\epsilon_0 \frac{\epsilon_r - 1}{\epsilon_r + 2} d\mathbf{r}$$

When a fluctuation $\Delta\epsilon_r$ in ϵ_r causes $d\alpha$ to fluctuate by $d\alpha_{\text{ex}}$,

$$d\alpha + d\alpha_{\text{ex}} = 3\epsilon_0 \frac{\epsilon_r + \Delta\epsilon_r - 1}{\epsilon_r + \Delta\epsilon_r + 2} d\mathbf{r}$$

Comparison of the above two equations leads to

$$d\alpha_{\text{ex}} \cong 3\epsilon_0 \frac{\Delta\epsilon_r}{\epsilon_r + 2} d\mathbf{r} \cong \epsilon_0 \Delta\epsilon_r d\mathbf{r}$$

when ϵ_r is close to unity.

Problem 2.25: Statistical mechanics for an open system gives the following relationship between the mean square fluctuation in n_p , the number of polymer chains in volume V , and the mean of n_p :

$$\langle \Delta n_p^2 \rangle = k_B T \left(\frac{\partial n_p}{\partial \mu_p} \right)_{T,p}$$

Derive Eq. (2.107) using this relationship and the Gibbs-Duhem theorem, $n_p d\mu_p + n_s d\mu_s = 0$.

Solution 2.25: From the Gibbs-Duhem theorem,

$$\frac{\partial \mu_p}{\partial n_p} = - \frac{n_s}{n_p} \frac{\partial \mu_s}{\partial n_p}$$

Because

$$-\Delta\mu_s = \Pi \frac{V_m}{N_A}$$

where V_m is the molar volume of the solvent,

$$\langle \Delta n_P^2 \rangle = -k_B T \frac{n_P}{n_S} \frac{\partial n_P}{\partial \mu_S} = k_B T \frac{n_P}{n_S} \frac{N_A}{V_m} \frac{\partial n_P}{\partial \Pi}$$

Thus we obtain

$$\langle \Delta c_{\text{tot}}^2 \rangle = \frac{ck_B T}{V} \frac{\partial c}{\partial \Pi}$$

where $n_S V_m / N_A \cong V$ was used.

Problem 2.26: Show that

$$\int_V \frac{1}{c} \langle \Delta c(\mathbf{r}) \Delta c(0) \rangle d\mathbf{r} = k_B T \frac{\partial c}{\partial \Pi}$$

(another expression for Eq. 2.107).

Solution 2.26: From Eq. 2.105,

$$\psi_{cc}(0) \equiv \int_V d\mathbf{r}_1 \int_V d\mathbf{r}_2 \langle \Delta c(\mathbf{r}_1) \Delta c(\mathbf{r}_2) \rangle = V \int_V \langle \Delta c(\mathbf{r}) \Delta c(0) \rangle d\mathbf{r}$$

Then, with Eqs. (2.106) and (2.107),

$$\int_V \frac{1}{c} \langle \Delta c(\mathbf{r}) \Delta c(0) \rangle d\mathbf{r} = \frac{1}{cV} \psi_{cc}(0) = \frac{V}{c} \langle \Delta c_{\text{tot}}^2 \rangle = k_B T \frac{\partial c}{\partial \Pi}$$

Problem 2.27: For a diblock copolymer or a random copolymer consisting of monomers a and b that have different contrasts to the solvent, the refractive index fluctuation $\Delta_c n(\mathbf{r})$ due to concentration fluctuation has two parts:

$$\Delta_c n(\mathbf{r}) = \left(\frac{dn}{dc} \right)_a \Delta c_a(\mathbf{r}) + \left(\frac{dn}{dc} \right)_b \Delta c_b(\mathbf{r})$$

where $(dn/dc)_l$ is the differential refractive index of homopolymer l ($l = a, b$), and $\Delta c_l(\mathbf{r}) = c_l(\mathbf{r}) - c_l$ with $c_l = \langle c_l(\mathbf{r}) \rangle$ denotes the concentration fluctuation of monomer l . Following the procedure in Section 2.4.7.4, we find the excess scattering intensity from the solution of the copolymer in the low

concentration limit as

$$\frac{I_{\text{ex}}(\mathbf{k})}{I_0} = \frac{4\pi^2 n^2}{\lambda^4 r^2} \left[\left(\frac{dn}{dc} \right)_a^2 \psi_{\text{aa}}(\mathbf{k}) + 2 \left(\frac{dn}{dc} \right)_a \left(\frac{dn}{dc} \right)_b \psi_{\text{ab}}(\mathbf{k}) + \left(\frac{dn}{dc} \right)_b^2 \psi_{\text{bb}}(\mathbf{k}) \right]$$

where

$$\psi_{ll'}(\mathbf{k}) \equiv \int_V d\mathbf{r}_1 \int_V d\mathbf{r}_2 \langle \Delta c_l(\mathbf{r}_1) \Delta c_{l'}(\mathbf{r}_2) \rangle \exp[i\mathbf{k} \cdot (\mathbf{r}_1 - \mathbf{r}_2)] (l, l' = a, b)$$

with $\psi_{\text{ab}}(\mathbf{k}) = \psi_{\text{ba}}(\mathbf{k})$. Because $\langle \Delta c_l(\mathbf{r}_1) \Delta c_{l'}(\mathbf{r}_2) \rangle = \langle c_l(\mathbf{r}_1) c_{l'}(\mathbf{r}_2) \rangle - c_l c_{l'}$,

$$\psi_{ll'}(\mathbf{k}) = \frac{MVN}{cN_A} \frac{c_l c_{l'}}{N_l N_{l'}} S_{ll'}(\mathbf{k}) - (2\pi)^3 V c_l c_{l'} \delta(\mathbf{k})$$

where $c = c_a + c_b$ is the total concentration, M and N refer to the whole chain, N_l is the number of l monomers in the polymer chain, and $S_{ll'}(\mathbf{k})$ is defined in Problem 2.18. After eliminating the unscattered beam,

$$\begin{aligned} \frac{I_{\text{ex}}(\mathbf{k})}{I_0} &= \frac{4\pi^2 n^2}{\lambda^4 r^2} \frac{MVN}{cN_A} \left[\frac{C_a^2}{N_a^2} \left(\frac{dn}{dc} \right)_a^2 S_{\text{aa}}(\mathbf{k}) + 2 \frac{c_a c_b}{N_a N_b} \left(\frac{dn}{dc} \right)_a \left(\frac{dn}{dc} \right)_b S_{\text{ab}}(\mathbf{k}) \right. \\ &\quad \left. + \frac{C_b^2}{N_b^2} \left(\frac{dn}{dc} \right)_b^2 S_{\text{bb}}(\mathbf{k}) \right] \end{aligned}$$

Answer the following questions assuming the whole chain follows the Gaussian statistics.

- (1) Show that, for the random copolymer, Eq. 2.114 (in the low concentration limit) holds with dn/dc replaced by the effective differential refractive index of the copolymer as a whole, $(c_a/c)(dn/dc)_a + (c_b/c)(dn/dc)_b$.
- (2) What is the radius of gyration $R_{g,\text{eff}}$ estimated from the linear relationship between \mathbf{k}^2 and the reciprocal of the scattering intensity in the small \mathbf{k} limit for the diblock copolymer?

Solution 2.27 (1):

$$\begin{aligned} \frac{I_{\text{ex}}(\mathbf{k})}{I_0} &= \frac{4\pi^2 n^2}{\lambda^4 r^2} \frac{MV}{cN_A} \left[c_a^2 \left(\frac{dn}{dc} \right)_a^2 + 2c_a c_b \left(\frac{dn}{dc} \right)_a \left(\frac{dn}{dc} \right)_b \right. \\ &\quad \left. + c_b^2 \left(\frac{dn}{dc} \right)_b^2 \right] f_D(kR_g) \\ &= \frac{4\pi^2 n^2}{\lambda^4 r^2} \frac{cMV}{N_A} \left[\frac{c_a}{c} \left(\frac{dn}{dc} \right)_a + \frac{c_b}{c} \left(\frac{dn}{dc} \right)_b \right]^2 f_D(kR_g) \end{aligned}$$

Solution 2.27 (2): In the small \mathbf{k} limit,

$$\begin{aligned} \frac{I_{\text{ex}}(\mathbf{k})}{I_0} &= \frac{4\pi^2 n^2}{\lambda^4 r^2} \frac{MV}{cN_A} \left[\left(\frac{dn}{dc} \right)_a^2 c_a^2 \left(1 - \frac{1}{3} k^2 R_{\text{ga}}^2 \right) \right. \\ &\quad + 2 \left(\frac{dn}{dc} \right)_a \left(\frac{dn}{dc} \right)_b c_a c_b \left(1 - \frac{1}{2} k^2 (R_{\text{ga}}^2 + R_{\text{gb}}^2) \right) \\ &\quad \left. + \left(\frac{dn}{dc} \right)_b^2 c_b^2 \left(1 - \frac{1}{3} k^2 R_{\text{gb}}^2 \right) \right] \\ &\cong \frac{4\pi^2 n^2}{\lambda^4 r^2} \frac{cMV}{N_A} \left[\frac{c_a}{c} \left(\frac{dn}{dc} \right)_a + \frac{c_b}{c} \left(\frac{dn}{dc} \right)_b \right]^2 \frac{1}{1 + \frac{1}{3} k^2 R_{\text{g,eff}}^2} \end{aligned}$$

with

$$R_{\text{g,eff}}^2 = \frac{\frac{c_a^2}{c^2} \left(\frac{dn}{dc} \right)_a^2 R_{\text{ga}}^2 + \frac{c_b^2}{c^2} \left(\frac{dn}{dc} \right)_b^2 R_{\text{gb}}^2 + 3 \frac{c_a c_b}{c^2} \left(\frac{dn}{dc} \right)_a \left(\frac{dn}{dc} \right)_b (R_{\text{ga}}^2 + R_{\text{gb}}^2)}{\left[\frac{c_a}{c} \left(\frac{dn}{dc} \right)_a + \frac{c_b}{c} \left(\frac{dn}{dc} \right)_b \right]^2}$$

Problem 2.28: In the preceding question, what happens to the light scattering of the diblock copolymer solution if the solvent is selected so that (1) $(dn/dc)_a = 0$, (2) $(dn/dc)_b = 0$, (3) $(c_a/c)(dn/dc)_a + (c_b/c)(dn/dc)_b = 0$?

Solution 2.28 (1): $R_{\text{g,eff}} = R_{\text{gb}}$ (a is invisible).

Solution 2.28 (2): $R_{\text{g,eff}} = R_{\text{ga}}$.

Solution 2.28 (3):

$$\frac{I_{\text{ex}}(\mathbf{k})}{I_0} \cong \frac{4\pi^2 n^2}{\lambda^4 r^2} \frac{cMV}{N_A} \left(\frac{dn}{dc} \right)_a^2 \frac{c_a^2}{c^2} \frac{2}{3} k^2 (R_{\text{ga}}^2 + R_{\text{gb}}^2)$$

Note that $I_{\text{ex}}(0) = 0$. The condition of the zero average differential refractive index is sometimes called *optical theta*.

Problem 2.29: What is the scattering from a telechelic molecule in which two identical small spheres are attached to the ends of a flexible chain that is isorefractive with the solvent? Assume the flexible chain follows the Gaussian statistics of N segments.

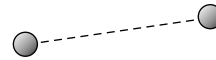


Solution 2.29: Two spheres are at \mathbf{r}_i and \mathbf{r}_j , separated by a distance between the two Gaussian chain ends. The scattering comes from the two spheres only.

Their structure factor is

$$\begin{aligned}
 S_1 &= \frac{1}{2} \sum_{i=1}^2 \sum_{j=1}^2 \langle \exp[i\mathbf{k} \cdot (\mathbf{r}_i - \mathbf{r}_j)] \rangle = 1 + \langle \exp[i\mathbf{k} \cdot (\mathbf{r}_1 - \mathbf{r}_2)] \rangle \\
 &= 1 + \int d(\mathbf{r}_1 - \mathbf{r}_2) (2\pi N b^2 / 3)^{-3/2} \exp\left(-\frac{3(\mathbf{r}_1 - \mathbf{r}_2)^2}{2N b^2}\right) \exp[i\mathbf{k} \cdot (\mathbf{r}_1 - \mathbf{r}_2)] \\
 &= 1 + \exp\left(-\frac{1}{6} N b^2 \mathbf{k}^2\right) = 1 + \exp(-R_g^2 \mathbf{k}^2)
 \end{aligned}$$

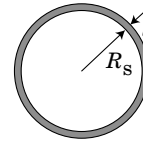
Problem 2.30: What is the scattering from a telechelic molecule in which two identical small spheres are attached to the end of a rodlike molecule of length L that is isorefractive with the solvent?



Solution 2.30: Two spheres are at \mathbf{r}_i and \mathbf{r}_j separated by L . The scattering comes from the two spheres only. Let the angle between \mathbf{k} and the rod be θ .

$$S_1 = 1 + \langle \exp[i\mathbf{k} \cdot (\mathbf{r}_1 - \mathbf{r}_2)] \rangle = 1 + \frac{1}{2} \int_0^\pi \sin\theta d\theta \exp(ikL \cos\theta) = 1 + \frac{\sin kL}{kL}$$

Problem 2.31: What is the scattering from a spherical molecule of radius R_s uniformly coated with a layer of thickness l ? Assume that only the coated layer is visible, i.e., the interior of the sphere is isorefractive with the solvent, and $l \ll R_s$.



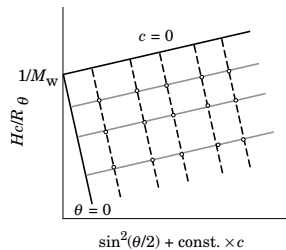
Solution 2.31: The single-scatterer structure factor is

$$\begin{aligned}
 S_1 &= N \langle \exp[i\mathbf{k} \cdot (\mathbf{r}_1 - \mathbf{r}_2)] \rangle = N \frac{1}{4\pi R_s^2 l} \int_{R_s}^{R_s+l} r^2 dr \int_0^\pi \sin\theta d\theta \int_0^{2\pi} d\phi \exp(ikr \cos\theta) \\
 &= N \frac{4\pi}{4\pi R_s^2 l} \int_{R_s}^{R_s+l} r^2 dr \frac{\sin kr}{kr} = N \frac{\sin kR_s}{kR_s}
 \end{aligned}$$

where N is the number of small molecules that coat the sphere surface.

Problem 2.32: Draw a sketch of the Zimm plot for a solution of a polymer with the same M_w and R_g but with A_2 just the opposite in sign to the one shown in Figure 2.49.

Solution 2.32:



2.5 SIZE EXCLUSION CHROMATOGRAPHY AND CONFINEMENT

2.5.1 Separation System

Size exclusion chromatography (SEC) has been widely used since its introduction during the 1960s. It offers a simple yet unbiased method to characterize the molecular weight distribution of a polymer. Although it uses a flow system, the separation principle and the analysis are based on a static property of the polymer molecules in solution. We briefly look at the separation system here before learning the principle.

Figure 2.54 illustrates the separation system. A high-pressure liquid pump draws a solvent called a **mobile phase** from the reservoir and pumps it into a column or a series of columns at a constant flow rate. At one time, a small amount of a dilute solution of polymer dissolved in the same solvent is injected into the stream from a sample loop by changing the position of the injection valve. The column is packed with porous materials, typically polymeric beads with many tiny through holes (pores).

The polymer molecules are partitioned between the small confines of the **pore**, called the **stationary phase**, and the interstitial space between the beads (mobile phase). Polymer molecules with a dimension smaller than the pore size enter the pore more easily than larger polymer molecules do. As the injected polymer solution is transported along the column, low-molecular-weight components are frequently partitioned to the stationary phase, whereas high-molecular-weight components remain mostly in the mobile phase (see Fig. 2.55). Therefore, it takes a longer time for the low-molecular-weight components to reach the column outlet. The band of the polymer in the mobile phase is narrow when injected but spreads according to the molecular weight distribution as the solution moves along the column.

The liquid that comes off the column is called the **eluent**. A detector with a flow cell is placed downstream to measure the concentration (mass/volume) of the polymer in the eluent. A differential refractometer is most commonly used to measure

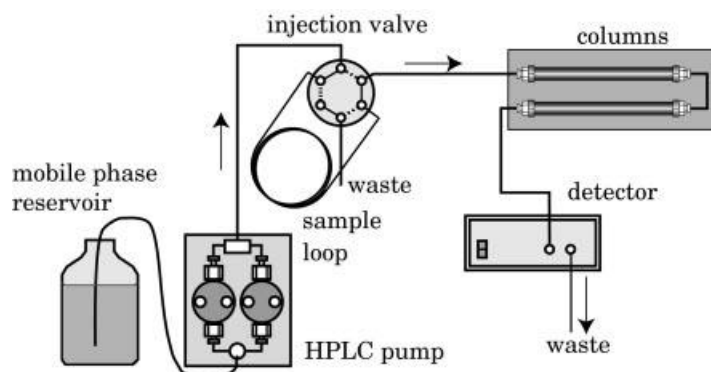


Figure 2.54. Schematic of the size exclusion chromatography system.

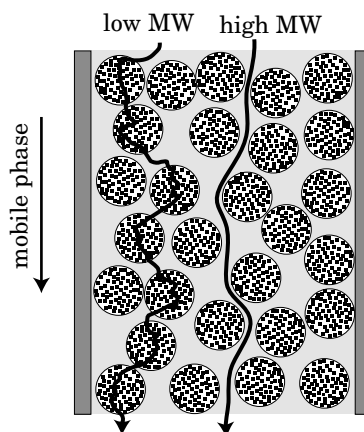


Figure 2.55. Transport of polymer molecules in the size exclusion column. High-molecular-weight (MW) components stay mostly in the mobile phase, whereas low-MW components are partitioned to the stationary phase more frequently.

the difference in the refractive index between the eluent and the pure solvent (Section 2.4.7). The difference is proportional to the concentration, with dn/dc being the proportionality constant. If the polymer has an ultraviolet absorption but the solvent does not, one can use an ultraviolet detector. The absorbance is proportional to the concentration by Beer's law.

Figure 2.56 shows the signal intensity of the detector plotted as a function of **retention time** (t_R), the time measured from the injection of the polymer solution. The **retention volume** (V_R), the cumulative volume of the fluid out of the column since the injection, can also be used for the abscissa. The curve is called a **retention curve** or a **chromatogram**. The height of a point on the curve above the baseline is proportional to the concentration at a given retention time. The signal maximizes at the peak retention time (t_p). The integral of the curve is proportional to the total

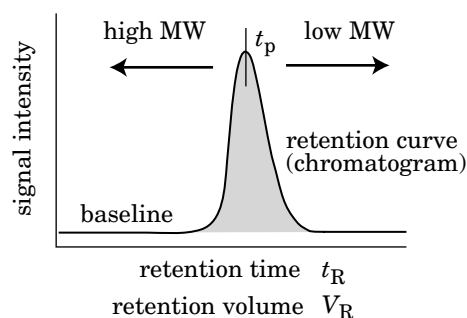


Figure 2.56. Typical SEC chromatogram. The signal intensity proportional to the eluent concentration is plotted.

amount of the polymer injected. The spread of the polymer band by the column is translated into a broadened chromatogram. Because high-molecular-weight components elute earlier, the time axis can be regarded as a reversed molecular weight axis.

SEC has other names. When the mobile phase is an organic solvent, SEC is also called **gel permeation chromatography (GPC)**. When it is aqueous, SEC is also called **gel filtration chromatography (GFC)** or aqueous GPC.

2.5.2 Plate Theory

Plate theory is useful to explain the band broadening during the transport of polymer molecules along the column. In the theory, the whole length of the column is divided into N_{pl} plates of an equal height. Each plate consists of the mobile phase and the stationary phase. Figure 2.57 explains what is supposed to occur in the plates. In each plate, the polymer molecules are partitioned between the two phases. The mobile phase moves to the next plate in a given time t_1 (plate height/linear velocity of the mobile phase), whereas the stationary phase does not. The moved mobile phase establishes concentration equilibrium with the stationary phase in the next plate. Equilibration and transport of the mobile phase are repeated in all of the plates each time. As a result, a completely excluded polymer (too large to enter the pore) requires a time of $t_1 N_{pl}$ to reach the outlet. A lower-molecular-weight polymer molecule needs a longer time to come out of the column.

When equilibrium is reached in the plate, the polymer concentration is c_S in the stationary phase and c_M in the mobile phase. Their ratio is called the **partition coefficient K** :

$$K \equiv c_S/c_M \quad (2.124)$$

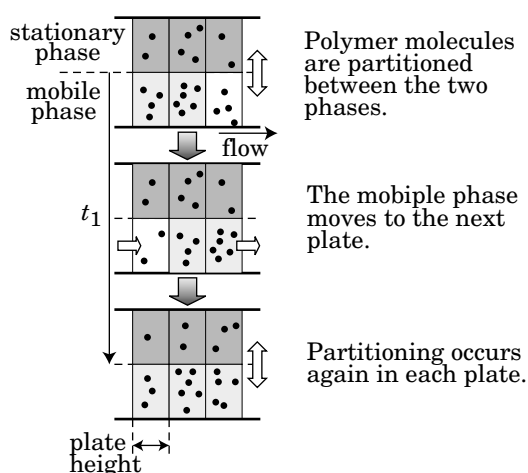


Figure 2.57. Plate theory in column chromatography.

When the concentration is sufficiently low ($c_M \ll c^*$, overlap concentration), K does not depend on c_M but depends on the ratio of the chain dimension to the pore size.

The **partition ratio** k' is defined as the ratio in the number of molecules between the two phases and given as

$$k' = KV_S/V_M \quad (2.125)$$

where V_S and V_M are the volumes of the two phases. The polymer molecules are partitioned with a probability of $k'/(1+k')$ to the stationary phase and with a probability of $1/(1+k')$ to the mobile phase. Partitioning in each occurs independently of the other plates and of the equilibration at other times. If the retention time of a particular polymer molecule is $t_R = t_1(N_{pl} + N_{ex})$, then this polymer molecule has been partitioned N_{ex} times to the stationary phase and N_{pl} times to the mobile phase before it reaches the outlet. Then,

$$k' = N_{ex}/N_{pl} \quad (2.126)$$

From Eqs. 2.125 and 2.126, we find that K depends linearly on t_R by

$$K = \frac{V_M}{V_S} \left(\frac{t_R}{t_1 N_{pl}} - 1 \right) \quad (2.127)$$

as seen in Figure 2.58, where $t_1 N_{pl}$ is the retention time for a completely excluded component.

2.5.3 Partitioning of Polymer with a Pore

2.5.3.1 Partition Coefficient Figure 2.59 illustrates equilibrium of polymer molecules between the pore space (stationary phase) and the surrounding fluid

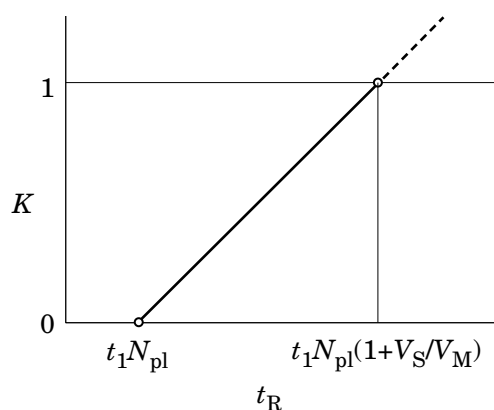


Figure 2.58. The partition coefficient K has a linear relationship with the retention time t_R . At $t_R = t_1 N_{pl}$, $K = 0$ (total exclusion). K does not exceed 1 in SEC unless there is an attractive interaction between the polymer and the pore surface.

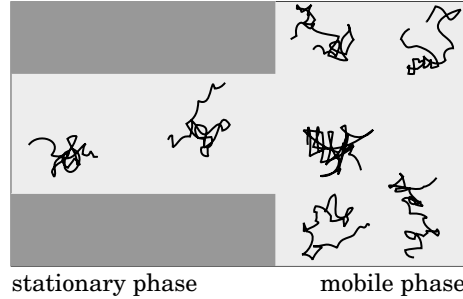


Figure 2.59. Polymer chains are partitioned between the stationary phase (pore space) and the mobile phase (surrounding fluid).

(mobile phase). The concentration equilibrium is reached when the chemical potential of the polymer molecule becomes equal between the two phases. At low concentrations, the solution is ideal. The chemical potential of the polymer molecule (μ_M) in the mobile phase of concentration (c_M) is given by

$$\mu_M = \mu^\circ + k_B T \ln(c_M/c^\circ) \quad (2.128)$$

where μ° is the chemical potential in a reference state of concentration c° in the ideal solution. When the polymer molecule is brought into the stationary phase, its entropy changes by ΔS and its enthalpy by ΔH . The entropy change is related to the decrease in the available space the centroid of the molecule can reach as well as the decrease in the total number of conformations. Because of these geometrical restrictions, $\Delta S < 0$. The enthalpy change is due to interactions of the polymer molecule with the pore surface and can be positive or negative. When the polymer chain enters the pore, surface–monomer contacts replace some of the monomer–solvent contacts, resulting in the enthalpy change. The chemical potential in the stationary phase (μ_S) of concentration (c_S) is then given by

$$\mu_S = \mu^\circ + k_B T \ln(c_S/c^\circ) - T\Delta S + \Delta H \quad (2.129)$$

The concentration equilibrium is dictated by $\mu_S = \mu_M$:

$$k_B T \ln(c_S/c^\circ) - T\Delta S + \Delta H = k_B T \ln(c_M/c^\circ) \quad (2.130)$$

which gives the partition coefficient $K = c_S/c_M$:

$$K = \exp\left(\frac{\Delta S}{k_B} - \frac{\Delta H}{k_B T}\right) \quad (2.131)$$

Because of the specific nature in the three-way interactions between polymer, surface, and solvent, there is hardly a universal method that allows us to predict ΔH

for a given combination of the polymer, surface, and solvent. In contrast, ΔS is universal because it is determined by the geometrical confinement of the polymer molecule by the pore. In ideal SEC, the stationary phase is designed to provide purely entropic effects for any combination of polymer and solvent as long as the solvent is good to the polymer. Then, $\Delta H = 0$ and

$$K = \exp(\Delta S/k_B) \quad (2.132)$$

Because $\Delta S < 0$, $K < 1$. With Eq. 2.127, we then find that t_R ranges between $t_1 N_{pl}$ and $t_1 N_{pl}(1 + V_S/V_M)$.

In a different mode of chromatography, ΔS is rather suppressed and the differences in ΔH between different polymers are utilized to analyze the chemical composition of the polymer. If $\Delta H > 0$, the pore wall repels the polymer. Otherwise, it adsorbs the polymer.

Recall that a polymer chain is described by a thin thread in the crudest approximation. This geometrical object interacts with the pore, another geometrical object. The confinement effect is manifested in the partition coefficient and the change in the chain conformation. We can expect an interesting relationship between the chain and the geometry of the pore. However, the geometry in the porous medium used in SEC is far from simple. The pore is rather highly tortuous. Theories have been developed for some simple geometries such as a slit, a square tube, and a cylinder.

2.5.3.2 Confinement of a Gaussian Chain We learn here how a Gaussian chain changes upon confinement by various geometries such as a slit, a square tube, and a cylindrical tube. It is possible to obtain a formula for the partition coefficient in each of the three geometries.

We first recall that the Gaussian transition probability $G(\mathbf{r}, \mathbf{r}')$ given by Eq. 1.34 can be factored into three independent components G_x , G_y , and G_z , where G_z is given by

$$G_z(z, z') = \frac{1}{2\pi^{1/2}R_g} \exp\left[-\frac{(z - z')^2}{4R_g^2}\right] \quad (2.133)$$

for example, for chains with radius of gyration R_g . When the Gaussian chain is brought into a slit of width d extending in x and y directions (Fig. 2.60), G_x and G_y do not change because each component is independent. Only G_z experiences a change. Casassa²⁷ calculated G_z for a one-dimensional random walker starting at z' to reach z after necessary number of steps without touching the slit walls. The result is

$$G_{z,\text{slit}}(z, z') = \frac{2}{d} \sum_{k=1}^{\infty} \sin \frac{k\pi z}{d} \sin \frac{k\pi z'}{d} \exp[-(k\pi R_g/d)^2] \quad (2.134)$$

Figure 2.61 compares the two distribution functions for the chain end z when the other end is at $z' = d/2$. $R_g = d/4$ was assumed.

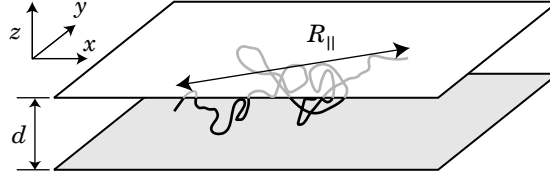


Figure 2.60. Polymer chain confined to a slit of width d . The chain has a dimension of $R_{||}$ along the slit walls. Its dimension in z direction is bound to d .

The partition coefficient K_{slit} is then calculated as the average of $G_z(z, z'; N)$ with respect to z and z' :

$$K_{\text{slit}} = d^{-1} \int_0^d dz \int_0^d dz' G_z(z, z') = \frac{8}{\pi^2} \sum_{k:\text{odd}} k^{-2} \exp[-(k\pi R_g/d)^2] \quad (2.135)$$

When $R_g \gg d$, the first term dominates:

$$K_{\text{slit}} \cong \exp[-(\pi R_g/d)^2] \quad (2.136)$$

It is now clear that K_{slit} decreases sharply as R_g increases and becomes comparable to d .

Because there is no confinement in the x and y directions, G_x and G_y do not change. The mean square end-to-end distance does not change its x and y components. Thus, the chain dimension $R_{||}$ along the slit wall is given by

$$R_{||}^2 = \langle R_{Fx}^2 \rangle + \langle R_{Fy}^2 \rangle = \frac{2}{3} Nb^2 \quad (2.137)$$

Confinement by a square tube extending in the x direction and having a square cross section of length d changes each of G_y and G_z in the same way as the slit does

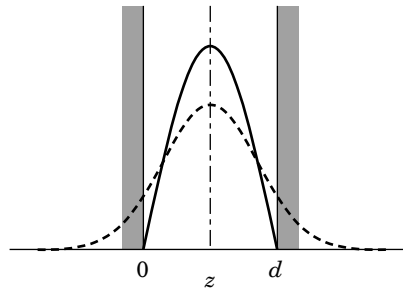


Figure 2.61. Density profile of the end of the Gaussian chain when the other end is at $z = d/2$. The density is compared for the confined chain (solid line) in a slit of walls at $z = 0$ and $z = d$ and the unconfined chain (dashed line). $R_g = d/4$ was assumed.

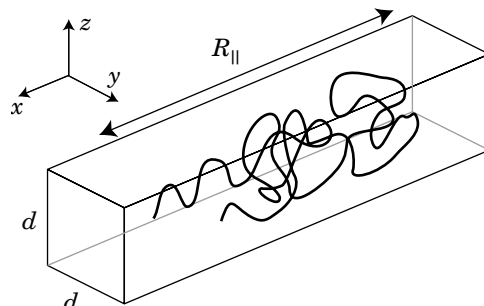


Figure 2.62. Polymer chain confined to a square tube of side d . The chain has a dimension of R_{\parallel} along the tube. Its dimensions in y and z directions are bound to d .

on G_z (Fig. 2.62). Confinement in one direction contributes to decreasing the partition coefficient by a factor of K_{slit} . The confinement in the y and z directions results in the partition coefficient of K_{slit}^2 . The chain dimension along the x direction is unchanged from that of the unconfined chain:

$$R_{\parallel}^2 = \langle R_{\text{Fx}}^2 \rangle = \frac{1}{3}Nb^2 \quad (2.138)$$

The three relationships in Eqs. 2.136–2.138 apply to other, non-Gaussian ideal chains. When the ideal chain is sufficiently long, then Eqs. 2.134 and 2.135 also apply.

The partition coefficient for a cylindrical pore was obtained similarly.²⁷ Likewise, the partition coefficient was calculated for a rodlike molecule in some simple geometries.²⁸ Figure 2.63 compares the partitioning of a Gaussian chain and a rodlike molecule in a cylindrical pore of radius R_p .²⁹ The plot of K is given as a

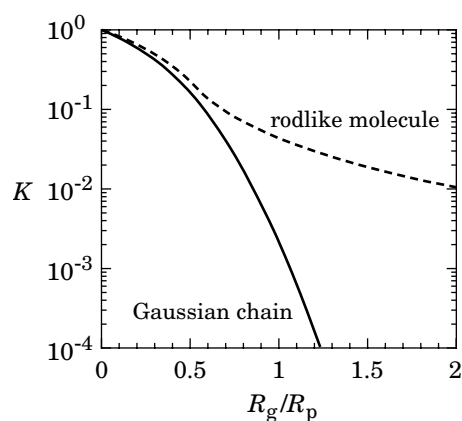


Figure 2.63. Partition coefficients K of a Gaussian chain and a rodlike molecule in a cylindrical pore of radius R_p as a function of R_g/R_p . (From Ref. 29.)

function of R_g/R_p . At $R_g = R_p$, only 1 of about 470 Gaussian chains finds itself in the pore. For the rodlike molecule ($R_g = L/12^{1/2}$; at $R_g = R_p$, the rod length is $3^{1/2} \times$ pore diameter), this odd is as large as 1 of 23 rods. The rod can align along the pore channel to fit in.

2.5.3.3 Confinement of a Real Chain The Gaussian chain is folded back into a dense packing of monomers when confined. In a real chain, overlay of monomers into the same space is prohibited. We can therefore expect that the real chain is more extended in the confined space compared with the free space. It is, however, all but impossible to treat the confinement of the real chain theoretically. We do not have a formula for the partition coefficient of the real chain even in simple confining geometries. Fortunately, it is possible to obtain an asymptotic functional relationship between ΔS and the chain length N for sufficiently long chains in a simple geometrical consideration.

We consider a real chain consisting of N monomers of size b and confined to a cylindrical pore of diameter d . When the chain dimension R_g in the free solution is smaller than the pore size, the chain does not feel much of the effect of the pore wall. As R_g exceeds d , the chain must adopt a conformation extending along the pore because of the excluded volume effect. As R_g increases further, the confined chain will look like a train of spheres of diameter d (see Fig. 2.64). The excluded volume effect prohibits the spheres from overlapping with each other. Therefore, the spheres can be arranged only like a shish kebab. The partial chain within each sphere follows a conformation of a real chain in the absence of confinement. The number n_d of monomers in the sphere is then given by

$$d \cong b n_d^{3/5} \quad (2.139)$$

where $n = 3/5$ was used (we will use the value in this section). The confined chain consists of N/n_d spheres. The length $R_{||}$ of the chain in the tube is then given as

$$R_{||} \cong d(N/n_d) \cong dN(b/d)^{5/3} \cong d(R_g/d)^{5/3} \quad (2.140)$$

Unlike a Gaussian chain, $R_{||}$ increases linearly with N . Note that R_g refers to the radius of gyration of unconfined chains.

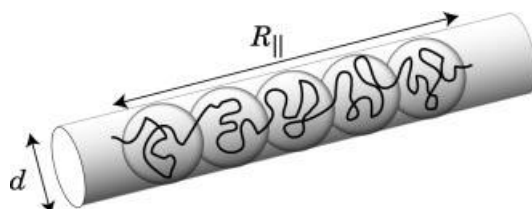


Figure 2.64. Real chain confined to a cylindrical pore of diameter d . The chain is regarded as a packed array of spheres of diameter d in one dimension. Within each sphere, the chain is three-dimensional.

Now we calculate the partition coefficient. The polymer chain consists of N/n_d spheres of size d . This sequence of self-avoiding spheres has the same end-to-end distance in the three-dimensional space as the chain of N monomers does (Problem 2.33). Therefore, grouping the monomers into spheres of n_d monomers does not introduce an artificial change in the statistical property of the chain. How the spheres are arranged in the three-dimensional space determines the overall conformation of the chain. We imagine a cubic lattice and place the spheres on the grid points separated by d . In the absence of the cylindrical pore, the number of possible grid points available to place the next sphere is five (six minus one, one being the preceding sphere; see Fig. 2.65 (a)). Thus the total number of the arrangement of the N/n_d spheres is roughly $5^{N/n_d}$. The condition that the spheres do not overlap decreases the total number, but the correction is small. Within the cylindrical pore, in contrast, there is only one possibility to place the next sphere, once the second sphere is placed (Fig. 2.65 (b)). There is only one possibility or two for the conformation of the whole sequence of spheres. The partition coefficient is calculated as the ratio of the possible numbers of arrangement:

$$K \cong \frac{1}{5^{N/n_d}} \quad (2.141)$$

Because $K = \exp(\Delta S/k_B)$, the entropy change ΔS is expressed as

$$-\Delta S/k_B = -\ln K \cong N/n_d \cong N(b/d)^{5/3} \cong (R_g/d)^{5/3} \quad (2.142)$$

The decrease in the entropy, $-\Delta S$, grows linearly with N , i.e., a longer chain experiences a greater restriction on its conformation in the pore. It is interesting to see that the same power law, $-\Delta S \sim N$, also applies to the ideal chain if we replace $5/3 = 1/\nu$ by 2. The proportionality to N is common between the ideal chain and the real chain. This result is not a coincidence. If we follow the same discussion as above to calculate K for the ideal chain, the number of arrangement for the spheres in the pore is $2^{N/n_d}$, as opposed to $6^{N/n_d}$ in the free solution. The ratio leads to $-\Delta S/k_B \cong N/n_d \cong (R_g/d)^2$. The confinement of the Gaussian chain gives the same relationship: From $K = K_{\text{slit}}^2$ and Eq. 2.136, we find $-\Delta S/k_B \cong (R_g/d)^2$.

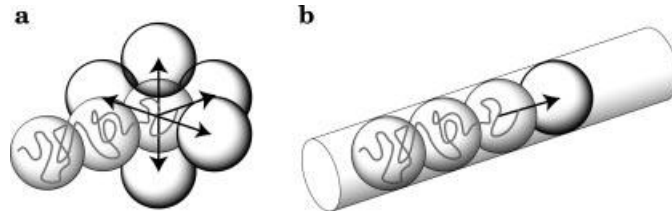


Figure 2.65. Conformation of a real chain. When the next sphere is attached to the growing end, there are five possible positions in the absence of the cylindrical pore (a), but only one is available within the pore (b).

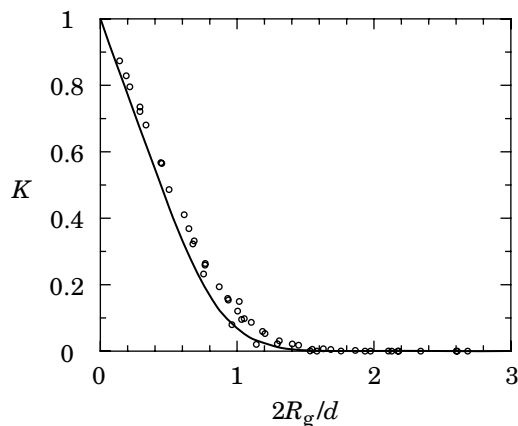


Figure 2.66. Partition coefficients K of a Gaussian chain (solid line) and a real chain (circles) with a radius of gyration R_g in a slit of width d . The data for the real chain were obtained in the computer simulation (From Ref. 5).

How about the confinement by the slit? The spheres are arranged in the two-dimensional space. The number of arrangements is now $3^{N/n_d}$. Then, $-\Delta S$ follows the same scaling relationship as Eq. 2.142 except the numerical coefficient. Figure 2.66 compares the partition coefficients of the Gaussian chain (solid line) and the real chain (circles) with a radius of gyration R_g in a slit of width d . The coefficients for the real chain were obtained in lattice computer simulations.⁵

The linear dimension of the chain in the slit is different from the counterpart in the cylindrical pore. Because the confined chain follows the conformation of two-dimensional excluded-volume chain,

$$R_{||} \cong d(N/n_d)^{3/4} \cong d(R_g/d)^{5/4} \quad (2.143)$$

Here we used the fact that, in two dimensions, the self-avoiding random walk has an exponent of $3/4$ in the relationship between R_F and N (Problem 1.13). We can also derive the above relationship by applying Flory's method that we used to derive the chain dimension in three dimensions (Problem 2.34).

As seen in the above examples, confinement lowers the number of dimensions available to a polymer chain. In the Gaussian chain, on the one hand, the confinement changes the confined components only. The root mean square end-to-end distance changes only by a numerical coefficient without changing the dependence of R_F on N . In the real chain, on the other hand, the decrease in the dimensionality changes qualitatively the relationship between N and $R_{||}$ from that in the free solution. The confinement manifests the excluded volume effect more prominently.

2.5.4 Calibration of SEC

We have learned in Section 2.5.2 that the retention time t_R of SEC increases linearly with K . We also learned in Section 2.5.3 that $K \cong (1/5)^{N/n_d}$ for the partitioning of

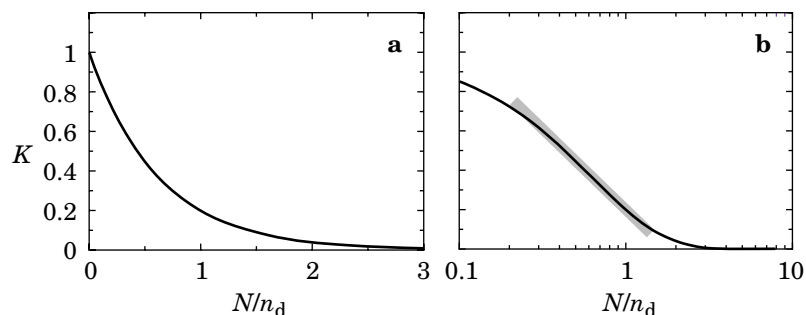


Figure 2.67. Sketch of the partition coefficients K of a real chain as a function of the number of blobs, N/n_d . In linear scale (a) and in semi-logarithmic scale (b) of N/n_d . The shaded region in (b) indicates a nearly straight portion of the plot.

the real chain with a cylindrical pore. The porous material used in SEC has a tortuous, interconnected pore structure. The pore resembles a cylindrical pore over a short distance.

Figure 2.67a is a plot of $K = (1/5)^{N/n_d}$ as a function of N/n_d . The plot of K_0 for the Gaussian chain with a cylindrical pore in Figure 2.63 is close to this plot when the abscissa is changed to $(R_g/R_p)^{5/3} \sim N$ and the ordinate is in linear scale. Therefore, we can extend the use of $K = (1/5)^{N/n_d}$, originally derived for sufficiently long chains, to shorter chains. The same plot in panel a, when the abscissa is in a log scale (Fig. 2.67b), is nearly straight in the middle range of K . An SEC column packed with such porous materials will have a linear relationship between t_R and $\log M$ in a certain range of the molecular weight M . The relationship is schematically depicted in Figure 2.68. The column is therefore able to resolve the molecular weight distribution in the logarithmic scale, but in a limited range. Above the upper threshold, t_R becomes insensitive to M . This limit is called the **exclusion limit**. Polymer chains with a molecular weight higher than the limit do not partition with the stationary phase and travel the column straight through to elute in $t_1 N_{pl}$. Below

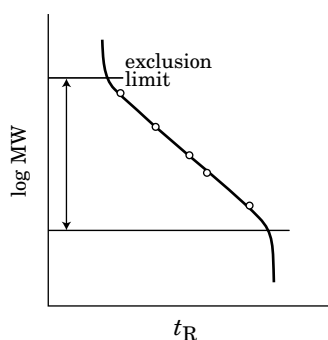


Figure 2.68. Calibration curve of a size-exclusion column. The column can analyze the molecular weight (MW) of the polymer only in the range indicated by the arrow.

the lower threshold, t_R becomes again insensitive to M . The pore size is too large to distinguish the polymer chain by its dimension.

The packing material with a greater pore size effectively increases n_d and shifts the range of molecular weight that the column can analyze to a greater molecular weight. The range can be broadened by mixing packing materials of different pore diameters at the expense of the resolution. A so-called linear column is prepared in this way. Another way is to connect columns of different pore diameters in series.

To relate the retention time to molecular weight for a given series of columns, we use molecular weight standards. They are commercially available. Manufacturers supply the data of M_w , M_n , and M_p , where M_p , the peak molecular weight, is the molecular weight at the peak of the SEC retention curve. A calibrated column can convert the retention curve into the plot of the molecular weight distribution.

2.5.5 SEC With an On-Line Light-Scattering Detector

Since approximately 1990, light-scattering detectors have been increasingly used as an on-line detector in SEC, providing more detailed information on the polymer chain conformation in the solution state. The detector has a flow cell with a small cell volume and measures the scattering intensities at different angles. The advantage of this scheme for characterization of polymer in solution is obvious. As the column separates the polymer according to molecular weight, each fraction is led to the light-scattering detector for instantaneous measurement of the scattering intensities [$I_{ex}(\theta)$], as illustrated in Figure 2.69. The concentration detector such as a refractive index detector and an ultraviolet absorption detector connected in series gives the estimate of the polymer concentration c . Then with the preinput data of dn/dc , a Zimm plot is prepared for each fraction. The plot is for one concentration only, but it is sufficiently low because of the band broadening (further dilution) by the SEC column of the already dilute injected solution.

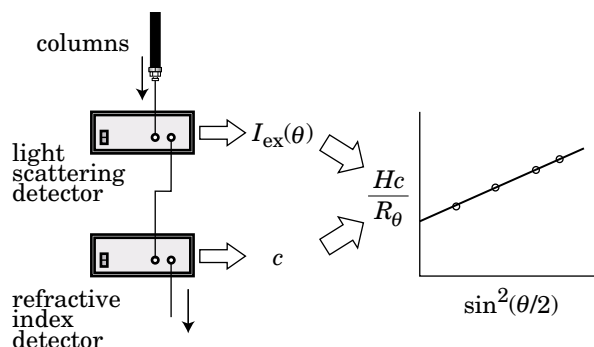


Figure 2.69. Use of an online light-scattering detector and a concentration detector in series allows a Zimm plot for every eluent. Thus, the molecular weight and radius of gyration can be estimated as a function of the retention time without using any standard.

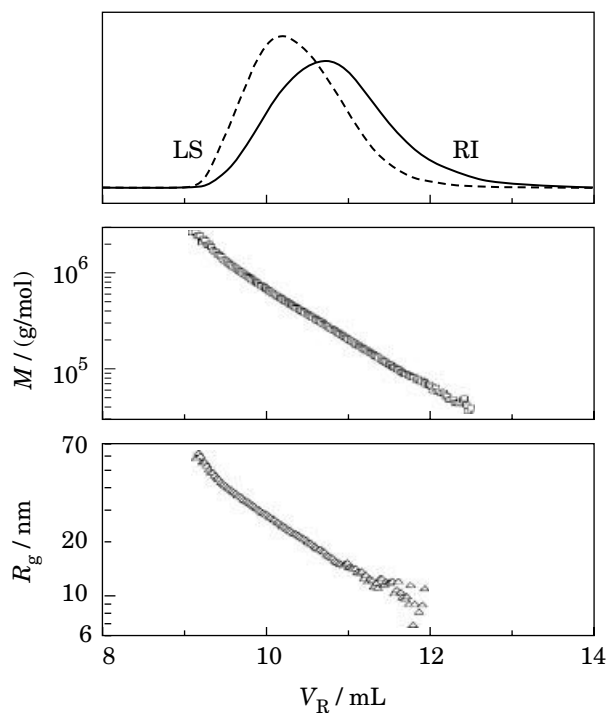


Figure 2.70. Typical examples of chromatograms. The solution is branched polyethylene in tetrahydrofuran. Top: light-scattering intensity I_{ex} (LS; 90°) and refractive index difference Δn (RI). Middle: molecular weight M . Bottom: radius of gyration R_g , plotted as a function of the retention volume V_R . (From Ref. 9.)

Thus A_2Mc is negligible in Eq. 2.116. Because the measurement is instantaneous, injection of a broad-distribution polymer sample results in a plot of the molecular weight M and the radius of gyration R_g as a function of the retention time. Thus we can obtain a plot of R_g as a function of M . In fact, Figure 1.38 was obtained in this way.

This method eliminates the need to fractionate the polydisperse polymer on a preparative scale and run the tedious light-scattering measurements for each fraction. Figure 2.70 shows an example of SEC chromatograms for branched polyethylene.⁹ Panel a shows the refractive index signal Δn , which is proportional concentration, and the light-scattering intensity I_{ex} at 90° . Because $I_{\text{ex}} \propto cM$, the peak of I_{ex} appears ahead of the peak in Δn . Panel b shows the molecular weight M , and panel c plots R_g . At both ends of the chromatogram, the concentration is low. The uncertainty in the estimates of M and R_g are larger at both ends.

Furthermore, an on-line viscosity detector can be connected in tandem to the concentration detector (and the light-scattering detector). As we will learn in Section 3.3, the solution viscosity gives an important piece of information on the state of polymer molecules in solution.

2.5.6 PROBLEMS

Problem 2.33: An excluded-volume chain of N monomers of size b has a dimension of $R_F \cong bN^\nu$. Grouping n_d monomers into one “big monomer” makes a chain of N/n_d big monomers with excluded volume. Within each big monomer, the chain is still an excluded-volume chain of monomer size b . Show that this coarse-grained chain has the same dimension as that of the original chain.

Solution 2.33: The size of the big monomer is bn_d^ν . Therefore, the dimension of the coarse-grained chain is $(bn_d^\nu)(N/n_d)^\nu = bN^\nu$, identical to R_F of the original chain. The choice of n_d is arbitrary.

Problem 2.34: Flory’s method, we learned in Section 1.4 to find the dimension of the real chain, can be extended to the confined real chain. Find the relationship between the dimension of the chain along the slit wall or the tube wall, $R_{||}$, and the degree of polymerization N for the confinement by (1) a slit of width d and (2) a tube of diameter d .

Solution 2.34 (1): The volume for a polymer chain confined to the slit is $R_{||}^2 d$. Then, the monomer density is $N/(R_{||}^2 d)$. The interaction term in Eq. 1.63 is now $b^3 N^2/(R_{||}^2 d)$. The free energy A_{ch} of the chain with a dimension of $R_{||}$ is Flory’s method given as

$$\frac{A_{ch}}{k_B T} \cong \frac{R_{||}^2}{Nb^2} + b^3 \frac{N^2}{R_{||}^2 d}$$

At its minimum,

$$\frac{\partial}{\partial R_{||}} \frac{A_{ch}}{k_B T} \cong \frac{2R_{||}}{Nb^2} - 2b^3 \frac{N^2}{R_{||}^3 d} = 0$$

Therefore,

$$R_{||} \cong b^{5/4} N^{3/4} / d^{1/4} = d(bN^{3/5}/d)^{5/4} = d(R_g/d)^{5/4}$$

which is identical to Eq. 2.143.

Solution 2.34 (2): In the tube, the volume for the polymer chain is $R_{||} d^2$. Then,

$$\frac{A_{ch}}{k_B T} \cong \frac{R_{||}^2}{Nb^2} + b^3 \frac{N^2}{R_{||} d^2}$$

At its minimum,

$$\frac{\partial}{\partial R_{||}} \frac{A_{ch}}{k_B T} \cong \frac{2R_{||}}{Nb^2} - b^3 \frac{N^2}{R_{||}^2 d^2} = 0$$

Therefore,

$$R_{\parallel} \cong b^{5/3}N/d^{2/3} = d(bN^{3/5}/d)^{5/3} = d(R_g/d)^{5/3}$$

which is identical to Eq. 2.140.

Problem 2.35: Repeat the preceding problem for the theta chains.

Solution 2.35 (1): The interaction term in Eq. 1.63 is $b^6N^3/(R_{\parallel}^2d)^2$. The free energy A_{ch} of the chain with a dimension of R_{\parallel} is given as

$$\frac{A_{\text{ch}}}{k_B T} \cong \frac{R_{\parallel}^2}{Nb^2} + b^6 \frac{N^3}{R_{\parallel}^4 d^2}$$

At its minimum,

$$\frac{\partial}{\partial R_{\parallel}} \frac{A_{\text{ch}}}{k_B T} \cong \frac{2R_{\parallel}}{Nb^2} - 4b^6 \frac{N^3}{R_{\parallel}^5 d^2} = 0$$

Therefore,

$$R_{\parallel} \cong b^{4/3}N^{2/3}/d^{1/3} = d(bN^{1/2}/d)^{4/3} = d(R_g/d)^{4/3}$$

Solution 2.35 (2): The volume is $R_{\parallel}d^2$. Then,

$$\frac{A_{\text{ch}}}{k_B T} \cong \frac{R_{\parallel}^2}{Nb^2} + b^6 \frac{N^3}{R_{\parallel}^2 d^4}$$

At its minimum,

$$\frac{\partial}{\partial R_{\parallel}} \frac{A_{\text{ch}}}{k_B T} \cong \frac{2R_{\parallel}}{Nb^2} - 2b^6 \frac{N^3}{R_{\parallel}^3 d^4} = 0$$

Therefore,

$$R_{\parallel} \cong b^2N/d = d(bN^{1/2}/d)^2 = d(R_g/d)^2$$

Note that these results for the theta chains are different from the chain dimensions of ideal chains in the slit and the tube. The confined ideal chains have the dimension of $\sim N^{1/2}$ in both confining geometries. The difference between the ideal chain and the theta chain shows up because of the third virial coefficient A_3 . Compensation of the excluded volume effect by the attractive polymer–polymer interaction allows the theta chain to have the same dimension as that of the ideal chain, but it is valid only in the three-dimensional free solution. In spaces of a reduced dimensionality, the same attractive interaction cannot mask the excluded volume.

APPENDIX 2.A: REVIEW OF THERMODYNAMICS FOR COLLIGATIVE PROPERTIES IN NONIDEAL SOLUTIONS

2.A.1 Osmotic Pressure

We briefly review here thermodynamics of a nonideal binary solution. The osmotic pressure Π is the extra pressure needed to equilibrate the solution with the pure solvent at pressure p across a semipermeable membrane that passes solvent only. The equilibration is attained when the chemical potential μ_S^* of the pure solvent becomes equal to the chemical potential μ_S of the solvent molecule in solute volume fraction ϕ at temperature T :

$$\mu_S^*(T, p) = \mu_S(T, p + \Pi, \phi) \quad (2.A.1)$$

We separate the right-hand side into two parts:

$$\mu_S(T, p + \Pi, \phi) = \mu_S^*(T, p + \Pi) + \Delta\mu_S \quad (2.A.2)$$

where $\Delta\mu_S$ denotes the change in the chemical potential from μ_S^* . Colligative properties make $\Delta\mu_S$ negative. Because the volume of a liquid depends little on the pressure,

$$\mu_S^*(T, p + \Pi) = \mu_S^*(T, p) + \int_p^{p+\Pi} \frac{\partial \mu_S^*}{\partial p} dp = \mu_S^*(T, p) + v^* \Pi \quad (2.A.3)$$

with v^* being the volume of the solvent molecule in the liquid phase. From Eqs. 2.A.1 to 2.A.3, we find

$$\Pi = -\frac{\Delta\mu_S}{v^*} \quad (2.A.4)$$

2.A.2 Vapor Pressure Osmometry

The colligative property shows up also in the vapor pressure of the solution. The vapor pressure p of the solvent above the solution is lower than the vapor pressure p^* of pure solvent. The vapor phase is nearly ideal. Therefore, the chemical potential of the solvent molecule in the vapor phase is given by $\mu^\circ(T) + k_B T \ln(p/p^\circ)$, where $\mu^\circ(T)$ is the chemical potential at a reference pressure p° . The vapor–liquid equilibrium for pure solvent is dictated by

$$\mu^\circ(T) + k_B T \ln(p^*/p^\circ) = \mu_S^*(T, p^*) \quad (2.A.5)$$

For a solution with a polymer volume fraction at ϕ , the equilibrium is given by

$$\mu^\circ(T) + k_B T \ln(p/p^\circ) = \mu_S(T, p, \phi) \quad (2.A.6)$$

From Eqs. 2.A.2, 2.A.5, and 2.A.6, we find

$$k_B T \ln(p/p^*) = \Delta\mu_S + \mu_S^*(T, p) - \mu_S^*(T, p^*) \quad (2.A.7)$$

Because $\mu_S^*(T, p) = \mu_S^*(T, p^*) + v^*(p - p^*)$ and $\Delta\mu_S = -v^*\Pi$,

$$\frac{\Pi v^*}{k_B T} = -\ln(p/p^*) + \frac{v^*(p - p^*)}{k_B T} \quad (2.A.8)$$

The second term on the right-hand side is much smaller compared with the first term. Thus,

$$\frac{\Pi v^*}{k_B T} = -\ln(p/p^*) \cong \frac{p^* - p}{p^*} \quad (2.A.9)$$

This equation gives the principle of **vapor pressure osmometry**: In place of measuring Π directly, we can measure the drop in the vapor pressure of the solvent above the solution to estimate Π .

APPENDIX 2.B: ANOTHER APPROACH TO THERMODYNAMICS OF POLYMER SOLUTIONS

Once we have obtained the free energy or the chemical potential expressed as a function of ϕ , we can forget that it was derived for a two-component incompressible fluid consisting of polymer and solvent. We can neglect the presence of solvent molecules and assume that polymer chains are suspended in “vacuum” at volume fraction ϕ . The system is essentially a single-component nonideal gas whose free energy is given by Eq. 2.7. ΔA_{mix} is then the free-energy change of “vaporization” of polymer molecules from their liquid state. The osmotic pressure Π can be obtained directly from ΔA_{mix} (Problem 2.4). In this scenario, the interaction is present only between two monomers of polymer: $\chi = -Z \varepsilon_{PP}/(2k_B T)$.

The Gibbs free energy change ΔG_{mix} is given by

$$\Delta G_{\text{mix}} = \Delta A_{\text{mix}} + \Pi \Delta V_{\text{mix}} \quad (2.B.1)$$

where $\Delta V_{\text{mix}} = V(1 - \phi)$. It can be shown that this ΔG_{mix} is equal to $n_P \Delta \mu_P$ (Problem 2.5). Note that this ΔG_{mix} is different from the one we find in the mixing of n_P polymer chains and n_S solvent molecules at a constant total volume.

APPENDIX 2.C: CORRELATION FUNCTION OF A GAUSSIAN CHAIN

The segment density autocorrelation function the Gaussian chain is calculated as follows.

$$\begin{aligned} \frac{N}{\rho} \langle \rho(\mathbf{r})\rho(0) \rangle &= \int_0^N dn \int_0^N dn' (2\pi|n - n'|b^2/3)^{-3/2} \exp\left(-\frac{3\mathbf{r}^2}{2|n - n'|b^2}\right) \\ &= 2 \int_0^N dn \int_0^n dn' (2\pi|n - n'|b^2/3)^{-3/2} \exp\left(-\frac{3\mathbf{r}^2}{2|n - n'|b^2}\right) \end{aligned} \quad (2.C.1)$$

We change the variable of integration from n' to $m = n - n'$ and then exchange the order of the double integral:

$$\frac{N}{\rho} \langle \rho(\mathbf{r})\rho(0) \rangle = 2 \int_0^N dm (N - m) (2\pi m b^2/3)^{-3/2} \exp\left(-\frac{3\mathbf{r}^2}{2m b^2}\right) \quad (2.C.2)$$

We change the variable of integration further from m to x where $x^2 = 3\mathbf{r}^2/(2b^2m)$. With $u \equiv 3\mathbf{r}^2/(2b^2N) = r^2/(4R_g^2)$ and $m = Nu/x^2$, Eq. 2.C.2 is transformed to

$$\frac{N}{\rho} \langle \rho(\mathbf{r})\rho(0) \rangle = \frac{6N}{\pi^{3/2}b^2r} \left[\int_{u^{1/2}}^{\infty} \exp(-x^2) dx - u \int_{u^{1/2}}^{\infty} \frac{1}{x^2} \exp(-x^2) dx \right] \quad (2.C.3)$$

Using integration by parts, the integral in the second term is changed to

$$\int_{u^{1/2}}^{\infty} \frac{1}{x^2} \exp(-x^2) dx = u^{-1/2} \exp(-u) - 2 \int_{u^{1/2}}^{\infty} \exp(-x^2) dx \quad (2.C.4)$$

Then,

$$\frac{1}{\rho} \langle \rho(\mathbf{r})\rho(0) \rangle = \frac{6}{\pi^{3/2}b^2r} [(1 + 2u)\text{Erfc}(u^{1/2}) - u^{1/2}\exp(-u)] \quad (2.C.5)$$